A STUDY OF THE CHARACTERISTICS AND THE SIMULATION OF THE PLANETARY RADIATION ENVIRONMENT

by

Roger R. Hughes

Contract No. NAS 5-9785

November, 1965

Prepared by

Messinger Consultants Company
2360 Huntington Drive
San Marino, California 91108

For

The National Aeronautics and Space Administration
Goddard Space Flight Center
Greenbelt, Maryland

A STUDY OF THE CHARACTERISTICS AND THE SIMULATION OF THE PLANETARY RADIATION ENVIRONMENT

by
Roger R. Hughes

Contract No. NAS 5-9785

November, 1965

Prepared by

Messinger Consultants Company
2360 Huntington Drive
San Marino, California 91108

For

The National Aeronautics and Space Administration
Goddard Space Flight Center
Greenbelt, Maryland

TABLE OF CONTENTS

LIST OF ILLUSTRATIONS

LIST OF TABLES

THIS REPORT HAS BEEN ASSIGNED
MESSINGER CONSULTANTS COMPANY
TECHNICAL DOCUMENT NO. MCC-856-F

SECTION 1
INTRODUCTION

A spacecraft located in the vicinity of the earth receives radiant energy from two major sources, the sun and the earth. Therefore, if the environment to be experienced by the spacecraft is to be truly simulated in a space environment simulation facility, it is necessary to provide radiant flux to the target volume of the simulator which has the same intensity, spectrum, and distribution as that which occurs in space. Accordingly, the purposes of this study were to determine the relationships between the components of the radiant flux experienced by the spacecraft, determine the characteristics of the radiant flux reflected and/or emitted by the earth, and to define a technique whereby the radiant flux emanating from the earth can be simulated in the Space Environment Simulator at NASA Goddard Space Flight Center.

This report was prepared by Roger R. Hughes, Senior Physicist, Messinger Consultants Company. Mr. Walter Wallin, President, Wallin Optical Systems, Inc., 9186 Independence Avenue, Chatsworth, California, 91311, was the Senior Optical Design Consultant for this study and contributed to the technical content of this report.

This study described herein was conducted between January 11, 1965, and August 10, 1965, by Messinger Consultants Company, 2360 Huntington Drive, San Marino, California, 91108, under Contract NAS 5-9785.

SECTION 2
STATEMENT OF THE PROBLEM

The study described herein consisted of three major areas of analysis. These areas were (1) an analysis of the characteristics of the radiant flux which would be encountered by a spacecraft in the vicinity of the earth; (2) the definition of a method whereby the distribution of the radiant flux emanating from the earth could be reproduced within the target volume of the Space Environment Simulator; and (3) an estimate of what effect various approximations introduced into the simulated environment would have upon the simulation fidelity. Some of the specific areas to be investigated and specific tasks to be performed were as follows:

1. Establish the important geometrical relationships which govern the irradiance experienced by a spacecraft in the vicinity of the earth.

2. Calculate the irradiance produced, on a target surface element in the vicinity of the earth, by (a) radiant flux emitted by the sun to the target surface element, by (b) radiant flux emitted by the sun and reflected by the earth to the target surface element, and by (c) radiant flux emitted by the earth to the target surface element, as a function of the location and the orientation of the target surface element.

3. Calculate the total irradiance experienced by a target surface element in the vicinity of the earth as a function of the location and the orientation of the target surface element.

4. Define a method whereby the various geometrical properties of the radiant flux experienced by a spacecraft in the vicinity of the earth can be reproduced within the target volume of the Space Environment Simulator.

5. Determine the error introduced by failure to simulate the continuous field subtended by the earth at the spacecraft.

6. Determine the error introduced by failure to simulate the variable irradiation of the earth by the sun.

7. Determine the error introduced by failure to reproduce the total field subtended by the earth at the location whose environment is being simulated.

8. Given the spectral absorptivity of various materials used to coat the exterior of a spacecraft, determine how the absorptance of each material will vary in space as a function of the location and the orientation of the surface of the spacecraft.

9. Given the spectral absorptivity of various materials used to coat the exterior of a spacecraft, estimate the absorptance error introduced by mismatch between the true spectrum and the spectrum produced by the Planetary Radiation Environment Simulator.

SECTION 3
SUMMARY

The basic assumptions and definitions used to define the characteristics of the Solar Radiation Environment and the Planetary Radiation Environment are specified. The properties of the radiant flux emitted by the sun, the properties of the radiant flux emitted by the sun and reflected by the earth, and the properties of the radiant flux emitted by the earth are defined in detail. The relationship, between these three components of the radiant flux experienced by a spacecraft in the vicinity of the earth, is established and the irradiance produced on a target surface element by each component of the radiant flux, and the total irradiance experienced by the target surface element, is determined as a function of the location and the orientation of the target surface element. The average radiant emittance of the earth's surface as seen from various positions in space, and the ratio between the two spectral components of the radiant flux emanating from the earth, are determined as a function of orbital altitude and position.

The concept whereby the Planetary Radiation Environment can be simulated is presented and the basic relationships, which must be satisfied if the Planetary Radiation Environment is to be simulated using this concept, are established. It is shown that the radiant intensity of the flux emanating from each module of the Planetary Radiation Environment Simulator must be proportional to the cosine of the angle between the axis of the module and the direction of emission. The relationship between (a) the density of modules on the array reference surface, (b) the axial intensity of the radiant flux emanating from each module, and (c) the average radiant emittance seen at the earth's surface from the orbital position for which the environment is to be simulated, is defined. It is shown that the shape of the array reference surface is arbitrary so long as a uniform module density can be achieved on the surface and so long as the boundary of the array reference surface does not lie within the field subtended by the simulated planet at any position in the target volume.

The design of a module for the Planetary Radiation Environment Simulator

is discussed and several design concepts are presented. The various geometrical relationships which the radiant flux emanating from each module must satisfy are defined and the various parameters which must be varied in order to simulate any given orbit are determined.

It is shown that the limitations on simulation fidelity are primarily economic rather than technological. Because of this fact, it is desirable that the effect of certain kinds of errors be determined since the elimination of these errors will considerably increase the cost of the Planetary Radiation Environment Simulator. Specific errors treated include (a) the error introduced by failure to simulate the variable irradiation of the earth by the sun, (b) the error introduced by failure to simulate the smoothly continuous field subtended by the earth, (c) the error introduced by failure to simulate the field subtended by the earth at the position where the environment is being simulated and (d) the error introduced by failure of the modules to produce radiant flux with the correct spectrum.

SECTION 4
TECHNICAL DISCUSSION

CHARACTERISTICS OF THE SOLAR RADIATION ENVIRONMENT AND THE PLANETARY RADIATION ENVIRONMENT

Definitions and Basic Assumptions

Throughout the following discussion, the term "Solar Radiation Environment" refers to that region of space within which the density of the radiant flux emitted by the sun is a significant fraction of the total radiant flux density. In a like manner, the term "Planetary Radiation Environment" refers to that region of space within which the density of the radiant flux emanating from a planet is a significant fraction of the total radiant flux density. Thus, the earth is located in the Solar Radiation Environment, but the sun is not located within the Planetary Radiation Environment of the earth.

A spacecraft located in the vicinity of a planet lies within both the Solar Radiation Environment and the Planetary Radiation Environment since it receives radiant flux from two major sources: the sun and the planet. The resulting irradiance distribution experienced by a spacecraft over its surface is a function of (1) the radiative characteristics of the sun and the planet; (2) the relative size and location of the sun, the planet, and the spacecraft; and (3) the orientation of the spacecraft with respect to the directions to the sun and to the planet. Because of the small size of the target volume (that volume which contains the spacecraft) with respect to the distance to the planet (and to the sun), the field subtended by the planet (and that subtended by the sun), as seen from any position within the target volume, is virtually constant and symmetric about the same direction. Thus, the density of the radiant flux emanating from the planet (and the density of the radiant flux emitted by the sun) is essentially uniform throughout the target volume.

To illustrate the degree to which the radiant flux density is uniform, consider a 40-foot diameter target volume located 100 miles from the surface of an 8000-mile diameter spherical planet. The irradiance, produced on surface elements oriented normal to the direction to the center of the planet by radiant flux emanating from various points on the planet's surface, varies within the target volume from 0.01515% for the flux emanating from the closest point on the surface of the planet (a distance of 100 miles) to 0.00037% for flux emanating from the farthest point that can be seen on the planet's surface (a distance of 900 miles). If the surface of the planet were of uniform radiance, the variation in the irradiance produced on the surface elements by radiant flux emanating from the entire planet is 0.00037% (see Appendix II, equation II-8). Because the distance from the spacecraft to the sun is much greater than the distance from the spacecraft to the planet, the density of the radiant flux emitted by the sun would be even more uniform than that of the radiant flux emanating from the planet.

In order to characterize the Solar Radiation Environment and the Planetary Radiation Environment in the vicinity of the earth, it was necessary to establish the geometrical and spectral characteristics of the radiant flux emitted by the sun and emanating from the earth. These characteristics were established on the basis of the following considerations:

1. It was assumed that the density, of both the radiant flux emitted by the sun and the radiant flux emanating from the earth, is uniform throughout any size target volume (that volume which contains the spacecraft) for which simulation of the Solar Radiation Environment and the Planetary Radiation Environment is feasible.

2. The sun was assumed to be a spherical Lambertian radiator whose diameter is 864,100 miles and which is located 92,907,000 miles from the earth. (The sun subtends an angle of 0°32' at the mean earth-sun distance and was assumed

to be of uniform radiance for all wavelengths.) On the basis of this assumption, the geometrical and spectral characteristics of the radiant flux emitted by the sun are mutually independent. The spectrum of the sun was represented according to data obtained from the Handbook of Geophysics, U. S. Air Force Research Directorate, MacMillan, 1960, Table 16-8, "Spectral Irradiance Normal to the Sun's Rays Outside the Atmosphere," page 16-16.

3. The earth was assumed to be spherical and to have a radius of 3958.89 miles. (This is the radius of a sphere which has the same volume as the earth.)

4. It was assumed that the earth is in a state of thermal equilibrium. Thus, the radiant flux F_s which the earth receives from the sun must equal the sum of the radiant flux F_a reflected by the earth and the radiant flux F_e absorbed and re-emitted by the earth. That is

$$F_s = F_a + F_e \tag{4-1}$$

Defining R as the radius of the earth, A as the average albedo of the earth, W as the average radiant emittance of the earth, and E_{s_o} as the solar constant (see Appendix I for the definitions of albedo, radiant emittance, and the solar constant) then

$$F_s = \pi R^2 E_{s_o} \tag{4-2}$$

$$F_a = A F_s \tag{4-3}$$

$$F_e = 4 \pi R^2 W \tag{4-4}$$

Solving these four expressions simultaneously to eliminate F_s, F_a, and F_e, yields the following expression for the average radiant emittance of the earth.

$$W = \frac{(1 - A) E_{s_o}}{4} \tag{4-5}$$

Taking the average albedo A of the earth as 35% and the solar constant E_{s_o} as 130 watts-per-square-foot (data supplied by Goddard Space Flight Center), the average radiant emittance W of the earth is 21.125 watts-per-square-foot.

5. It was assumed that the albedo of an element of area on the earth's surface is independent of direction with respect to the surface normal; i.e., each surface element was assumed to be a Lambertian reflector (see Appendix I).

6. It was assumed that the emissivity of an element of area on the earth's surface is independent of direction with respect to the surface normal; i.e., each surface element was assumed to be a Lambertian radiator (see Appendix I).

7. It was assumed that local variations in the albedo and emissivity of the earth's surface, due to geographical factors (e.g., land, sea, clouds) and/or due to seasonal and diurnal temperature variations, can be ignored for the purpose of this analysis, since such variations are rapid and random with respect to the mean values.

8. Due to the lack of data concerning the spectrum of the radiant flux reflected by the earth and the spectrum of the radiant flux emitted by the earth, it was assumed (after conferring with Goddard Space Flight Center) that (a) the spectrum of the reflected radiant flux is identical to the solar spectrum and (b) the spectrum of the thermally emitted radiant flux is identically that of a 250°K blackbody. (Although this assumption is questionable, any error thus introduced will affect only the values calculated for the absorptance of various materials as a function of the location in the Planetary Radiation Environment. These values were used only to estimate the error introduced by mismatch between the true and the simulated spectrums.)

On the basis of the above considerations, it was possible to calculate the irradiance produced, on a target surface element, by radiant flux emitted by the sun, by radiant flux absorbed and re-emitted by the earth and by radiant flux reflected from the earth. These three components of the total irradiance experienced by a target surface element were calculated in terms of the geometrical relationships illustrated in figure 4-1 (using the computer programs SPACE and ORBVAR, see Appendix IV) and are discussed below.

Irradiance Due to Radiant Flux Emitted by the Sun

If the sun is assumed to be a spherical Lambertian radiator, then the equations governing the irradiance produced on a target surface element by radiant flux emitted by the sun can be specified, in terms of the parameters of figure 4-1, by making parametric substitutions into the equations of Appendix II. The equations thus determined are listed, in Appendix IV, as equations (IV-1) through (IV-11). The irradiance E_s, on a target surface element in the vicinity of the earth due to radiant flux emitted by the sun, is plotted as a function of Ψ in figure 4-2.

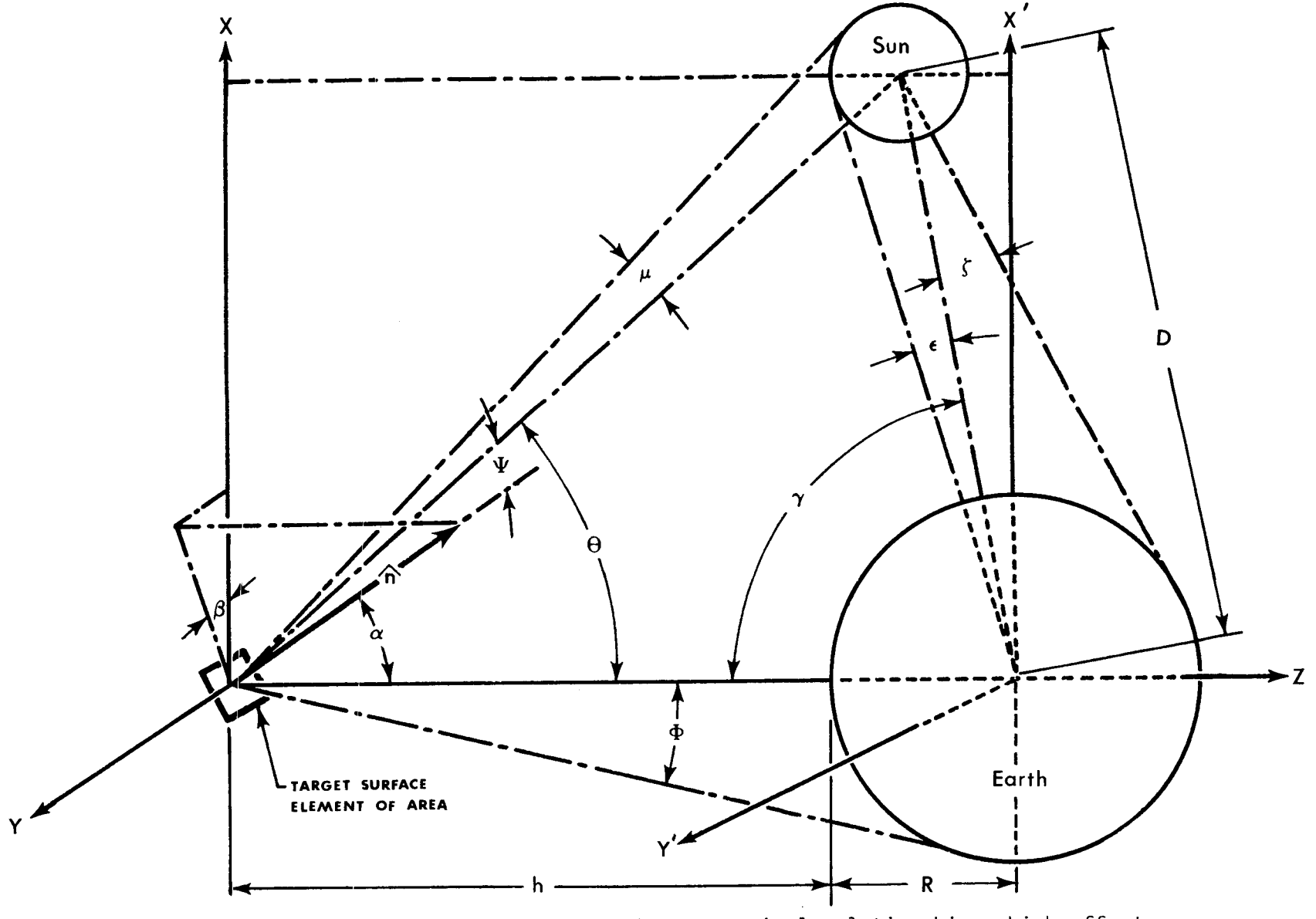

Figure 4-1. Schematic representation of the geometrical relationships which affect the irradiance experienced by a target surface element in space.

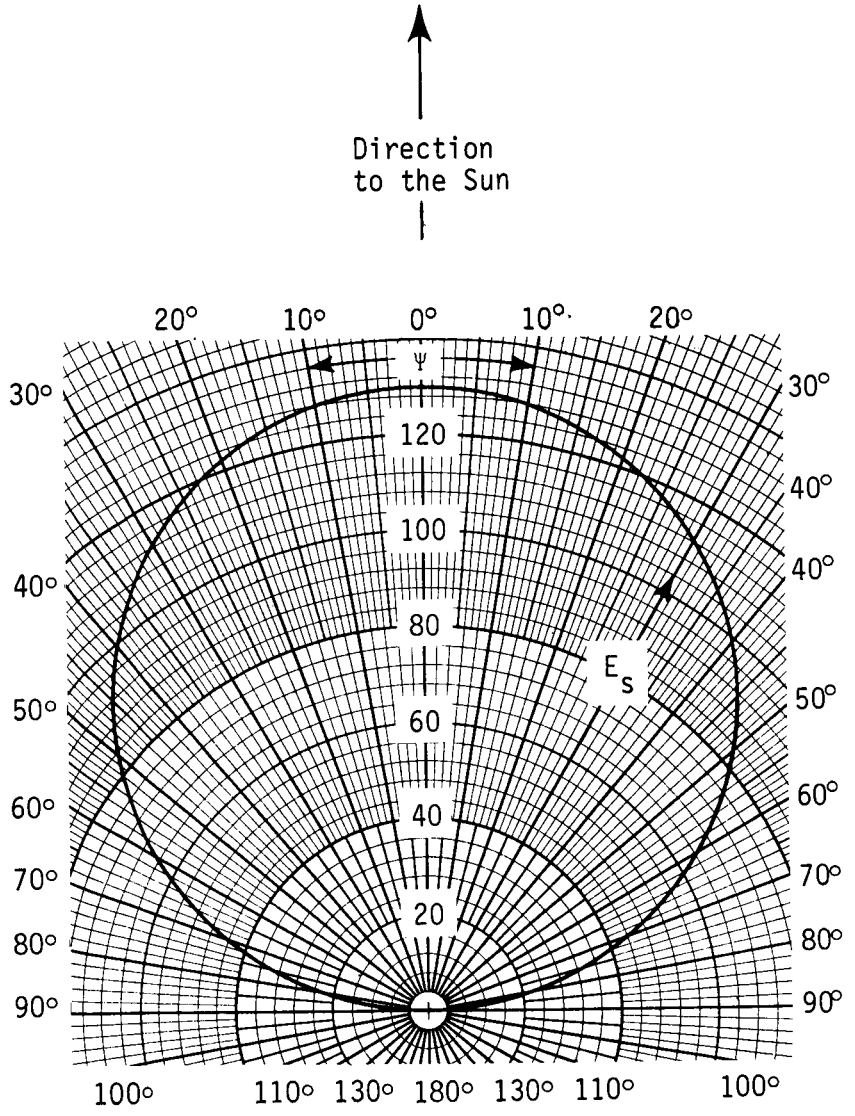

Figure 4-2. E_s (watts-per-square-foot) versus Ψ

Irradiance due to Radiant Flux Thermally Emitted by the Earth

If the earth is assumed to be a spherical Lambertian radiator of uniform radiance, then the equations governing the irradiance E_e produced on a target surface element by radiant flux absorbed and re-emitted by the earth can also be determined in terms of the parameters of figure 4-1, by making parametric substitutions into the equations of Appendix II. The equations thus defined are listed, in Appendix IV, as equations (IV-12) through (IV-21).

The irradiance E_{e_o}, on a target surface element which is oriented so that its normal $\hat{n}$ is in the direction toward the center of the earth ($\alpha = 0$), was calculated as a function of orbital altitude h using the computer program ORBVAR and is plotted versus h in figure 4-3. The normalized irradiance $\frac{E_e}{E_{e_o}}$ was calculated, as a function of the angle α between the normal $\hat{n}$ to the target surface element and direction to the center of the earth, using the computer program SPACE and is plotted versus α in figure 4-4 for orbital altitudes of 200, 300, 400, 500, 600, and 700 miles.

Irradiance Due to Radiant Flux Reflected from the Earth

If the earth is assumed to be a spherical Lambertian reflector of uniform albedo, then the equations governing the irradiance E_a produced on a target surface element by radiant flux reflected from the earth can be determined, in terms of the parameters of figure 4-1, by making parametric substitutions into the equations of Appendix III. The equations thus defined are listed, in Appendix IV, as equations (IV-22) through (IV-50).

The irradiance E_{a_o}, on a target surface element which is oriented so that its normal $\hat{n}$ is in the direction toward the center of the earth

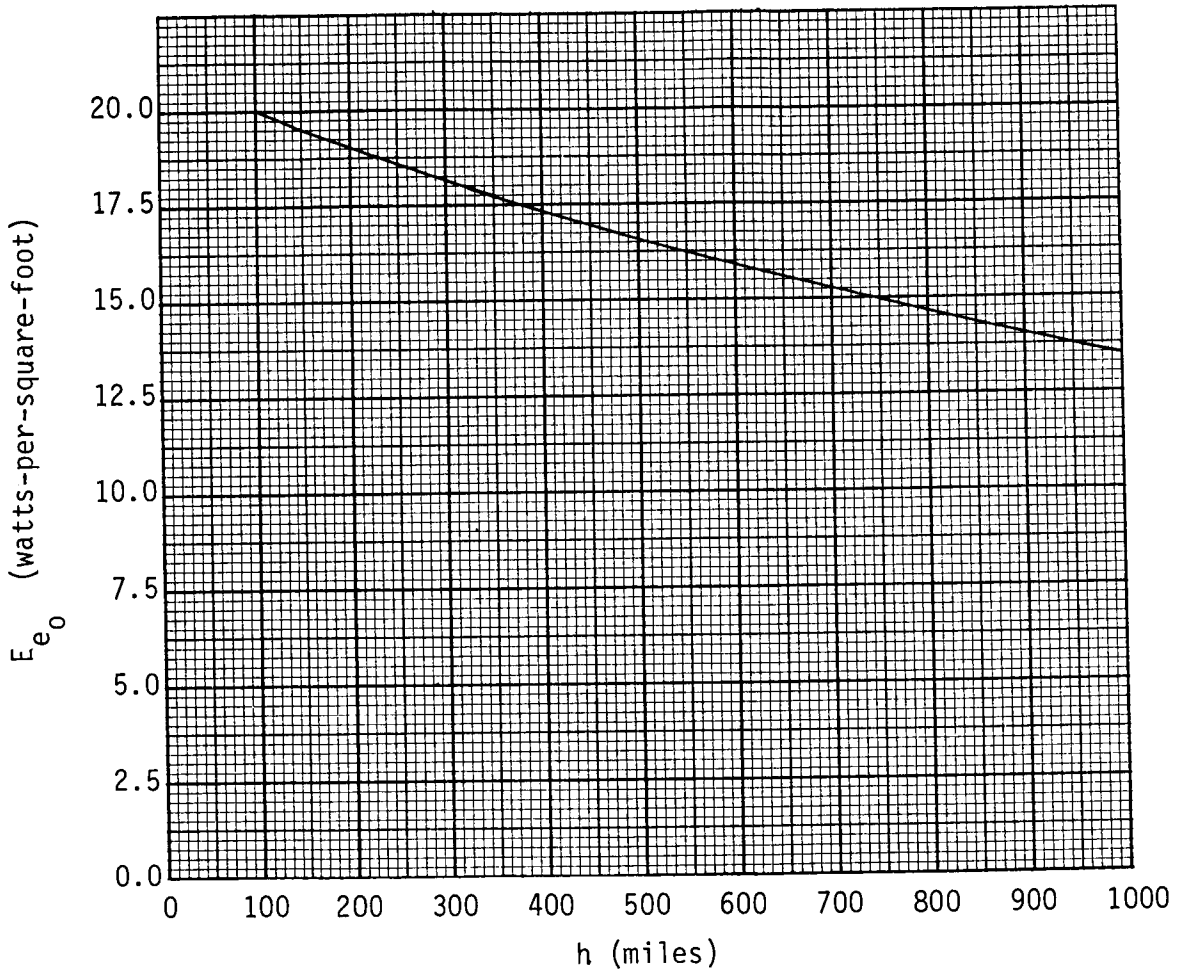

Figure 4-3. E_{e_o} versus h

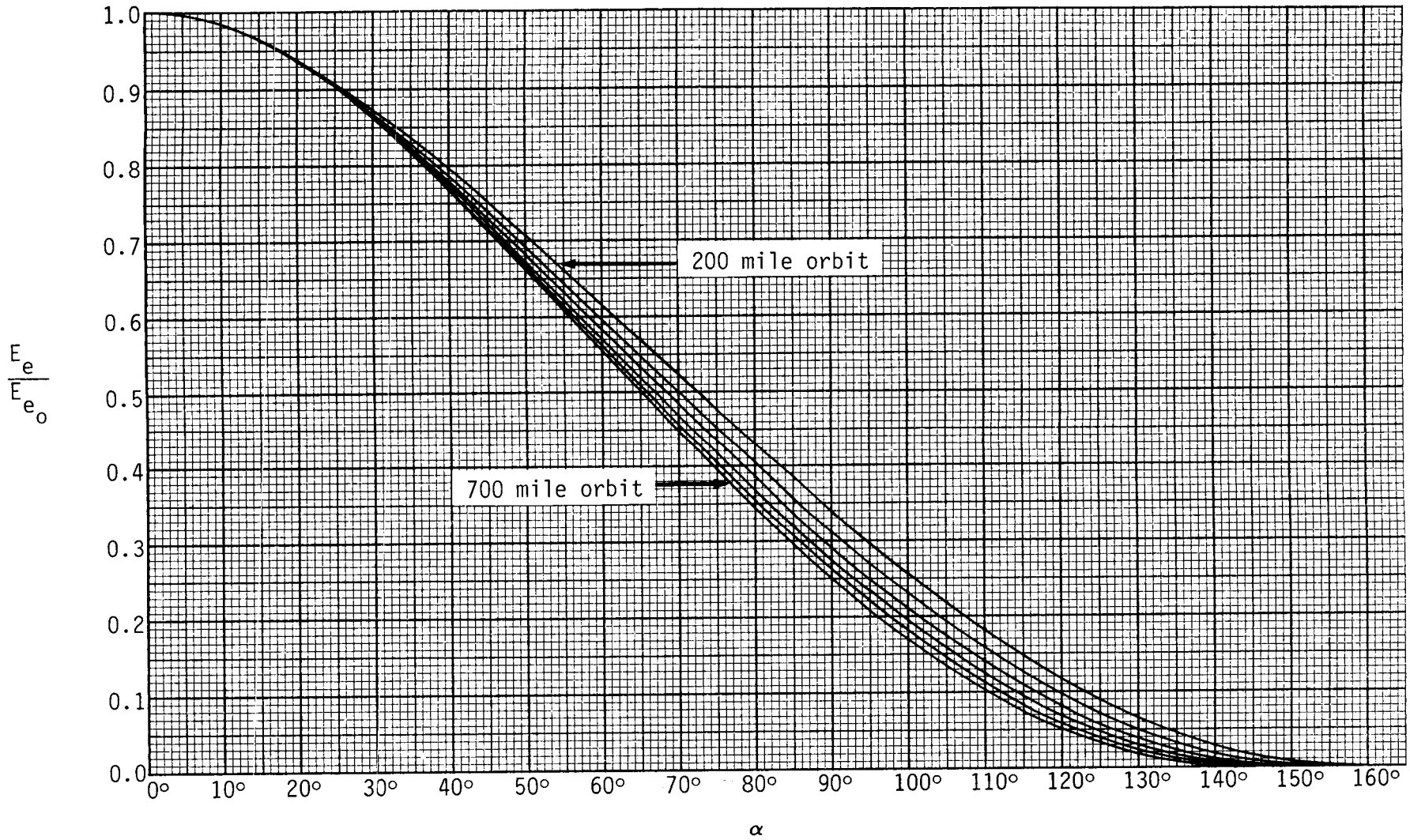

Figure 4-4. $\frac{E_e}{E_{e_o}}$ versus α for h from 200 miles to 700 miles in 100-mile increments

($\alpha = 0$), was calculated as a function of the angle γ at the center of the earth between the directions to the sun and to the target surface element, using the computer program ORBVAR, and is plotted versus γ in figure 4-5 for orbital altitudes from 100 to 1000 miles in 100-mile increments.

Total Irradiance Produced by Radiant Flux Emanating from the Earth

The total irradiance $E_{e_o} + E_{a_o}$ produced, by the radiant flux reflected and/or emitted by the earth, on a target surface element which is oriented so that its normal $\hat{n}$ is in the direction toward the center of the earth, was calculated as a function of the angle γ at the center of the earth between the directions to the sun and to the target surface element, using the computer program ORBVAR, and is plotted versus γ in figure 4-6 for orbital altitudes from 100 to 1000 miles in 100-mile increments. Using the computer program SPACE, the normalized total irradiance $\frac{E_a + E_e}{E_{a_o} + E_{e_o}}$ was calculated as a function of the angle α between the normal $\hat{n}$ to the target surface element and the direction to the center of the earth and is plotted versus α, for $\gamma = 0°$ and orbital altitudes from 200 to 700 miles in 100-mile increments, in figures 4-7 through 4-12 and, for $\gamma = 90°$ and orbital altitudes from 200 to 700 miles in 100-mile increments, in figures 4-13 through 4-18.

The ratio $\frac{E_{a_o}}{E_{e_o}}$ between the irradiance produced by the two spectral components of the radiant flux emanating from the earth was also calculated and is plotted versus γ, in figure 4-19, for orbital altitudes of 100 and 1000 miles.

The field half-angle Φ subtended by the earth was calculated as a function of the orbital altitude h, using the equation

$$\Phi = \arctan\left(\frac{R}{\sqrt{2Rh + h^2}}\right) \tag{4-6}$$

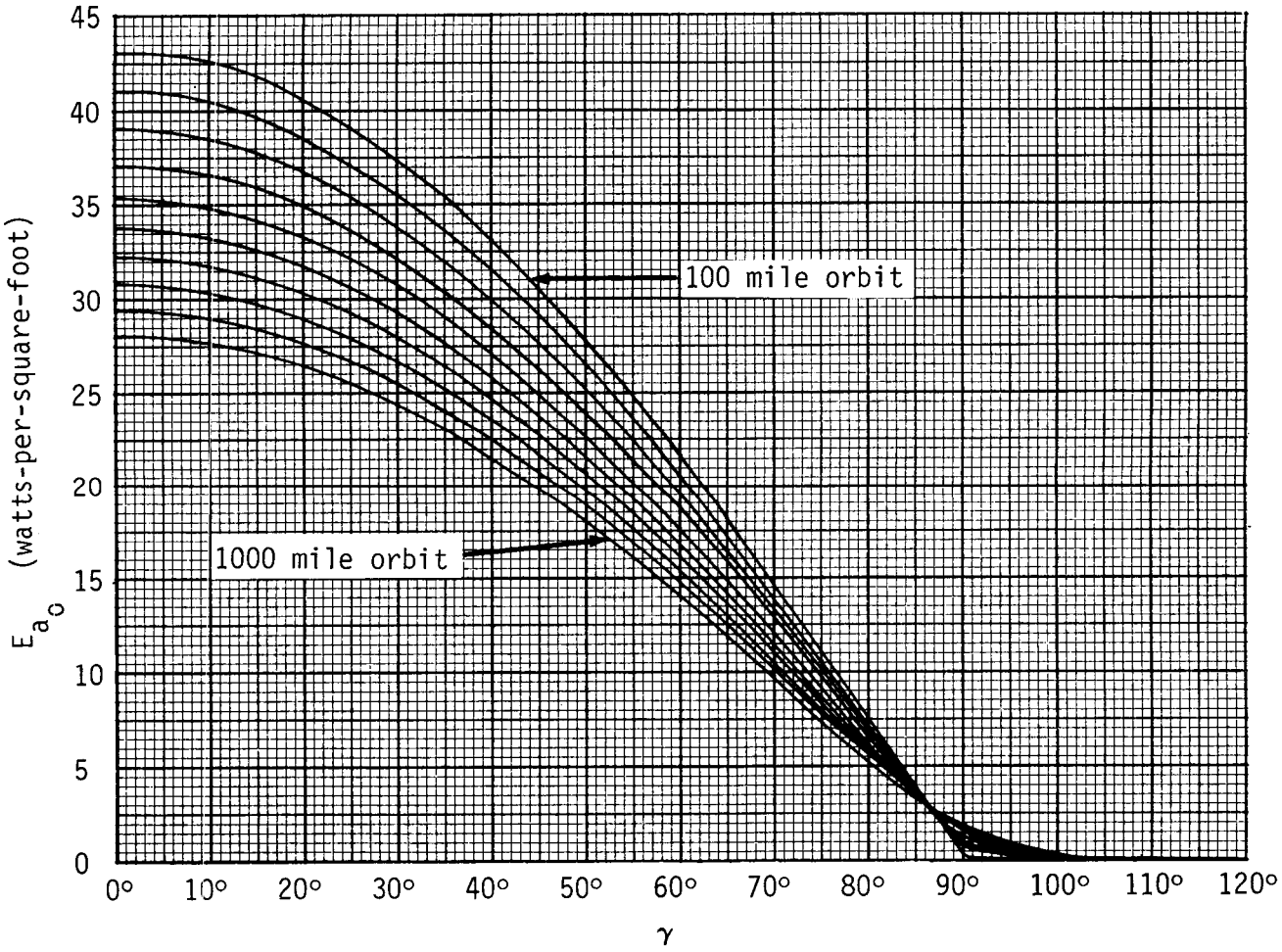

Figure 4-5. E_{a_o} versus γ for h from 100 miles to 1000 miles in 100-mile increments.

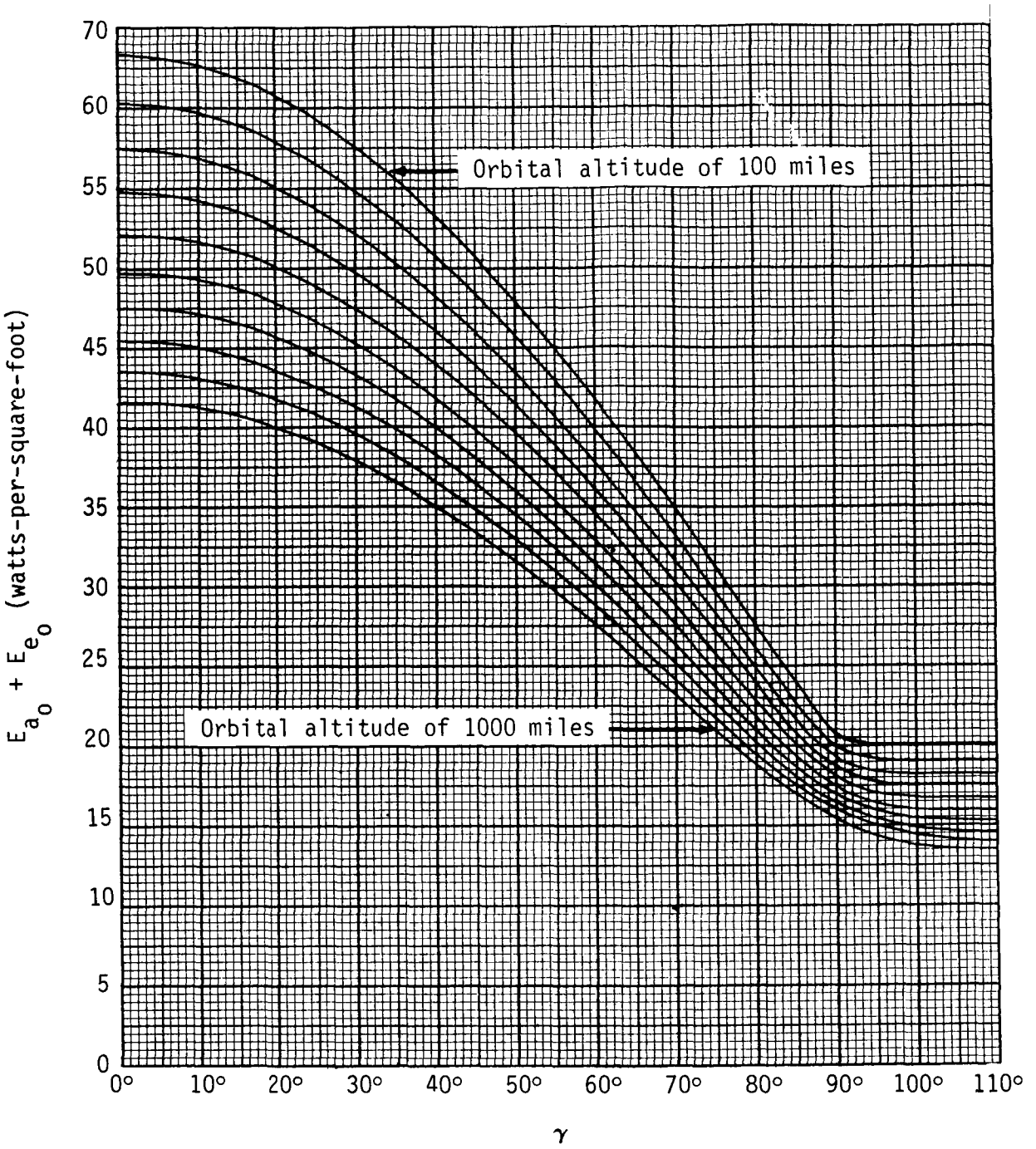

Figure 4-6. $E_{a_o} + E_{e_o}$ versus γ for h from 100 miles to 1000 miles in 100-mile increments.

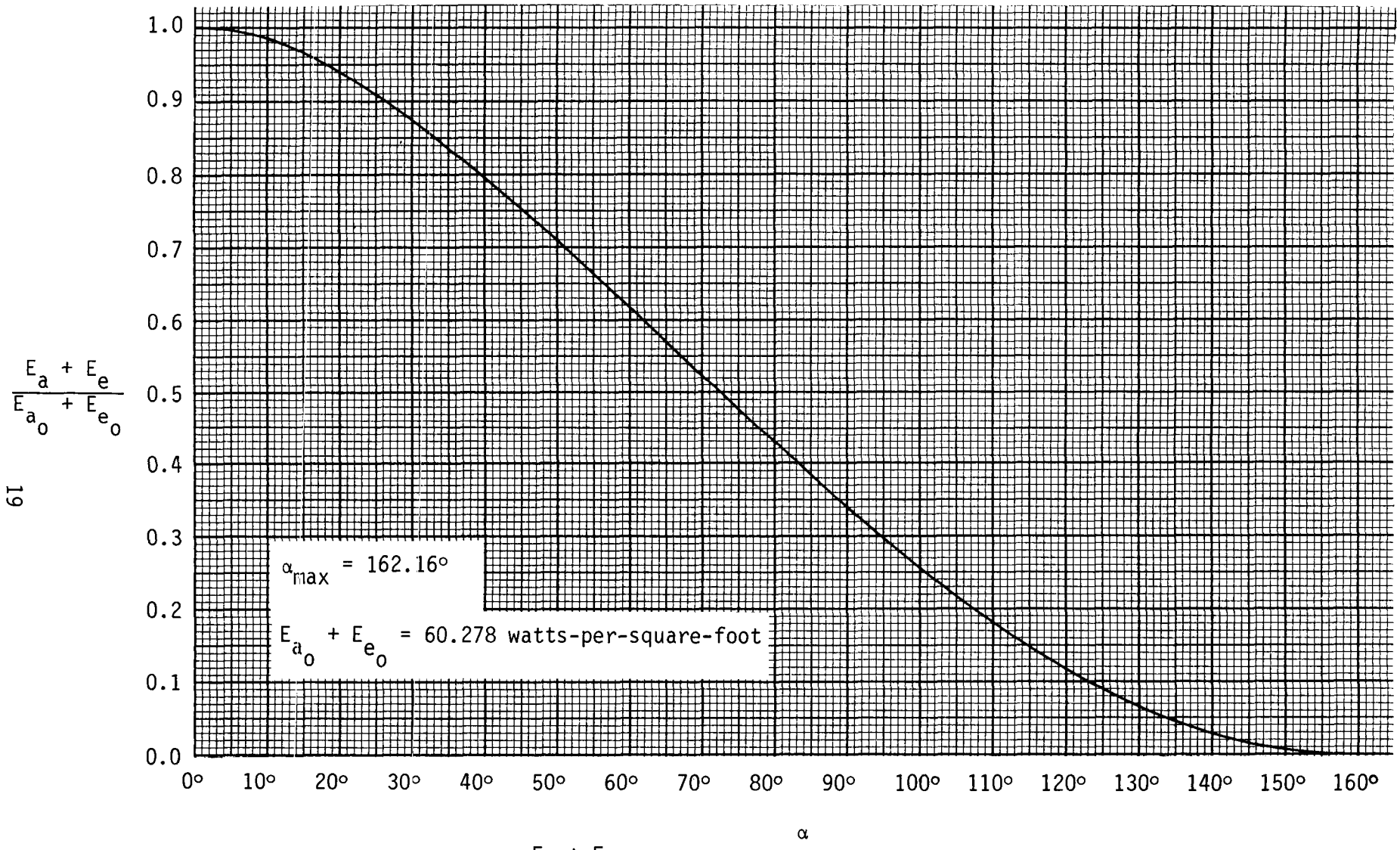

Figure 4-7. $\frac{E_a + E_e}{E_{a_o} + E_{e_o}}$ versus α when h = 200 miles and $\gamma = 0°$

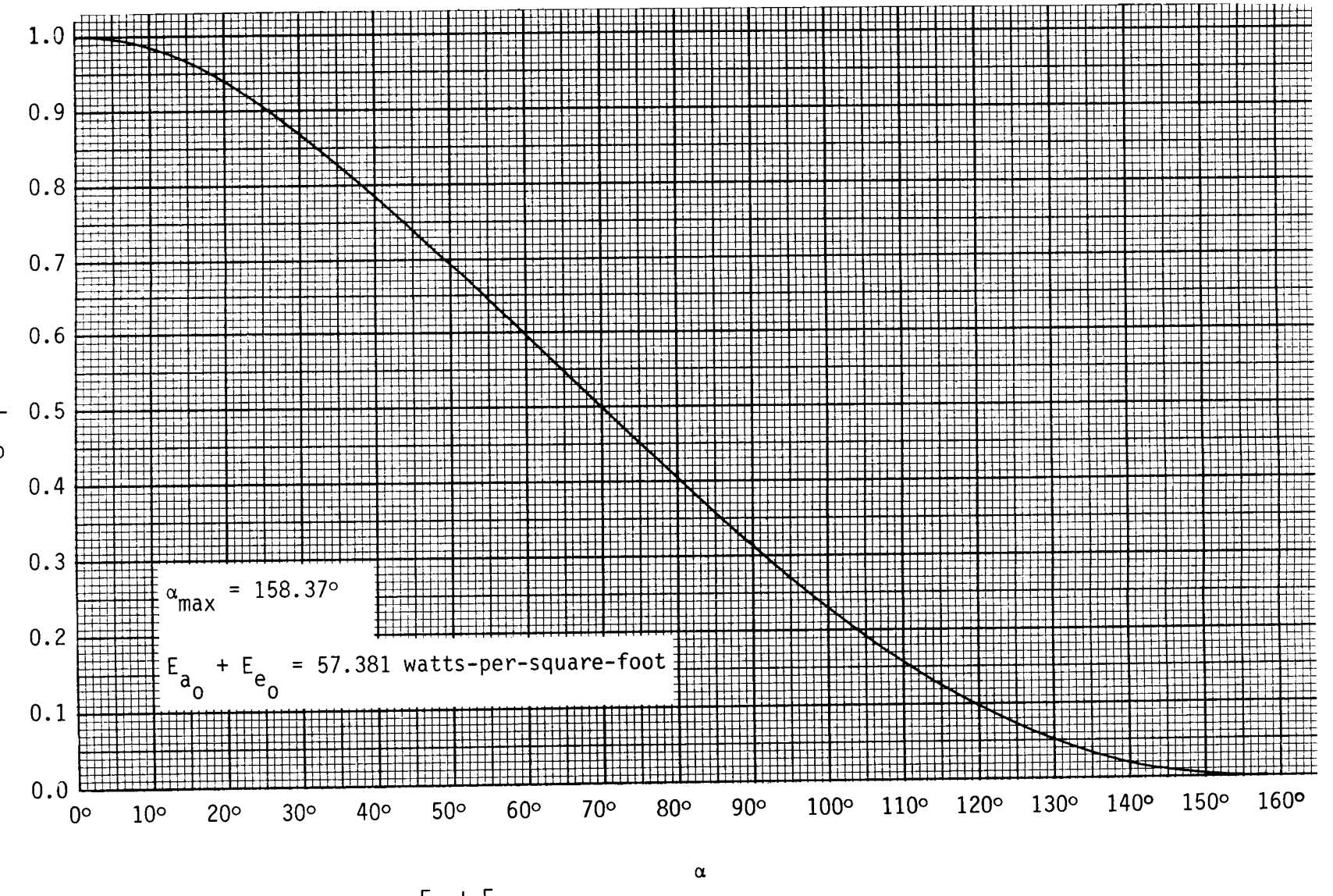

Figure 4-8. $\frac{E_a + E_e}{E_{a_o} + E_{e_o}}$ versus α when h = 300 miles and $\gamma = 0°$

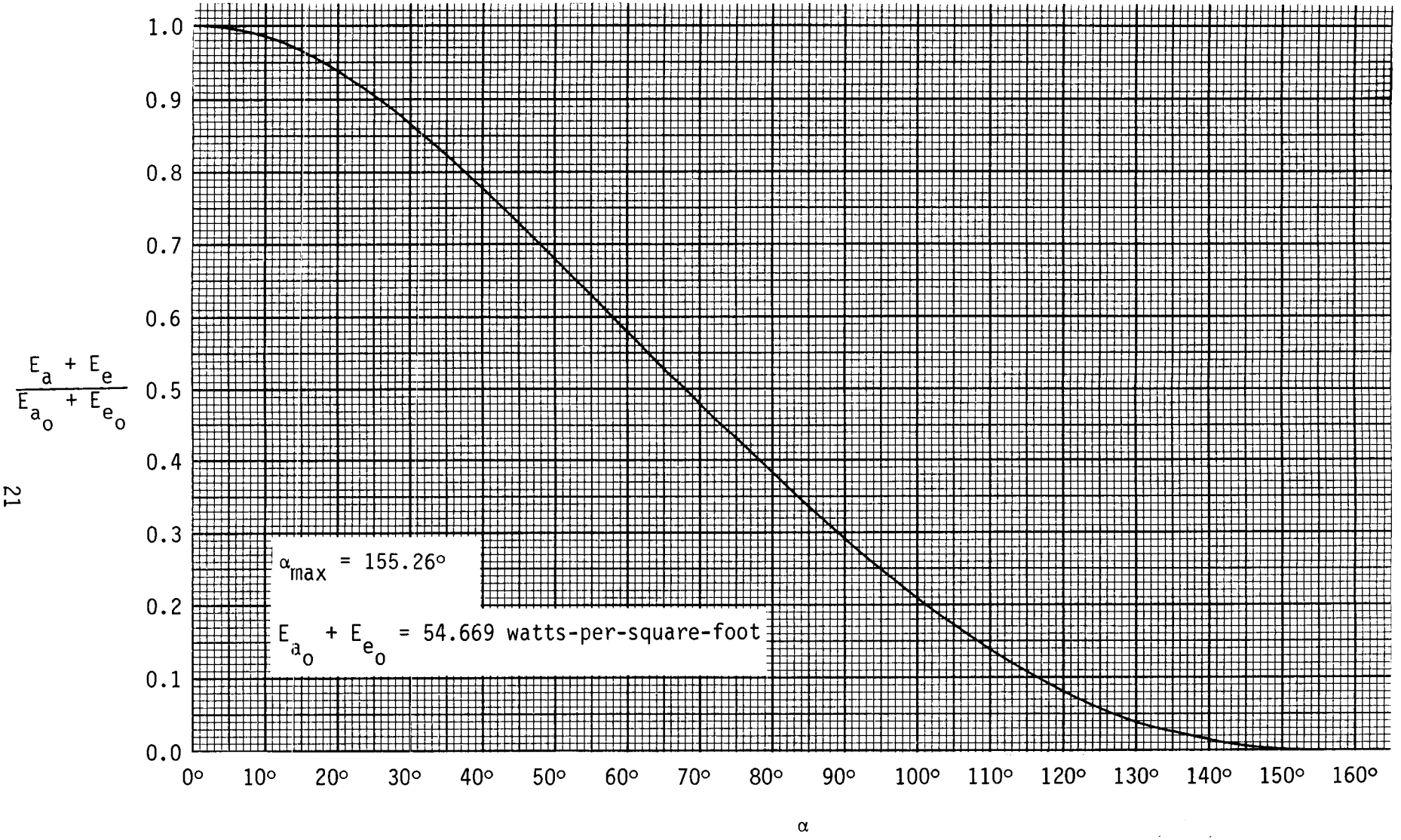

Figure 4-9. $\frac{E_a + E_e}{E_{a_o} + E_{e_o}}$ versus α when h = 400 miles and γ = 0°

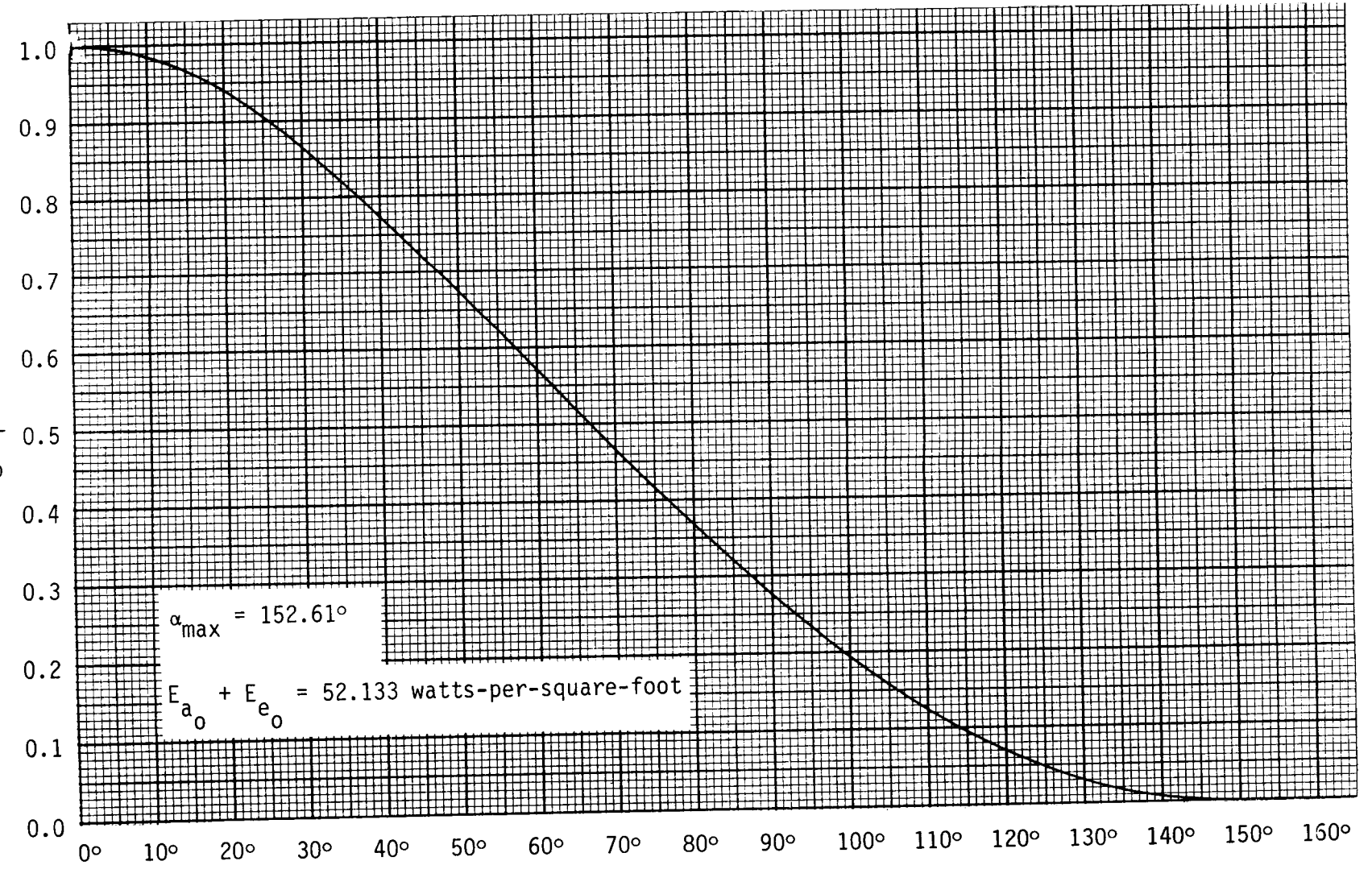

Figure 4-10. $\frac{E_a + E_e}{E_{a_o} + E_{e_o}}$ versus α when h = 500 miles and $\gamma = 0°$

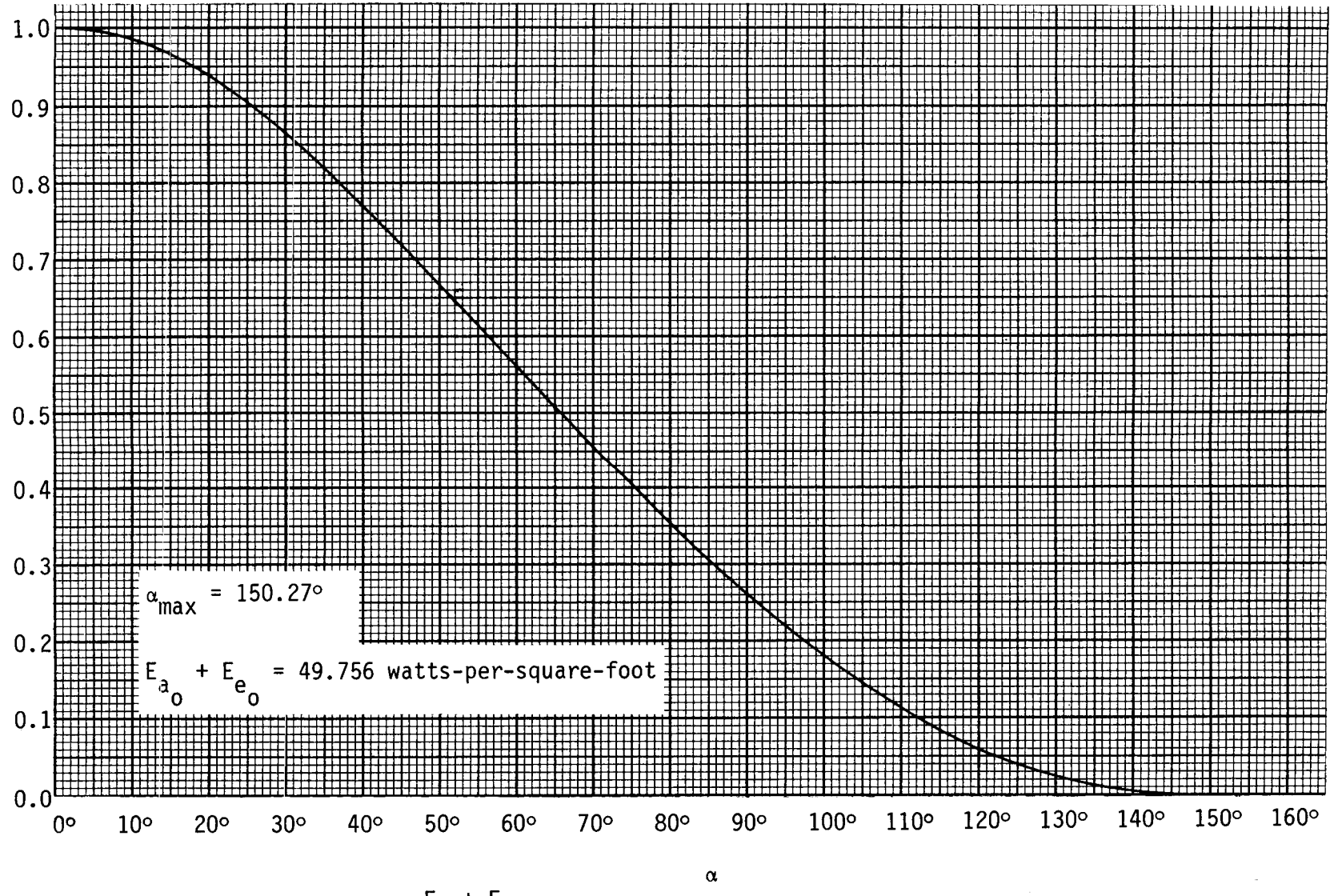

Figure 4-11. $\frac{E_a + E_e}{E_{a_o} + E_{e_o}}$ versus α when h = 600 miles and $\gamma = 0°$

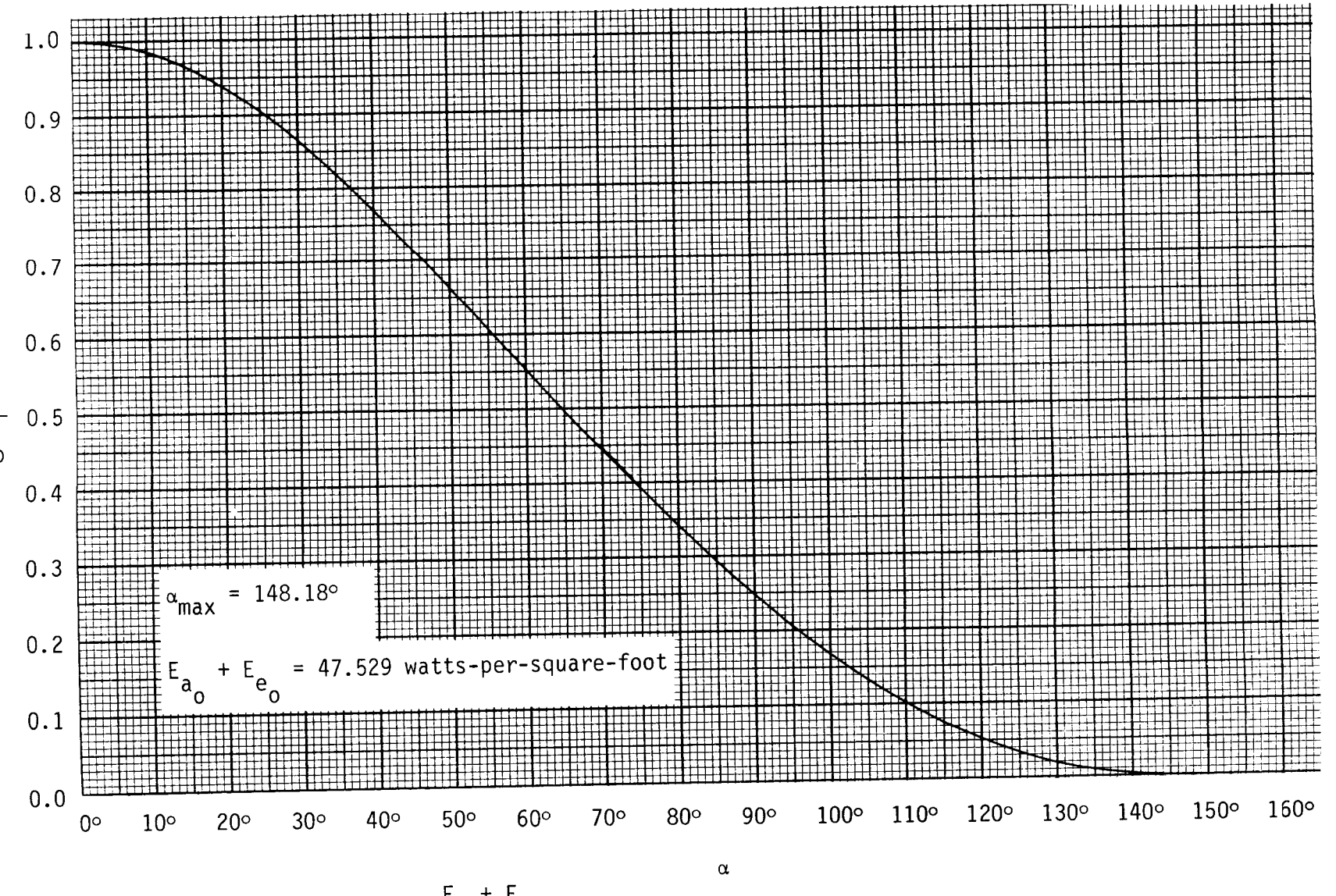

Figure 4-12. $\frac{E_a + E_e}{E_{a_o} + E_{e_o}}$ versus α when h = 700 miles and $\gamma = 0°$

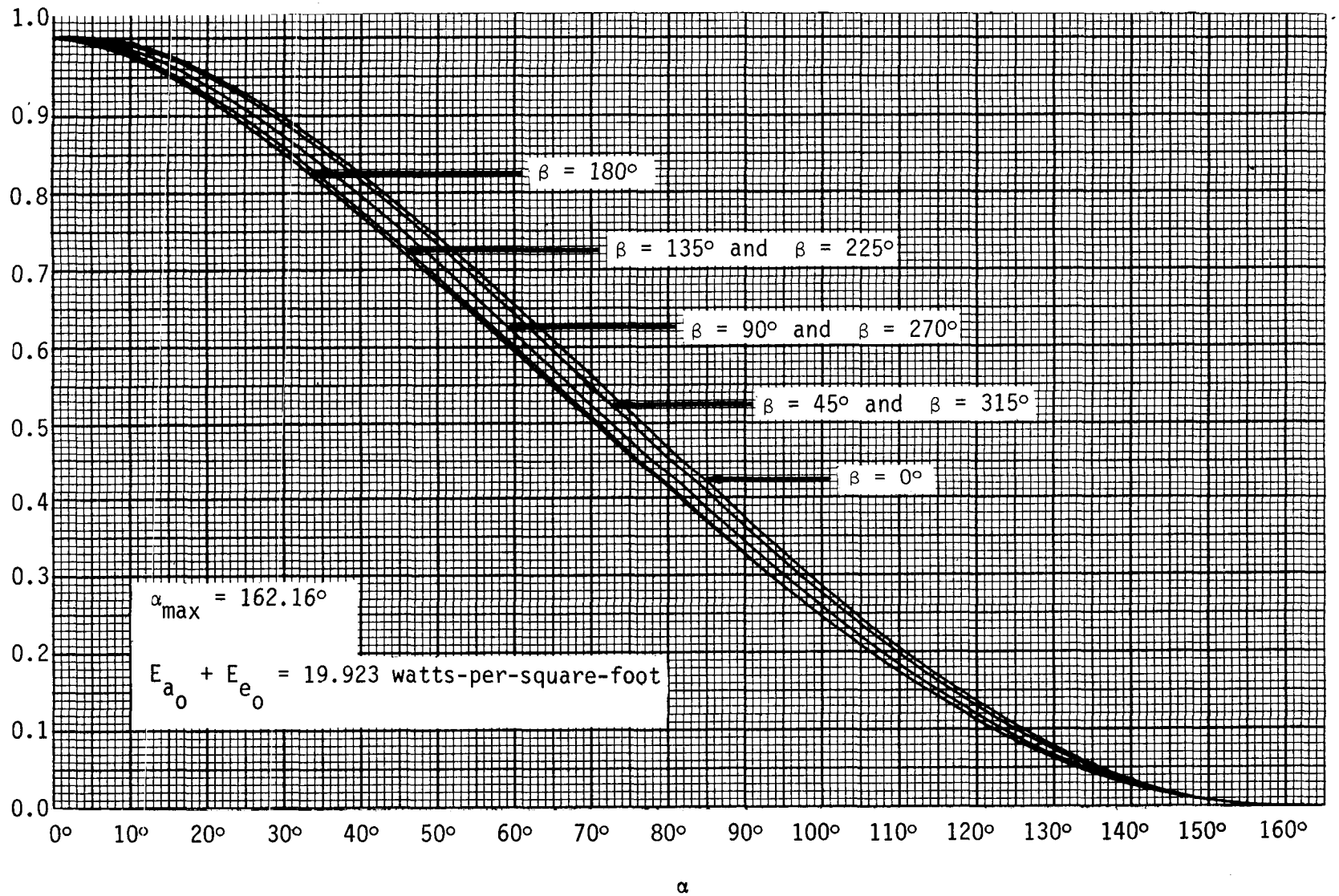

Figure 4-13. $\frac{E_a + E_e}{E_{a_o} + E_{e_o}}$ versus α when h = 200 miles and $\gamma = 90°$

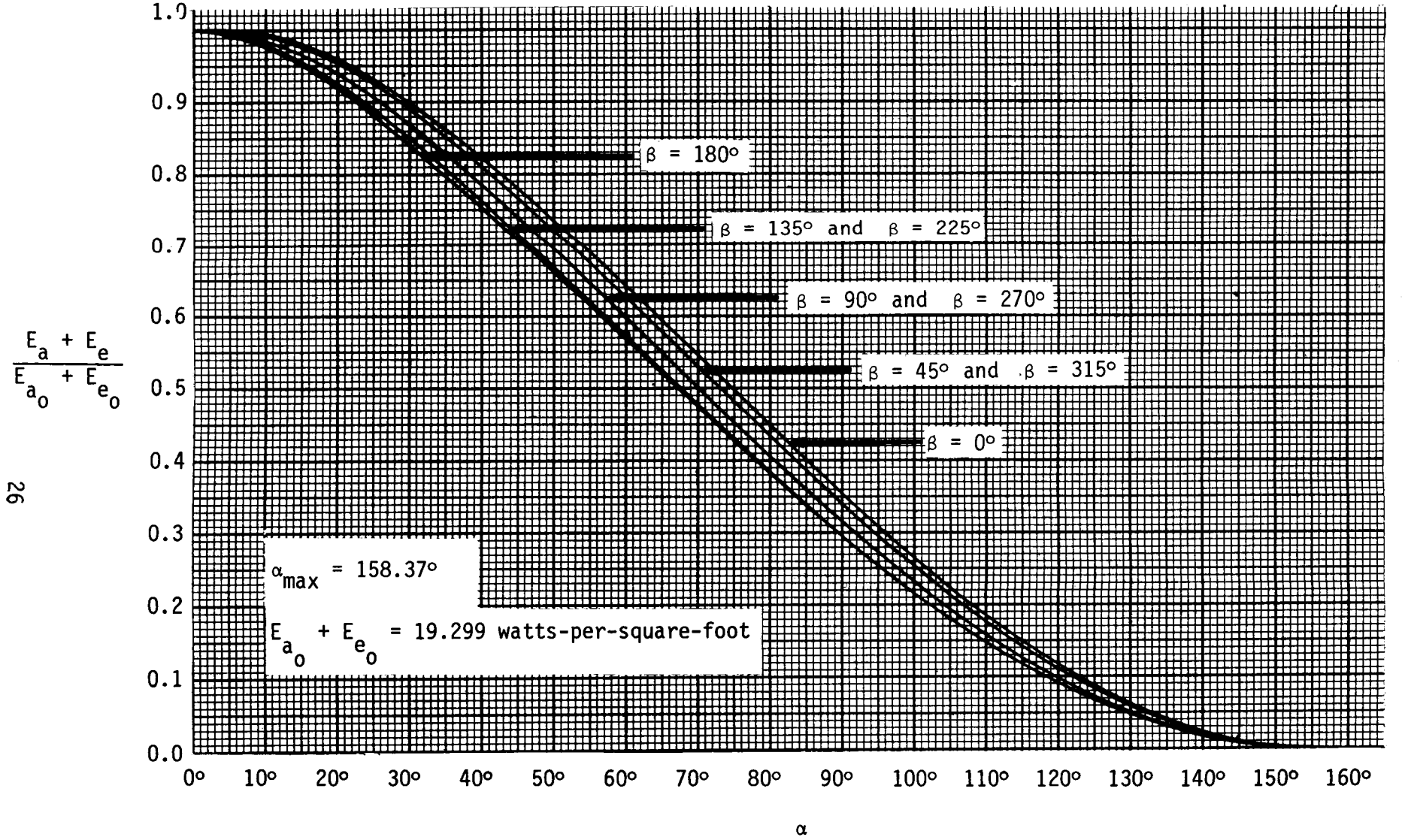

Figure 4-14. $\frac{E_a + E_e}{E_{a_o} + E_{e_o}}$ versus α when h = 300 miles and ϕ = 90°

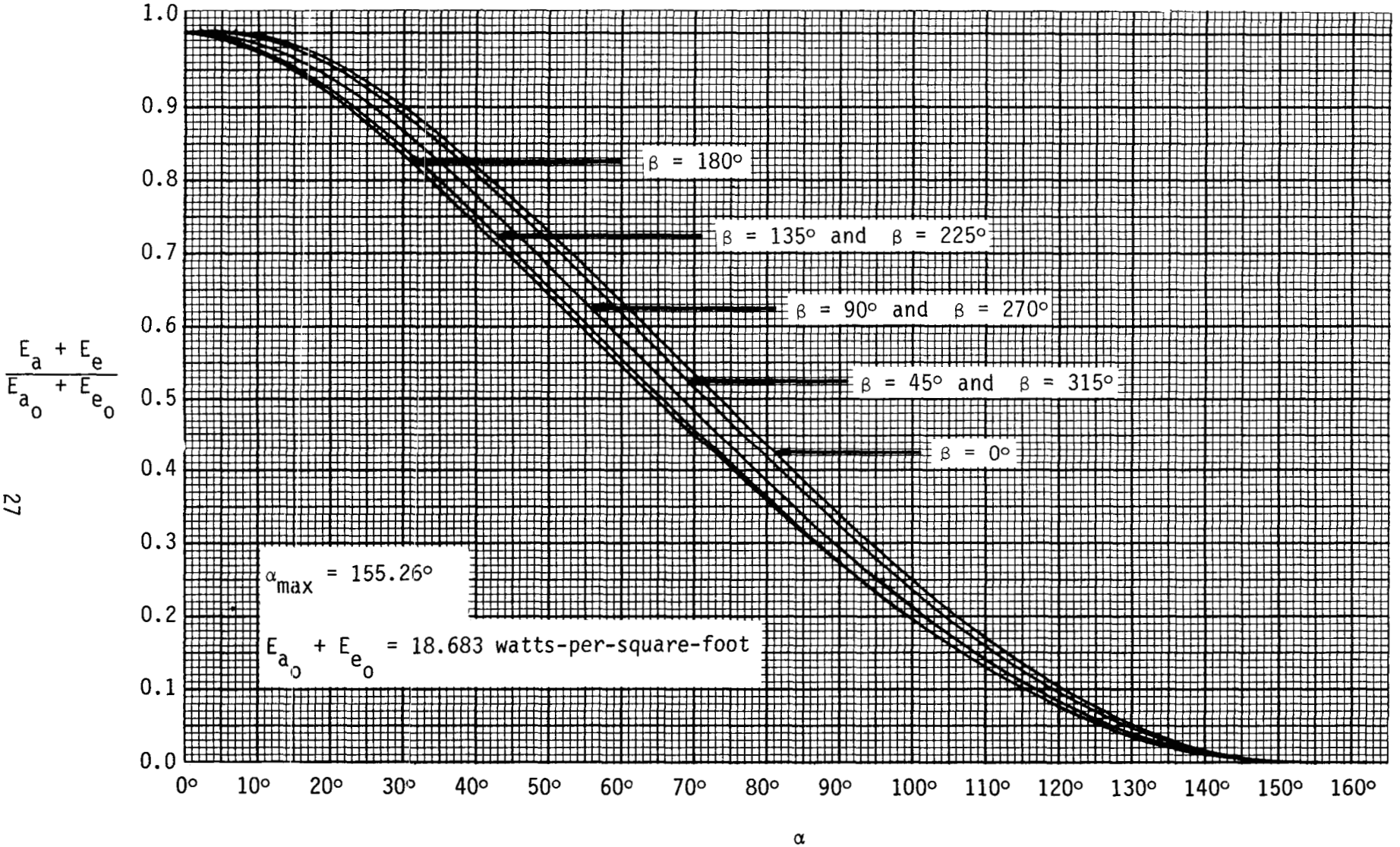

Figure 4-15. $\frac{E_a + E_e}{E_{a_o} + E_{e_o}}$ versus α when h = 400 miles and γ = 90°

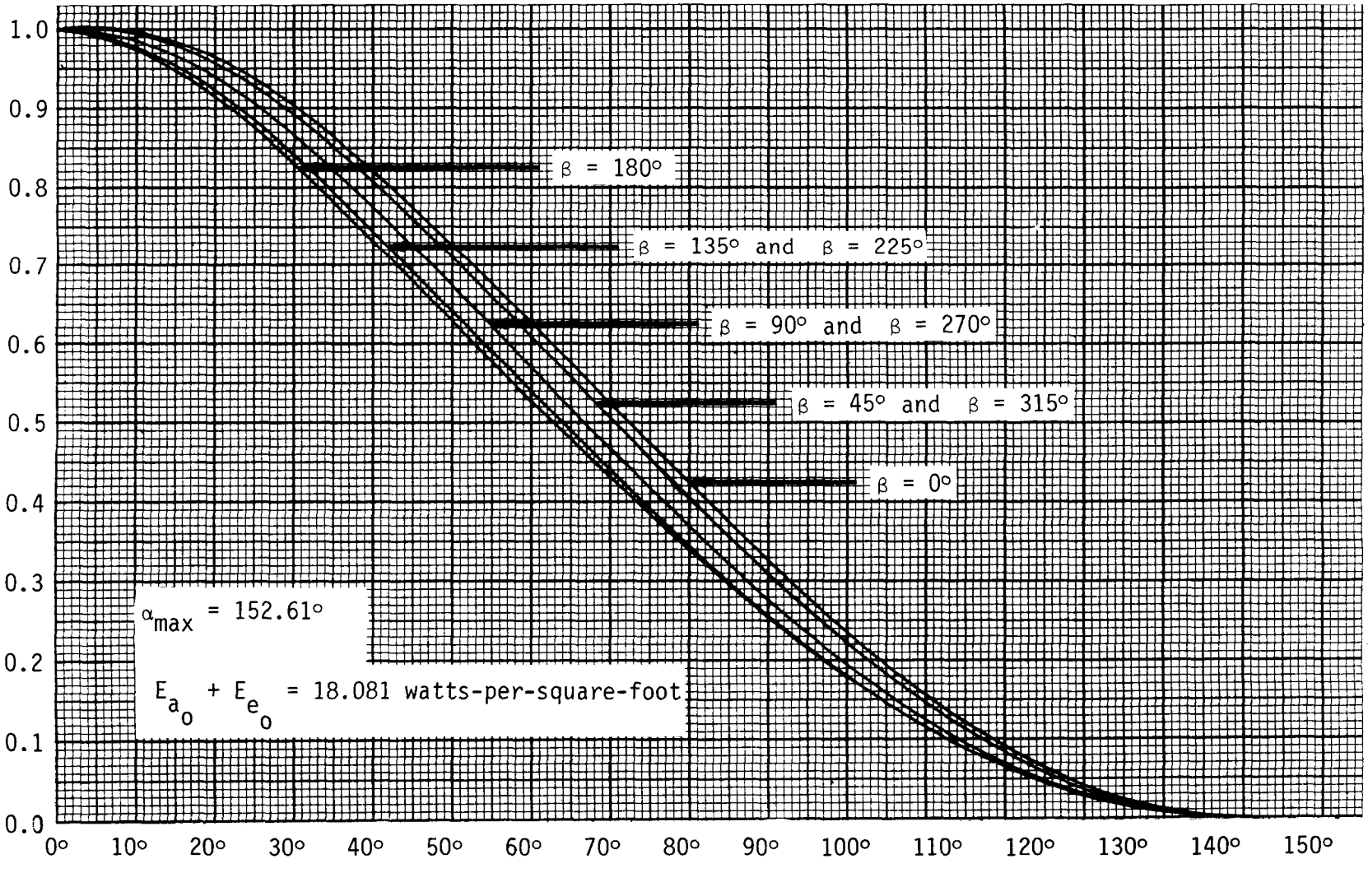

Figure 4-16. $\frac{E_a + E_e}{E_{a_o} + E_{e_o}}$ versus α when h = 500 miles and γ = 90°

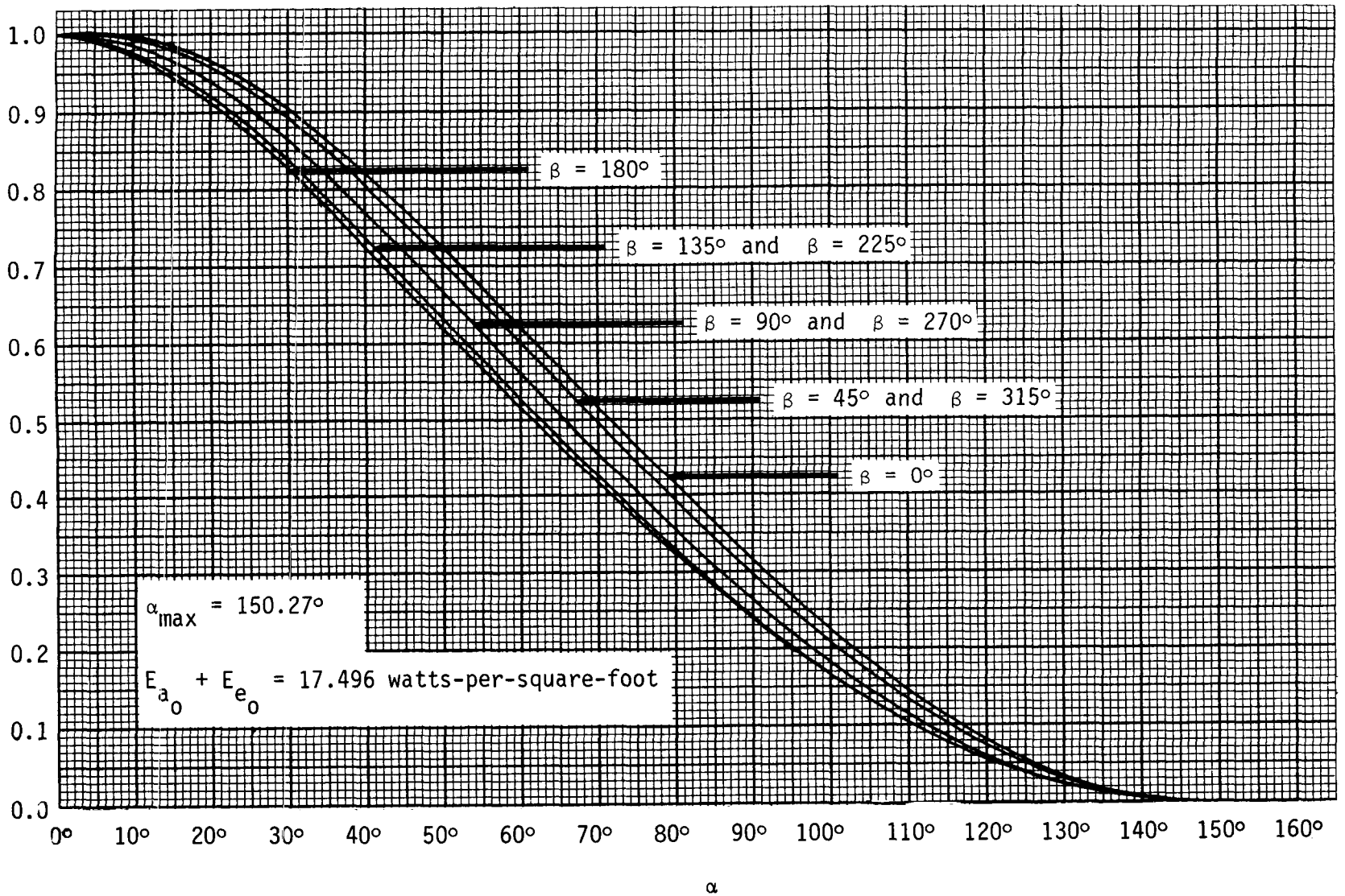

Figure 4-17. $\frac{E_a + E_e}{E_{a_o} + E_{e_o}}$ versus α when h = 600 miles and $\gamma = 90°$

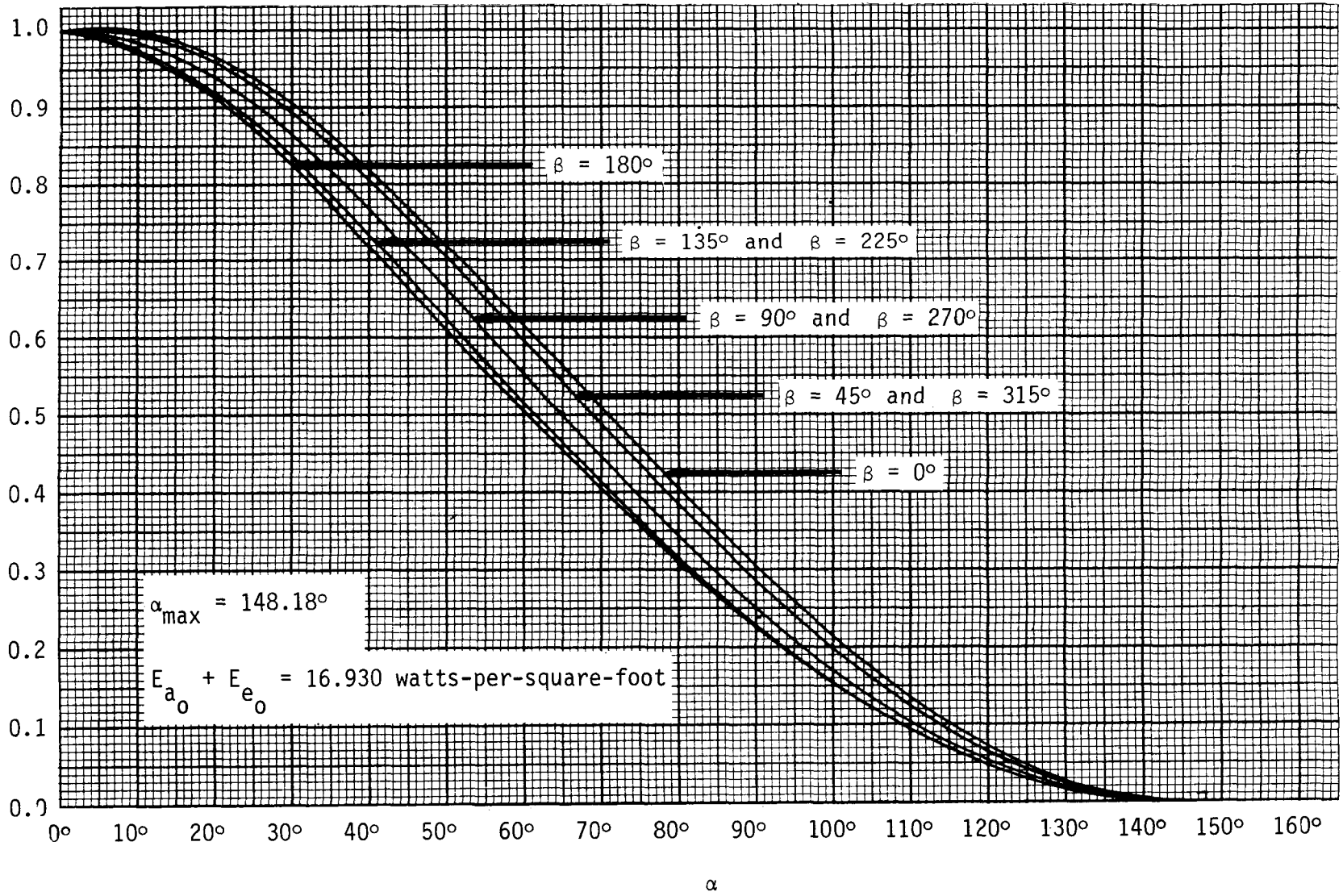

Figure 4-18. $\frac{E_a + E_e}{E_{a_o} + E_{e_o}}$ versus α when h = 700 miles and $\gamma = 90°$

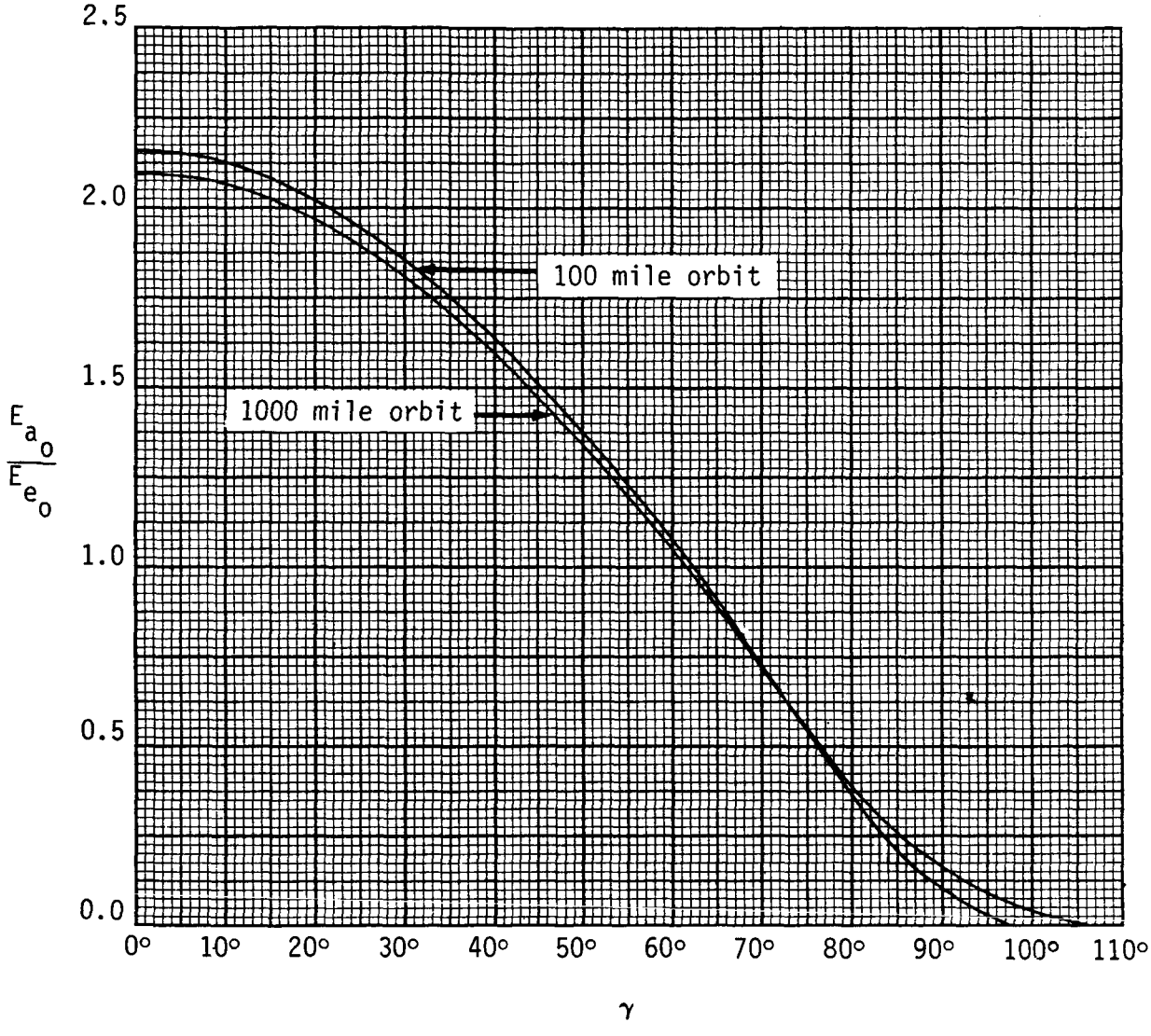

Figure 4-19. $\frac{E_{a_o}}{E_{e_o}}$ versus γ for h = 100 miles and h = 1000 miles

The field half-angle Φ and the total field angle 2Φ subtended by the earth are plotted versus h in figure 4-20. Finally, the average radiant emittance W_{ave} of the earth's surface, as seen from various target locations, was calculated using the relationship

$$W_{ave} = \frac{E_{e_o} + E_{a_o}}{\sin^2\Phi} \tag{4-7}$$

and is plotted versus γ, for orbital altitudes of 100 and 1000 miles, in figure 4-21.

Total Irradiance Experienced by a Target Surface Element in the Vicinity of the Earth

The total irradiance E experienced by a target surface element in the vicinity of the earth is given by

$$E = E_a + E_e + E_s \tag{4-8}$$

The total irradiance E was calculated as a function of α, using the computer program SPACE, at various locations (h, γ) in the vicinity of the earth (h is the orbital altitude; γ is the angle, at the center of the earth, between the directions to the sun and to the target surface element). E is plotted versus α, for h = 200 miles and $\gamma = 0°$ in figure 4-22; for h = 600 miles and $\gamma = 0°$ in figure 4-23; for h = 200 miles and $\gamma = 90°$ in figure 4-24; and for h = 600 miles and $\gamma = 90°$ in figure 4-25. If a spherical spacecraft was located at the position defined by the values of h and γ noted for each of these figures, then the plots represent the irradiance distribution on the surface of the spacecraft along the intersection between the sphere and the plane which contains the centers of the earth, the sphere, and the sun.

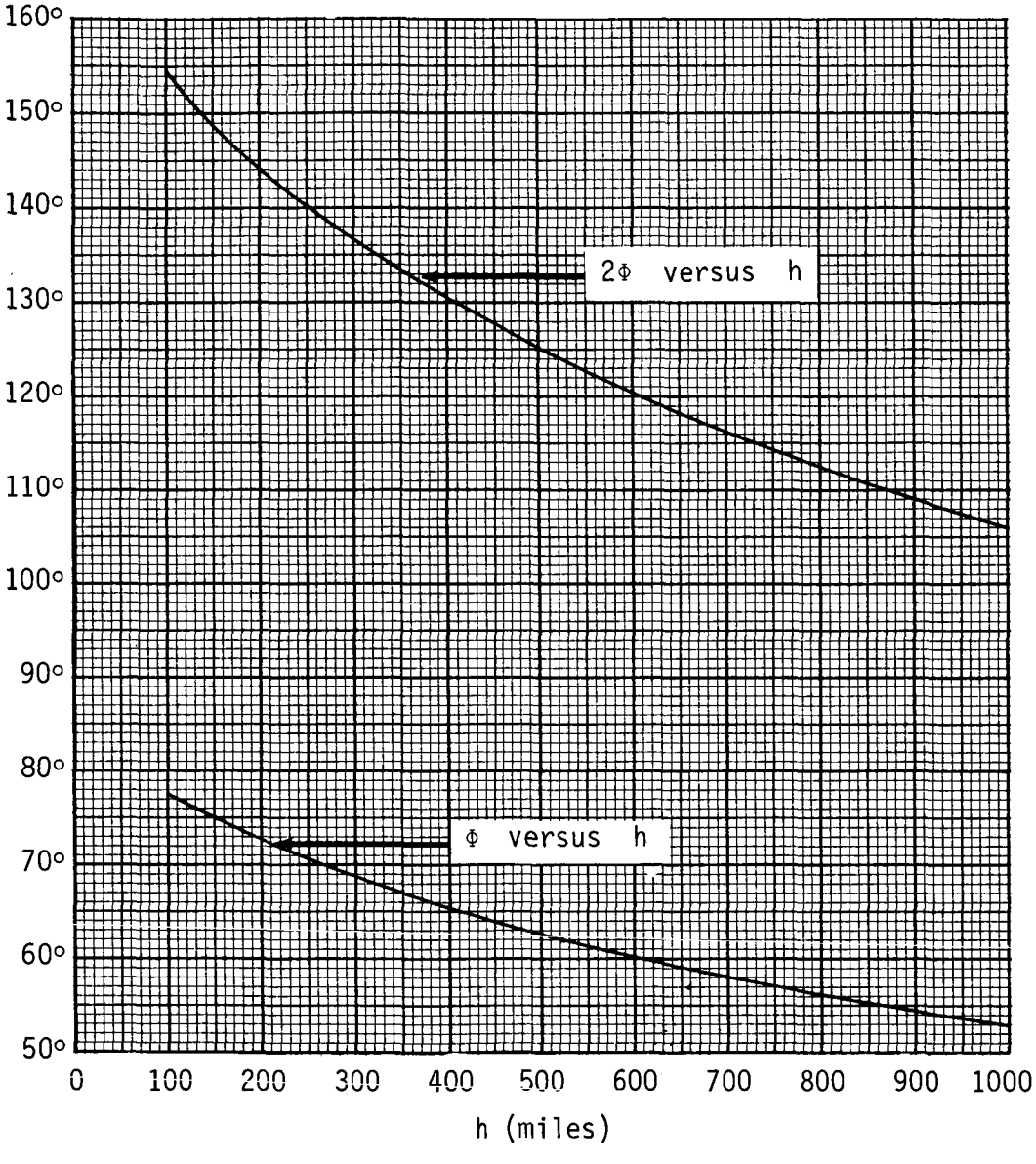

Figure 4-20. Φ and 2Φ versus h

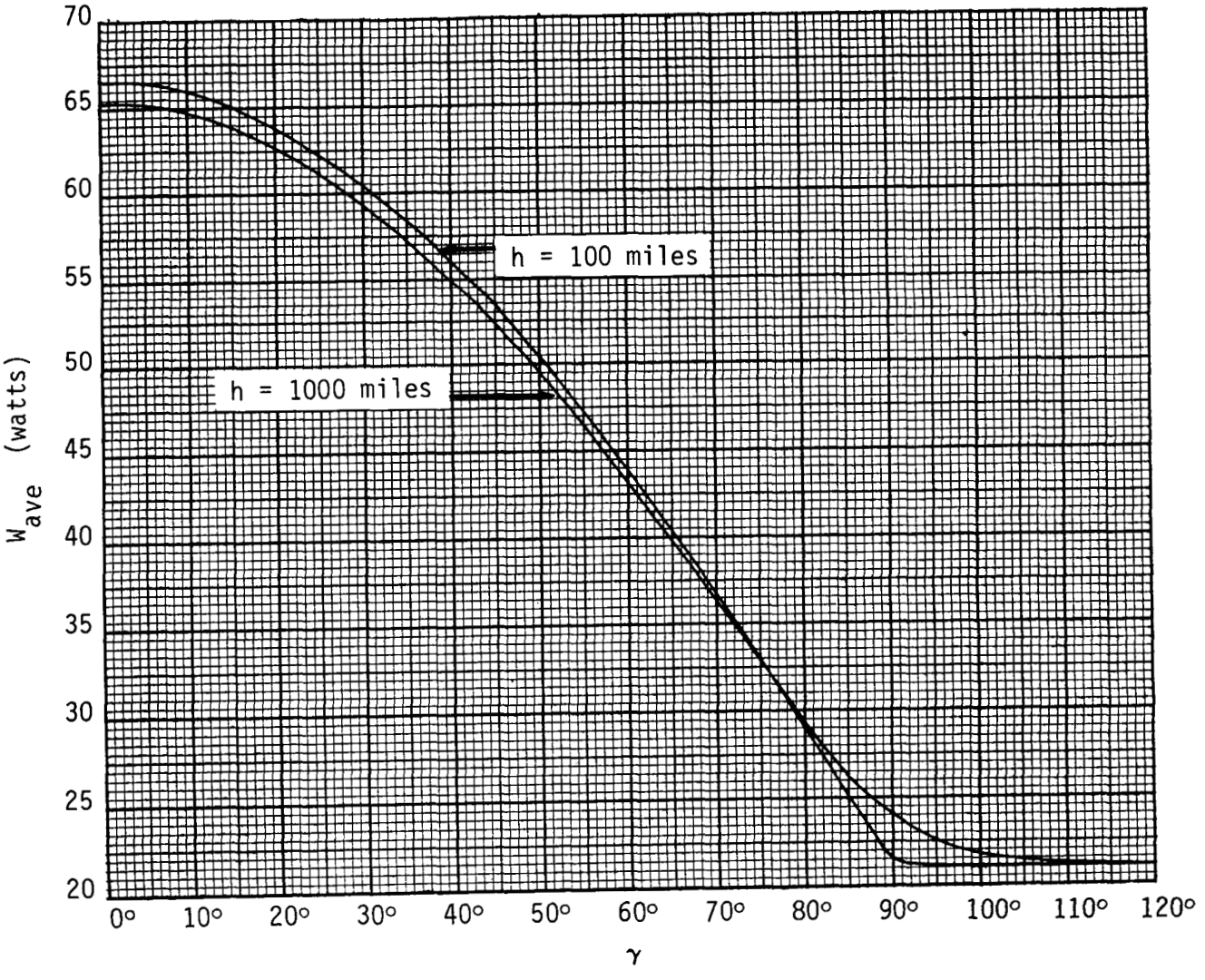

Figure 4-21. W_{ave} versus γ for h = 100 miles and h = 1000 miles

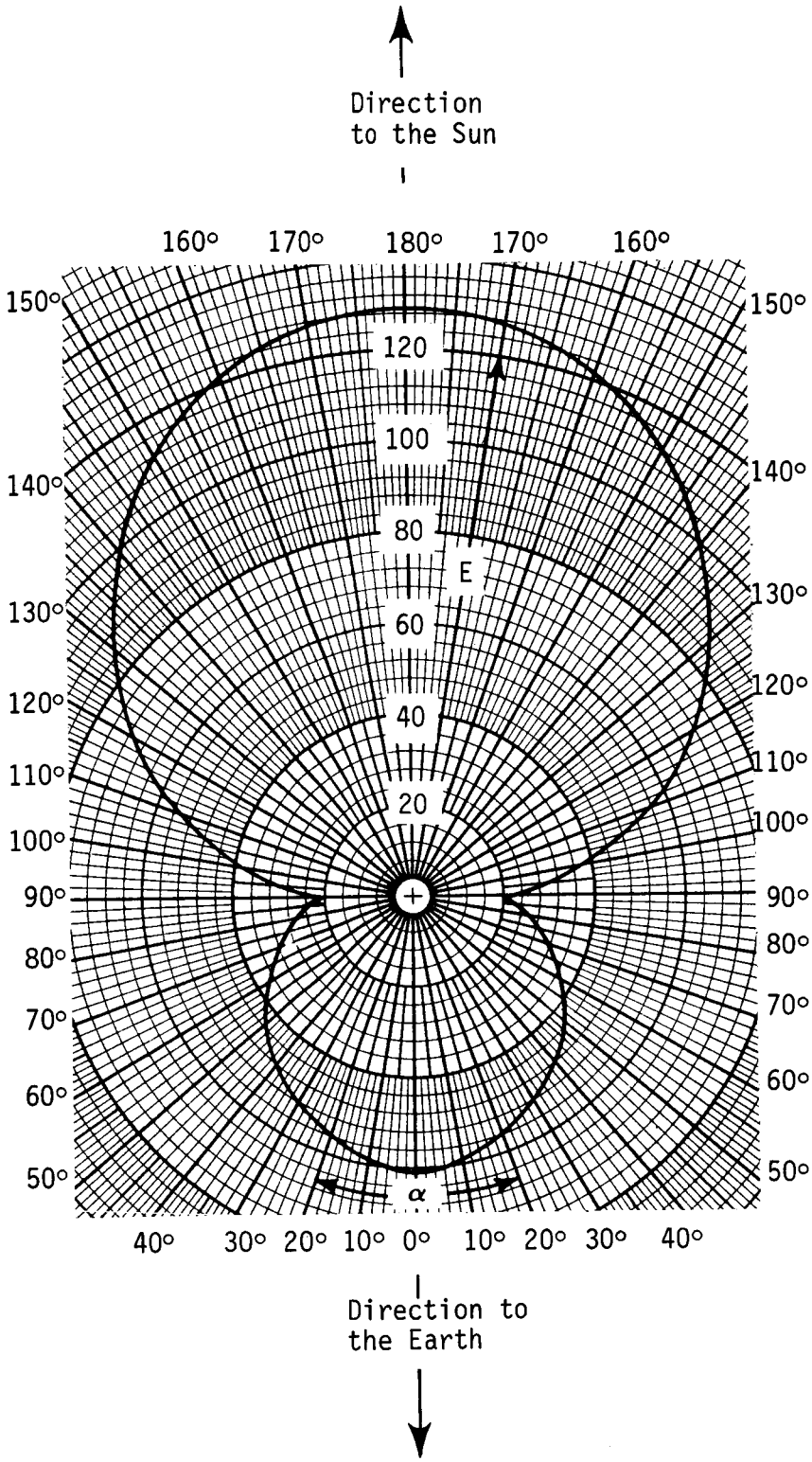

Figure 4-22. E (watts-per-square-foot) versus α when h = 200 miles and γ = 0°

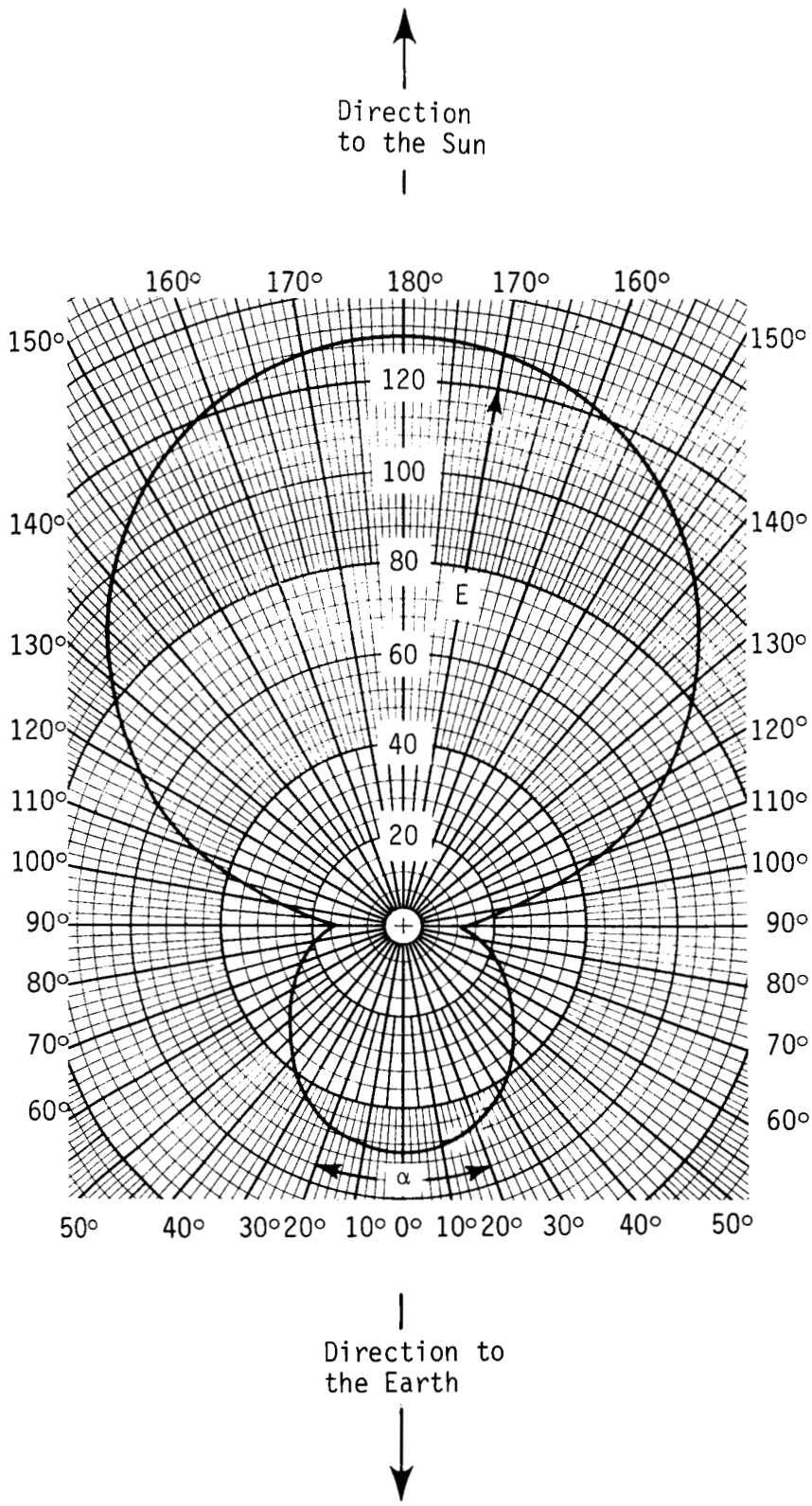

Figure 4-23. E (watts-per-square-foot) versus α when h = 600 miles and γ = 0°

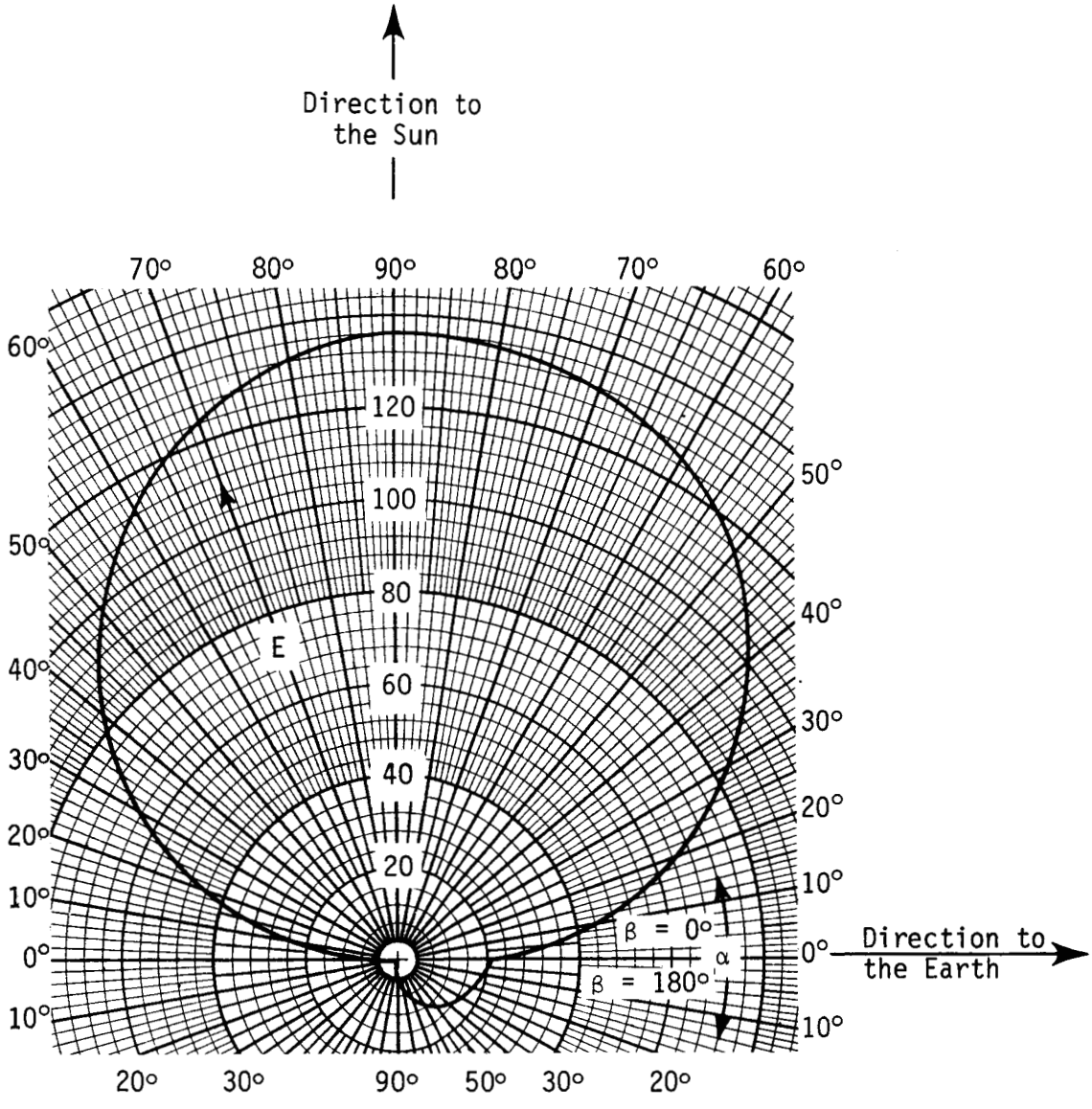

Figure 4-24. E (watts-per-square-foot) versus α when h = 200 miles and γ = 90°

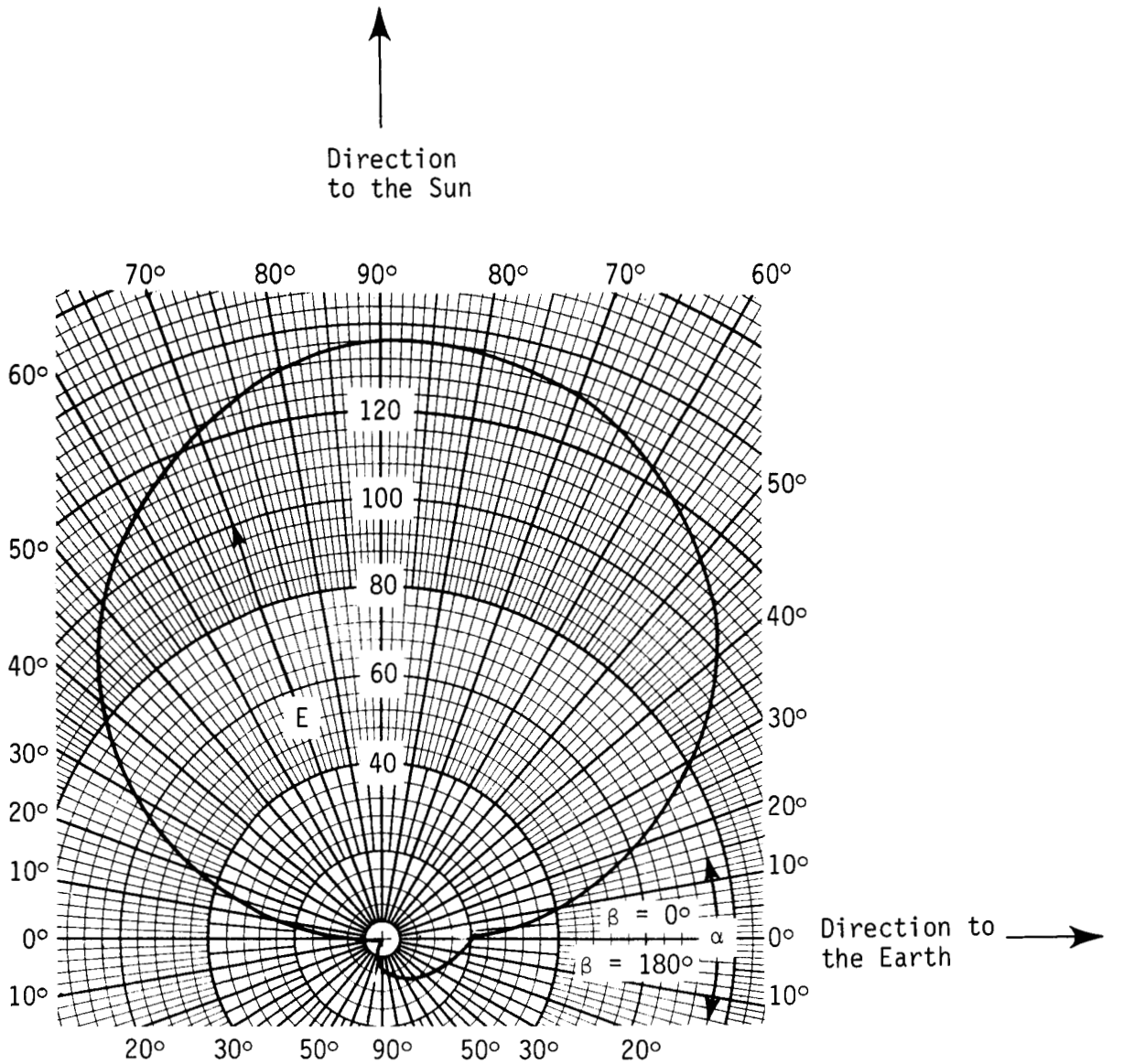

Figure 4-25. E (watts-per=square-foot) versus α when h = 600 miles and γ = 90°

CHARACTERISTICS OF THE PLANETARY RADIATION ENVIRONMENT SIMULATOR

The Simulation Concept

From the geometry of figure 4-1, it can be seen that, if a reference surface is inserted between the earth and the spacecraft so that all of the radiant flux emanating from the earth toward the spacecraft passes through this surface, it is impossible to determine, from the spacecraft, whether this radiant flux was emitted by the earth or by the reference surface. Thus, in order to exactly simulate the Planetary Radiation Environment of the earth within a finite volume, it is necessary to reproduce the distribution of the radiant flux emitted (by the earth) through every element of area on an appropriate reference surface. However, the Planetary Radiation Environment of the earth can be closely approximated by dividing the reference surface into many equal, small, finite areas and then by approximating the distribution of the radiant flux emitted through each area in the real case, with that produced by an appropriate source, optical-system combination. The simulated earth, rather than appearing as a continuous variably illuminated disk, will be seen as a pattern of many small spots of light which subtend the same total field, see figure 4-26.

In order to define the performance characteristics required of each source, optical-system combination (each module), consider the geometry represented schematically in figure 4-27, where: a multi-modular array of uncollimated projection systems has been located on the array reference surface so that the density D of the modules is uniform over the entire surface; the unit vector $\hat{r}$ defines the direction from the target surface element dT to an element of area dS on the array surface; R is the distance between dS and dT ; the radius vector $R\hat{r}$ locates dS with respect to dT ; and γ is the angle between $\hat{r}$ and the unit vector $\hat{m}$ normal to dS .

Defining $d\omega$ as the element of solid angle subtended by the element

Appearance of the Earth from Space (Continuous, Variably Illuminated Disk)

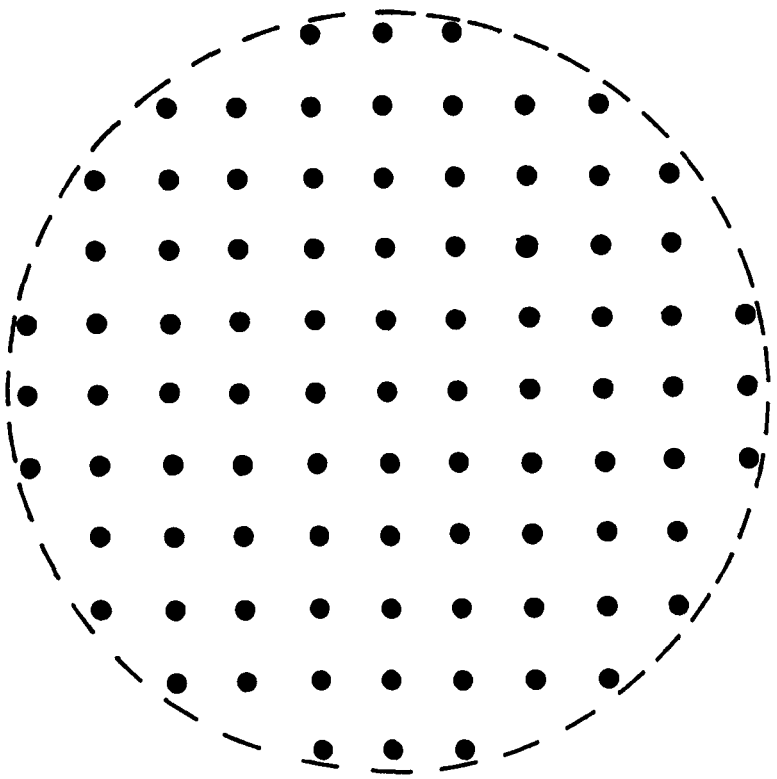

Appearance of the Simulated Earth (Many Small Spots of Light)

Figure 4-26. Schematic views of the real and the simulated appearance of the earth.

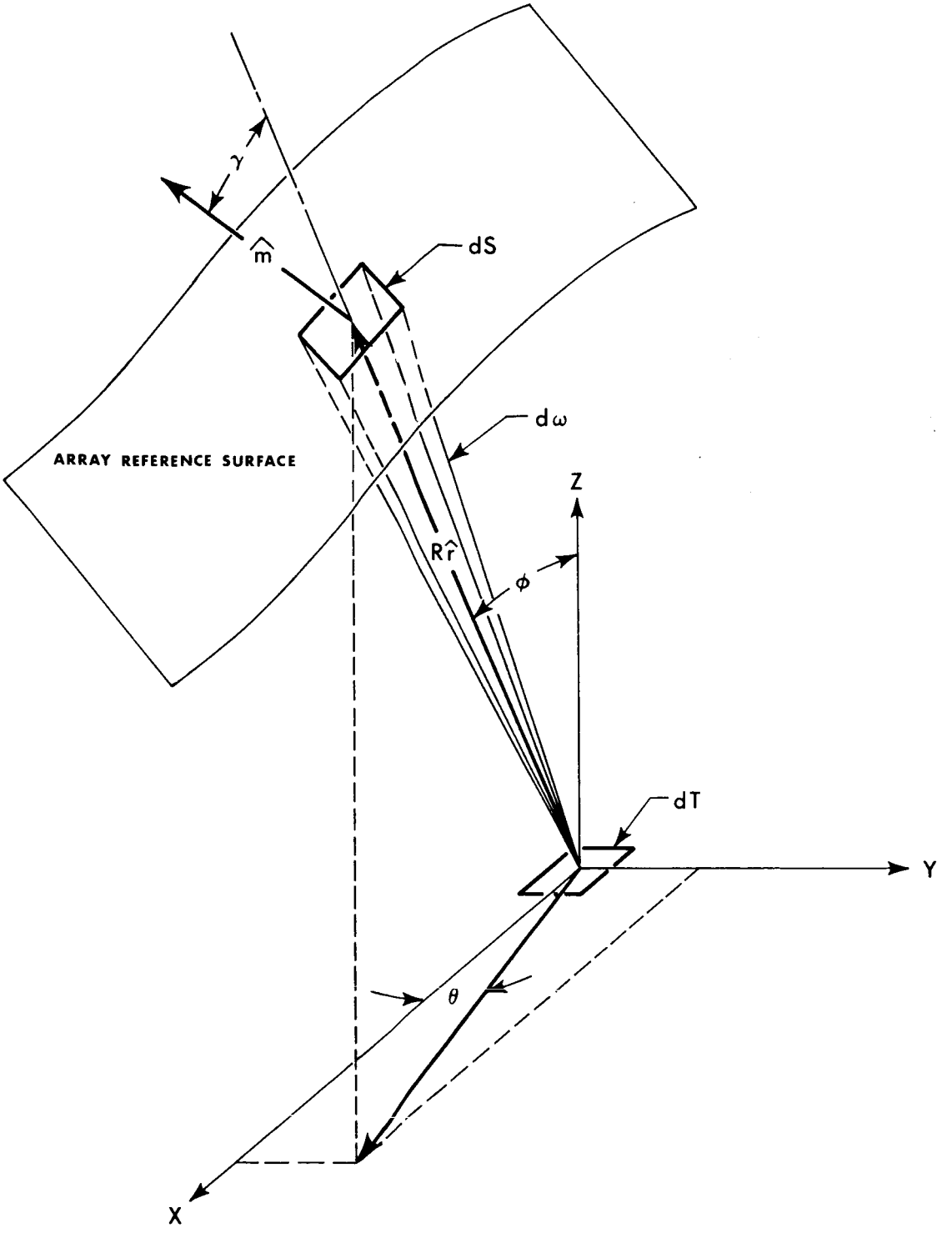

Figure 4-27. Schematic representation of geometrical relationships which affect the transfer of radiant flux from a multi-modular array of uncollimated projection systems to a target surface element.

of area dS on the array surface at the target surface element dT, then from the geometry of figure 4-27

$$d\omega = \frac{dS\ (\hat{m}\cdot\hat{r})}{R^2(\hat{r}\cdot\hat{r})} = \frac{dS\ \cos\ \gamma}{R^2} \tag{4-9}$$

The element of solid angle $d\omega$ can also be defined, in terms of the direction angles ϕ and θ (see Appendix I), as

$$d\omega = \sin\ \phi\ d\phi\ d\theta \tag{4-10}$$

Combining equations (4-9) and (4-10) yields the following expression for dS

$$dS = \frac{R^2 \sin\ \phi\ d\phi\ d\theta}{\cos\ \gamma} \tag{4-11}$$

Because there will be a finite distance between adjacent modules, the local module density D will, in reality, vary over the array reference surface. However, the performance characteristics required of each module can be determined by assuming that the module size and spacing are sufficiently small that the local module density D may be considered to be uniform over the entire surface. The effects introduced by finite module size and spacing can then be considered as simulation errors. Therefore, assuming that the value of D is constant over the surface, if I is now defined as the intensity of the radiant flux emitted by a module on dS in the direction $-\hat{r}$ toward the target surface element dT, then the irradiance dE produced on the target surface element by the radiant flux emitted by the N modules on dS is

$$dE = N\left(\frac{I\ \cos\ \phi}{R^2}\right) \tag{4-12}$$

By definition

$$N = D\ dS \tag{4-13}$$

If equation (4-11) is substituted into equation (4-13), the resulting expression is

$$N = \frac{D\, R^2 \sin\phi\, d\phi\, d\theta}{\cos\gamma} \tag{4-14}$$

which, when substituted into equation (4-12) yields

$$dE = \frac{D\, I \sin\phi \cos\phi\, d\phi\, d\theta}{\cos\gamma} \tag{4-15}$$

If the simulated earth is now taken such that it is centered on the Z-axis and subtends a field half-angle of Φ at the target surface element, then the total irradiance E on the target surface element is given by

$$E = D \int_0^{2\pi} d\theta \int_0^{\Phi} \left[I \left(\frac{\sin\phi \cos\phi}{\cos\gamma} \right) \right] d\phi \tag{4-16}$$

Because of the term $\cos\gamma$ in equation (4-16), the irradiance E will vary throughout the target volume for most reference surface geometries. This results because $\cos\gamma$ is dependent, not only upon ϕ and θ, but also upon the location and the orientation of the array surface element dS with respect to the target surface element dT. Therefore, in order to achieve uniform irradiance throughout the target volume (a fundamental characteristic of the Planetary Radiation Environment), it is necessary to eliminate the term $\cos\gamma$ from equation (4-16). The term $\cos\gamma$ can be eliminated only if I is proportional to $\cos\gamma$. For example, if

$$I = I_o \cos\gamma \tag{4-17}$$

where I_o is the intensity of the radiant flux emitted by a module in the direction $-\hat{m}$ (normal to the array surface element dS), then equation (4-16) becomes

$$E = D\, I_o \int_0^{2\pi} d\theta \int_0^{\Phi} \sin\phi \cos\phi \, d\phi \qquad (4\text{-}18)$$

Integrating equation (4-18) yields

$$E = \pi\, D\, I_o \sin^2\Phi \qquad (4\text{-}19)$$

Thus, both the irradiance E and the field half-angle Φ subtended by the simulated earth are constant and are independent of the geometry of the array reference surface (so long as it is large enough) and the location within the target volume if the following requirements are satisfied:

1. The modules are uniformly distributed over the array surface (D is constant).
2. The modules are oriented so that their respective axes of symmetry are normal to the array reference surface.
3. The intensity I of the radiant flux emitted by each module is proportional to the cosine of the angle of emission (e.g., $I = I_o \cos\gamma$).
4. The axial intensity I_o is the same for all modules.
5. The angular divergence of the radiant flux emitted by each module is restricted, by using appropriate field stops, to within an angle Φ with respect to the direction of the array field axis (parallel to the Z-axis of figure 4-27).

A more generalized expression for the irradiance E within the target volume could have been obtained by expressing the intensity I of the radiant flux emitted by a module as

$$I = I_o\, f(\phi,\theta) \cos\gamma \qquad (4\text{-}20)$$

which, when substituted into equation (4-16) results in the expression

$$E = D\, I_o \int_0^{2\pi} d\theta \int_0^{\Phi} f(\phi,\theta)\, \sin\phi \cos\phi\, d\phi \qquad (4\text{-}21)$$

Since equation (4-21) is independent of position parameters, then the irradiance E will be uniform (and the field half-angle subtended by the simulated earth will be constant) for all positions within that volume where the limits of integration apply. The function $f(\phi,\theta)$ permits a generalized masking of each module (identically with respect to the direction of the array axis) with graded masks in order to simulate the variable illumination of the earth and local variations in the albedo and/or emissivity of the earth's surface. Thus, using this design concept, virtually every aspect of the Planetary Radiation Environment can be simulated, except for the continuous field subtended by the earth. However, the incorporation of graded field masks will add, considerably, to the cost of the Planetary Radiation Environment Simulator. Therefore, the Planetary Radiation Environment Simulator will be defined by assuming that the radiant intensity I of each module, within an angle Φ with respect to the direction of the array field axis, is given by equation (4-17). (This is equivalent to assuming that the earth is a spherical Lambertian radiator of uniform radiance.) The effects introduced by ignoring the function $f(\phi,\theta)$ can then be evaluated as simulation errors.

The required axial intensity I_o of the radiant flux emitted by each module may be determined as follows: from equation (4-19)

$$I_o = \frac{E}{\pi\, D\, \sin^2\Phi} \qquad (4\text{-}22)$$

Defining W_{ave} as the average radiant emittance of the earth's surface, including both the reflected and emitted radiant flux, as seen from a given location in space, then from equation (4-7)

$$W_{ave} = \frac{E}{\sin^2 \Phi} \tag{4-23}$$

Therefore, if the earth is simulated as a spherical Lambertian radiator of uniform radiance, then, from equations (4-22) and (4-23), the axial intensity I_o required from each module is

$$I_o = \frac{W_{ave}}{\pi D} \tag{4-24}$$

From equation (4-24), it can be seen that the axial intensity I_o required from each module is directly proportional to the average radiant emittance W_{ave} seen at the earth's surface and is inversly proportional to the density D of the modules on the array reference surface.

The uniformity of the irradiance produced by the simulator within the target volume is a function of the uniformity of the density of the modules on the array reference surface. For example, defining S as the area of the array reference surface and locating N modules on this surface, then the average density D of the modules is

$$D = \frac{N}{S} \tag{4-25}$$

and the average irradiance E within the target volume is given by equation (4-19). The solid angle Ω subtended by the simulated earth is

$$\Omega = \int_0^{2\pi} d\theta \int_0^{\Phi} \sin \phi \, d\phi = 2\pi \, (1 - \cos \Phi) \tag{4-26}$$

Defining E_t as the irradiance produced at some position within the target volume by the N_t modules located on that portion (the area S_t) of the

array reference surface which can be seen within the solid angle Ω from the target position, then the module density D_t seen from this position is

$$D_t = \frac{N_t}{S_t} \tag{4-27}$$

Therefore, from equation (4-19),

$$U = \frac{E_t}{E} = \frac{\pi D_t I_o \sin^2\Phi}{\pi D I_o \sin^2\Phi} = \frac{D_t}{D} \tag{4-28}$$

where U represents the uniformity of the irradiance within the target volume.

Simulating the Environment Experienced by a Spacecraft which is Orbiting the Earth

From the geometry of figure 4-1, the geometrical parameters which must be varied to dynamically simulate the environment encountered by a spacecraft orbiting the earth are: (1) the field half-angle Φ subtended by the earth at the spacecraft; and (2) the angle Θ, taken at the spacecraft, between the directions to the centers of the sun and the earth. (Because of the great distance between the spacecraft and the sun, the field half-angle μ subtended by the sun at the spacecraft may be assumed to be constant.) Assuming that the spacecraft is in an elliptical orbit around the earth, the distance r between the center of the earth and the spacecraft is given by

$$r = h + R = \frac{a\,(1 - e^2)}{1 - e \cos T} \tag{4-29}$$

where e is the eccentricity and a is the semi-major axis of the elliptical orbit. The angle T is measured with respect to the direction to the apogee of the orbit (the direction for which the value of r is a

maximum). Thus, from the geometry of figure 4-1,

$$\sin \Phi = \frac{R}{h+R} = \frac{R\,(1 - e \cos T)}{a\,(1 - e^2)} \tag{4-30}$$

and

$$\Phi = \arctan \left[\frac{R\,(1 - e \cos T)}{\sqrt{a^2(1 - e^2)^2 - R^2(1 - e \cos T)^2}} \right] \tag{4-31}$$

The field half-angle Φ subtended by the earth at the spacecraft may be determined, as a function of time t, as follows.

The angular momentum m of an orbiting spacecraft is constant. Thus

$$m \equiv r^2 \frac{dT}{dt} = \frac{2\pi\, a^2 \sqrt{1 - e^2}}{\tau} \tag{4-32}$$

where τ is the orbital period. Substituting equation (4-29) into equation (4-32) yields

$$m\, dt = \left[\frac{a^2(1 - e^2)^2}{(1 - e \cos T)^2} \right] dT \tag{4-33}$$

By making the appropriate transformations, equation (4-33) can be integrated to obtain an expression for t in terms of the angle T and the constants of the orbit (e, τ). Thus

$$t = \frac{\tau \sqrt{1 - e^2}}{2\pi} \left(\frac{e \sin T}{1 - e \cos T} + \frac{2Q}{\sqrt{1 - e^2}} \right) \tag{4-34}$$

where

$$Q = \arctan\left[\sqrt{\left(\frac{1+e}{1-e}\right)}\ \tan\left(\frac{T}{2}\right)\right] \tag{4-35}$$

Thus, given the constants e, a, τ (of the spacecraft's orbit) and R (the radius of the earth); then if values of T are substituted into equations (4-31), (4-34) and (4-35), it is possible to plot a curve which defines how Φ (the field half-angle subtended by the simulated earth) must be varied during the dynamic simulation of that orbit.

The angle Θ, taken at the spacecraft, between the directions to the sun and to the earth may be determined as a function of time, as follows. From the geometry of figure 4-1

$$\Theta = \pi - (\gamma + \rho) \tag{4-36}$$

where γ is the angle, at the center of the earth, between the directions to the sun and to the spacecraft; ρ is the angle, at the center of the sun, between the directions to the earth and to the spacecraft. Define Γ as the angle between the normal to the plane of the spacecraft's orbit and the direction from the earth to the sun. Let p be the distance between the spacecraft and the reference plane which is normal to the earth-sun line and which intersects the plane of the spacecraft's orbit at the center of the earth. Defining r and T as before, then p is given by

$$p = r \sin\Gamma \cos(T + \delta) \tag{4-37}$$

where δ is the angle between the direction to the apogee of the orbit and the plane containing the earth-sun line and the normal to the spacecraft's orbit. If ξ is defined as the angle between the reference plane and the direction from the center of the earth to the spacecraft, then from the geometry of figure 4-1

$$\sin\xi = \frac{p}{r} = \sin\left(\frac{\pi}{2} - \gamma\right) \tag{4-38}$$

Using equations (4-37) and (4-38), and the trigonometric identities, γ may be expressed as

$$\gamma = \arctan\left[\frac{\sqrt{1 - \sin^2\Gamma \cos^2(\Upsilon + \delta)}}{\sin\Gamma \cos(\Upsilon + \delta)}\right] \tag{4-39}$$

From the geometry of figure 4-1, the angle ρ is given by

$$\rho = \arctan\left[\frac{r \cos(\frac{\pi}{2} - \gamma)}{D - p}\right] \tag{4-40}$$

where D is the radius of the earth's orbit. Substituting equation (4-37) into equation (4-40) yields

$$\rho = \arctan\left[\frac{\sqrt{1 - \sin^2\Gamma \cos^2(\Upsilon + \delta)}}{\left(\frac{D}{r}\right) - \sin\Gamma \cos(\Upsilon + \delta)}\right] \tag{4-41}$$

[Inclusion of the angle ρ in equation (4-36) corrects for parallax. However, near the earth, the term $\left(\frac{D}{r}\right)$ of equation (4-41) is so large that $\rho \simeq 0$]. Combining equations (4-36), (4-39) and (4-41) to eliminate ρ and γ yields

$$\Theta = \arctan\left[\frac{\sqrt{1 - \sin^2\Gamma \cos^2(\Upsilon + \delta)}}{\left(\frac{r}{D}\right) - \sin\Gamma \cos(\Upsilon + \delta)}\right] \tag{4-42}$$

Since the angle Υ varies with time, then, from equation (4-42), Θ varies with time for all orbits except those which lie in the reference plane ($\Gamma = 0$ or $\Gamma = \pi$). Given the radius R of the earth, the radius D of the earth's orbit, and the constants e, a, τ, Γ and δ which define the orbit of the spacecraft; then, if various values of Υ are substituted into equations (4-29), (4-35), (4-34), and (4-42) to determine the corresponding values for r, Q, t and Θ, it is possible to plot

a curve which defines how Θ (the angle between the direction of the solar field axis and the direction of the array field axis, see figure 4-28) must be varied in order to dynamically simulate that orbit.

In reality, the radius D of the earth's orbit and the angle Γ between the earth-sun line and the normal to the plane of the spacecraft's orbit are not constant; they both vary with time t. Defining e' as the eccentricity and a' as the semi-major axis of the earth's orbit, then on the basis of equation (4-29)

$$D = \frac{a'\left[1 - (e')^2\right]}{1 - e' \cos \omega} \tag{4-43}$$

where ω is the angle between the earth-sun line and the direction to the aphelion of the earth's orbit (the direction for which the value of D is a maximum). Defining ω_0 as the value of ω at the time (t=0) when the spacecraft is launched into orbit then, on the basis of equations (4-34) and (4-35)

$$t = \frac{\tau'\sqrt{1 - (e')^2}}{2\pi}\left[\frac{e' \sin \omega}{1 - e' \cos \omega} + \frac{2Q'}{\sqrt{1 - (e')^2}} - C\right] \tag{4-44}$$

where τ' is the orbital period of the earth (one year), and where

$$Q' = \arctan\left[\sqrt{\left(\frac{1 + e'}{1 - e'}\right)} \quad \tan\left(\frac{\omega}{2}\right)\right] \tag{4-45}$$

$$C = \frac{e' \sin \omega_0}{1 - e' \cos \omega_0} + \frac{2Q'_0}{\sqrt{1 - (e')^2}} \tag{4-46}$$

$$Q'_0 = \arctan\left[\sqrt{\left(\frac{1 + e'}{1 - e'}\right)} \quad \tan\left(\frac{\omega_0}{2}\right)\right] \tag{4-47}$$

The cosine of the angle Γ is given by

$$\cos \Gamma = \sin \sigma \left\{\sin \eta \sin\left[2(\omega - \omega_0)\right] - \cos \eta \cos\left[2(\omega - \omega_0)\right]\right\} \tag{4-48}$$

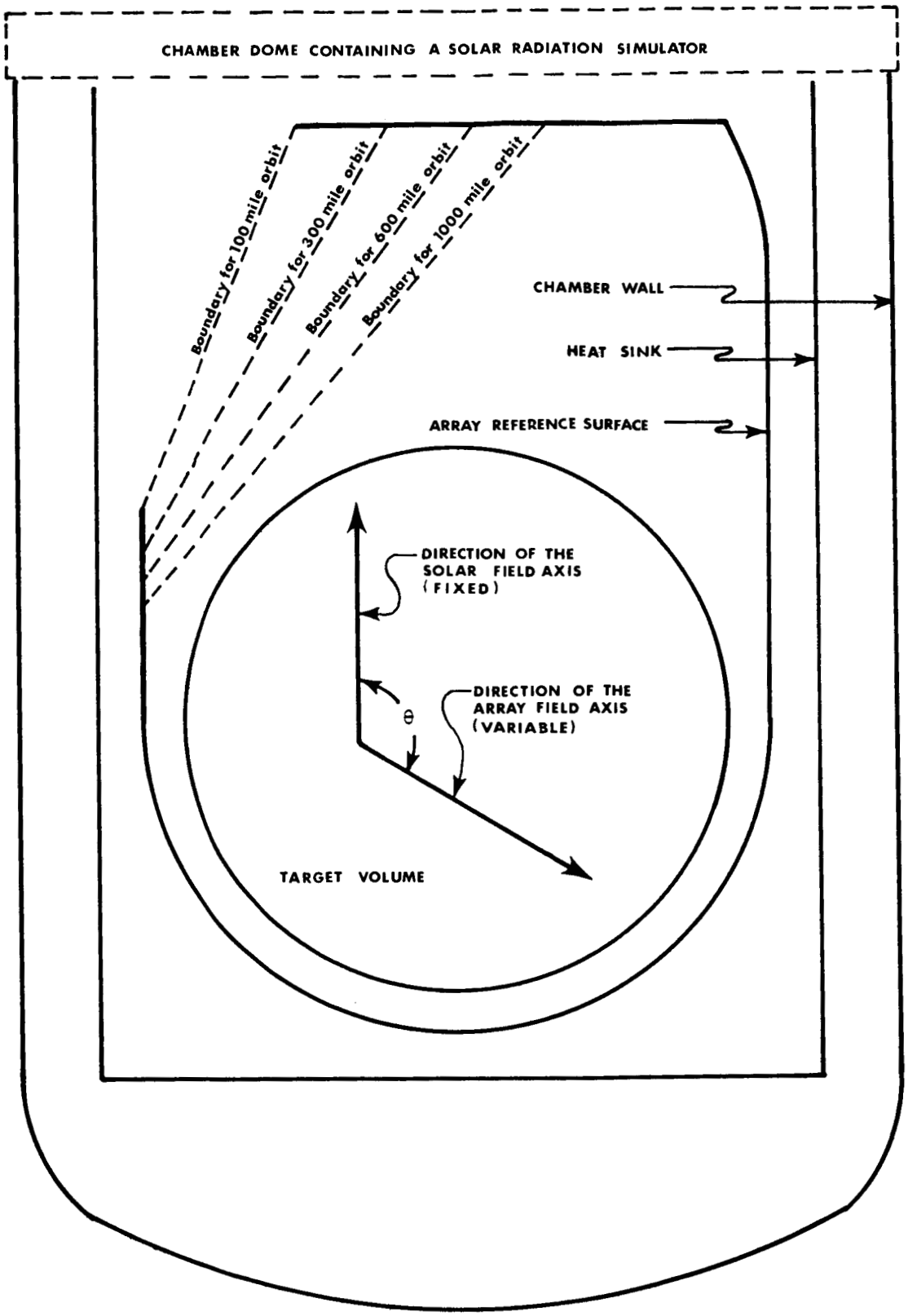

Figure 4-28. Schematic representation of the Space Environment Simulator showing the angle θ between the directions of the solar field axis and the array field axis.

where σ is the angle between the normal to the plane of the spacecraft's orbit and the normal to the earth's orbit (the polar axis), and η is the angle (when $t = 0$) between the earth-sun line and projection of the normal to the plane of the spacecraft's initial orbit into the plane of the earth's orbit. [The angles σ and η are, respectively, the co-latitude and the longitude of a spherical coordinate system (see Appendix I) whose polar axis is normal to the plane of the earth's orbit.] From the trigonometric identities,

$$\sin \Gamma = \sqrt{1 - \cos^2 \Gamma} \tag{4-49}$$

$$\Gamma = \arctan \left(\frac{\sin \Gamma}{\cos \Gamma} \right) = \arctan \left(\frac{\sqrt{1 - \cos^2 \Gamma}}{\cos \Gamma} \right) \tag{4-50}$$

From equations (4-43) through (4-50), it can be seen that the variation in D and Γ (especially in Γ) with respect to time can be ignored only when the total simulation time t_{max} is so small that $\omega_{max} \simeq \omega_o$. The average variation in ω is 0.9856 degrees-per-day.

Having established a method whereby Φ and Θ can be defined as a function of time t for any orbit, consider now the special case where the spacecraft's orbit is circular. For a circular orbit, $e = 0$ and r is constant. Thus, from equation (4-31)

$$\Phi = \arctan \left(\frac{R}{\sqrt{r^2 - R^2}} \right) = \text{constant} \tag{4-51}$$

and from equations (4-34) and (4-35)

$$t = \frac{\tau T}{2\pi} \tag{4-52}$$

Setting $\delta = 0$, then from equations (4-42) and (4-52)

$$\theta = \arctan\left[\frac{\sqrt{1 - \sin^2\Gamma \cos^2\left(\frac{2\pi t}{\tau}\right)}}{\left(\frac{r}{R}\right) - \sin\Gamma \cos\left(\frac{2\pi t}{\tau}\right)}\right] \tag{4-53}$$

If the earth's orbit is assumed to be circular, then $e' = 0$ and D is constant. Setting $\omega_o = 0$, then from equations (4-44) through (4-47)

$$t = \frac{\tau' \omega}{2\pi} \tag{4-54}$$

From equations (4-48) and (4-54)

$$\cos\Gamma = \sin\sigma \left[\sin\eta \sin\left(\frac{4\pi t}{\tau'}\right) - \cos\eta \cos\left(\frac{4\pi t}{\tau'}\right)\right] \tag{4-55}$$

If equation (4-55) is now substituted into equation (4-53) using the trigonometric identities, the result will be an expression which defines how θ must be varied in time in order to dynamically simulate a circular orbit of radius r and orbital period τ, assuming that the earth's orbit is also circular.

The axial intensity I_o of the radiant flux emitted by each module of the Planetary Radiation Environment Simulator is, from equation (4-24)

$$I_o = \frac{W_{ave}}{\pi D} \tag{4-56}$$

where D is the density of the modules on the array reference surface and W_{ave} is the average radiant emittance seen at the earth's surface, see equation (4-7). W_{ave} is plotted versus $\gamma \simeq \pi - \Theta$ in figure 4-21. Since I_o varies with W_{ave}, and since W_{ave} varies with γ and thus with Θ, then in order to dynamically simulate any orbit, the axial intensity I_o of the radiant flux emitted by each module must vary with Θ, increasing

as the value of Θ increases between 0 and π.

To summarize, in order to dynamically simulate the orbit of any spacecraft with a Space Environment Simulator such as that represented in figure 4-28, there are three parameters which must be varied with time. These are: (1) the angle Θ between the solar field axis and the array field axis; (2) the field half-angle Φ subtended by the simulated earth; and (3) the axial intensity I_0 of the radiant flux emitted by each module. In addition, the Space Environment Simulator must be equipped with a gimbal which will orient the spacecraft with respect to the directions of the solar field axis and the array field axis.

Design of a Module

From equations (4-17) and (4-20), it is required that the radiant intensity I_0 of the flux emitted by each module be proportional to the cosine of the angle of emission γ, where γ is measured from the axis of symmetry of the radiant flux distribution. The radiant intensity of a plane Lambertian radiator is, by definition (see Appendix I)

$$I = I_0 \cos \gamma \tag{4-57}$$

where I_0 is the radiant intensity in the direction of the surface normal ($\gamma = 0$).

The simplest module consists of a source which emits all of its radiant flux into a solid angle of 2π steradians (into a hemisphere) and whose radiant intensity distribution, within this solid angle, is given by equation (4-57). Both the zirconium arcs and tantalum carbide RF lamps (manufactured by Sylvania Electric Company) meet this requirement; however, both require elaborate and costly power supplies.

Next in order of simplicity is a module which consists of a hemispherical mirror and a source that radiates into a solid angle of 4π steradians

(a sphere) and whose radiant intensity I' is given by

$$I' = I'_o \cos \gamma \tag{4-58}$$

where I'_o is the radiant intensity along the axis of symmetry of the radiant flux distribution ($\gamma = 0$ or $\gamma = \pi$). The hemispherical mirror is located so that it is centered about the axis of symmetry of the radiant flux distribution in the direction $\gamma = \pi$ and so that it places an image of the source alongside the source. The radiant flux F_m emitted by the source into the solid angle Ω subtended by the mirror (2π steradians), is equal to the radiant flux emitted by the source into remaining solid angle (2π steradians). F_m is given by

$$F_m = \int_0^{\Omega} I' d\Omega = I'_o \int_0^{2\pi} d\theta \int_{\pi}^{\frac{\pi}{2}} \sin \gamma \cos \gamma \, d\gamma = \pi I'_o \tag{4-59}$$

Defining A_m as the reflectance of the mirror for the spectrum of the source, the total radiant flux F emitted by the module is

$$F = F_m (1 + A_m) = \pi I_o \tag{4-60}$$

where I_o is the axial intensity of the radiant flux emitted by the module. Defining P as the electrical input power to the source and C as the radiative efficiency of the source, then, by definition

$$C P = 2F_m \tag{4-61}$$

Combining equations (4-59) through (4-61) so as to eliminate I'_o, F, and F_m

$$I_o = \frac{C\ (1 + A_m)\ P}{2\pi} \tag{4-62}$$

Combining this expression and equation (4-24) yields an expression which defines the density D of modules required on the array reference surface if the Planetary Radiation Environment of the earth is to be simulated using a source whose input electrical power is P. That is

$$D = \frac{2W_{ave}}{C\ (1 + A_m)\ P} \tag{4-63}$$

where W_{ave} is the average radiant emittance of the earth as seen from the location whose environment is to be simulated. From figure 4-21, the value of W_{ave} ranges between 21.125 watts-per-square-foot and 66.611 watts-per-square-foot.

One source which emits radiant flux in accordance with equation (4-58) is the ribbon tungsten filament. (Ribbon tungsten filament lamps are available in 108-watt versions that are very compact.) Reliable values of the radiative efficiency C of tungsten filament lamps are not known, but according to Hardy and Perrin, Principles of Optics, it is 0.80 "or lower". Taking $C = 0.75$ as a conservative value and assuming that, for an evaporated aluminum mirror which has been exposed to the atmosphere, $A_m = 0.92$ (see Appendix V) for the spectrum of a tungsten filament lamp, then in order to simulate the maximum radiant emittance seen at the earth's surface,

$$D = \frac{2\ (66.611)}{0.75\ (1 + 0.92)\ P} = \frac{92.5153}{P} \tag{4-64}$$

Thus, if 108-watt ribbon tungsten filament lamps are used, the required module density is 0.8566 modules-per-square-foot and there must be one module for each 1.1674 square-foot of area on the array reference surface.

The lamps least naturally suited to provide the required radiant flux distribution are those whose radiant intensity distribution approximates that of a cylindrical Lambertian radiator. The radiant intensity I' of a cylindrical Lambertian radiator is given by

$$I' = I'_{90} \sin \phi \tag{4-65}$$

where ϕ is the angle, at the center of the cylinder, between the axis of the cylinder and the direction of emission; I'_{90} is the radiant intensity in the directions where $\phi = 90°$ (in the directions perpendicular to the axis of the cylinder). This source category includes the short arc lamp, the capillary, and the tungsten-iodine lamp.

A compromise to the required cosine distribution can be obtained, using this type source, by locating the source coaxially within an appropriate reflector (see Appendix VI). However, because of the shadows introduced by the ends of the lamp, there will be an axially symmetric solid angle $\Omega_s = 2\pi (1 - \cos \gamma_s)$ which contains no radiant flux. (γ_s is the field half-angle subtended, at the secondary focus, by the obstruction which is causing the shadow.) If an array of these modules was located on a spherical reference surface of radius R, then there would be a volume of radius $R \sin \gamma_s$ (centered within the target volume) which would receive no radiant flux from the array of modules. If these modules were located on a plane, then all parts of the target volume would be uniformly irradiated; however, the simulated earth would have a dark region, at the center of its field, which subtends the solid angle Ω_s. Thus, before this module configuration can be used for the Planetary Radiation Environment Simulator, a technique must be defined whereby radiant flux with the correct intensity and distribution can be introduced into the solid angle Ω_s.

A compromise to the required cosine distribution can also be obtained, using this type of source, by locating the source on the axis of an

appropriate reflector so that its axis is perpendicular to the axis of the reflector. If the source were a cylindrical Lambertian radiator, then the intensity I' of the radiant flux emitted by the source in a direction ϕ with respect to the axis of the reflector, is given by

$$I' = I'_{90} \sqrt{1 - \sin^2\phi \cos^2\theta} \tag{4-66}$$

where I'_{90} is again the radiant intensity in the direction perpendicular to the axis of the source; θ is the longitude of the ϕ,θ spherical coordinate system centered at the source and is the angle between the plane defined by the axes of the lamp and the reflector and the plane defined by axis of the reflector and the direction of emission. The intensity I of the radiant flux emanating from the module is equal to the sum of intensity I' of the radiant flux emitted by the source and the intensity I'_m of the reflected radiant flux in the direction γ with respect to the axis of the module. That is

$$I = I' + I'_m \tag{4-67}$$

If equations (4-57) and (4-66) are now substituted into equation (4-67), the resulting expression defines the intensity distribution required of the reflected radiant flux I'_m in order that the intensity I of the total radiant flux emanating from the module be proportional to $\cos\gamma$. This expression is

$$I'_m = I_o \cos\gamma - I'_{90} \sqrt{1 - \sin^2\gamma \cos^2\theta} \tag{4-68}$$

Defining A_m as the reflectance of the reflector for the spectrum of the source, then the axial intensity I_o of the total radiant flux emanating from the module is

$$I_o = \left(1 + A_m\right) I'_{90} \tag{4-69}$$

Substituting equation (4-69) into equation (4-68) yields

$$I'_m = I'_{90} \left[\left(1 + A_m\right) \cos \gamma - \sqrt{1 - \sin^2\gamma \cos^2\theta} \right] \qquad (4\text{-}70)$$

Therefore, if the radiant intensity distribution of the source is given by equation (4-66), then the radiant intensity distribution required of the reflected radiant flux is given by equation (4-70). Using these two equations, the shape of the required reflector can be determined by applying the methods described in Appendix VI to calculate coordinates over the surface. Because of the term $\cos^2\theta$ in equations (4-66) and (4-70), the reflecting surface thus defined will not be circularly symmetric about the axis of the module. It is probable that the reflecting surface will have an elliptic cross-section.

From the preceding, the most desirable module configuration (on the basis of simulation fidelity, simplicity and low cost-per-module) appears to be a ribbon tungsten filament lamp used with a hemispherical mirror. The major disadvantage of this module configuration is that, because of the low power output of the ribbon tungsten filament lamp, a great many modules will be needed to provide the maximum irradiance required in the target volume of the Planetary Radiation Environment Simulator. (It should be noted, however, that the use of more modules will increase the uniformity of the irradiance within the target volume.)

A possible alternative to the ribbon tungsten filament lamp is the C-13 tungsten filament projection lamp. Polar plots of the relative radiant intensity distribution of the C-13 tungsten filament projection lamp are shown, for two scanning directions, in figure 4-29. (The relative radiant intensity distribution within the solid angle where $90° \leq \phi \leq 180°$ is identical to that plotted in figure 4-29.) The distribution curve plotted from measurements taken in the plane normal to the axis of the cylindrical lamp envelope closely approximates that of a uniformly radiating source within an angle $\phi = 40°$ because the projected area of each coil of the filament is independent of ϕ in this plane. The decrease in the relative intensity for $\phi > 40°$ is a result of the fact that the field-of-

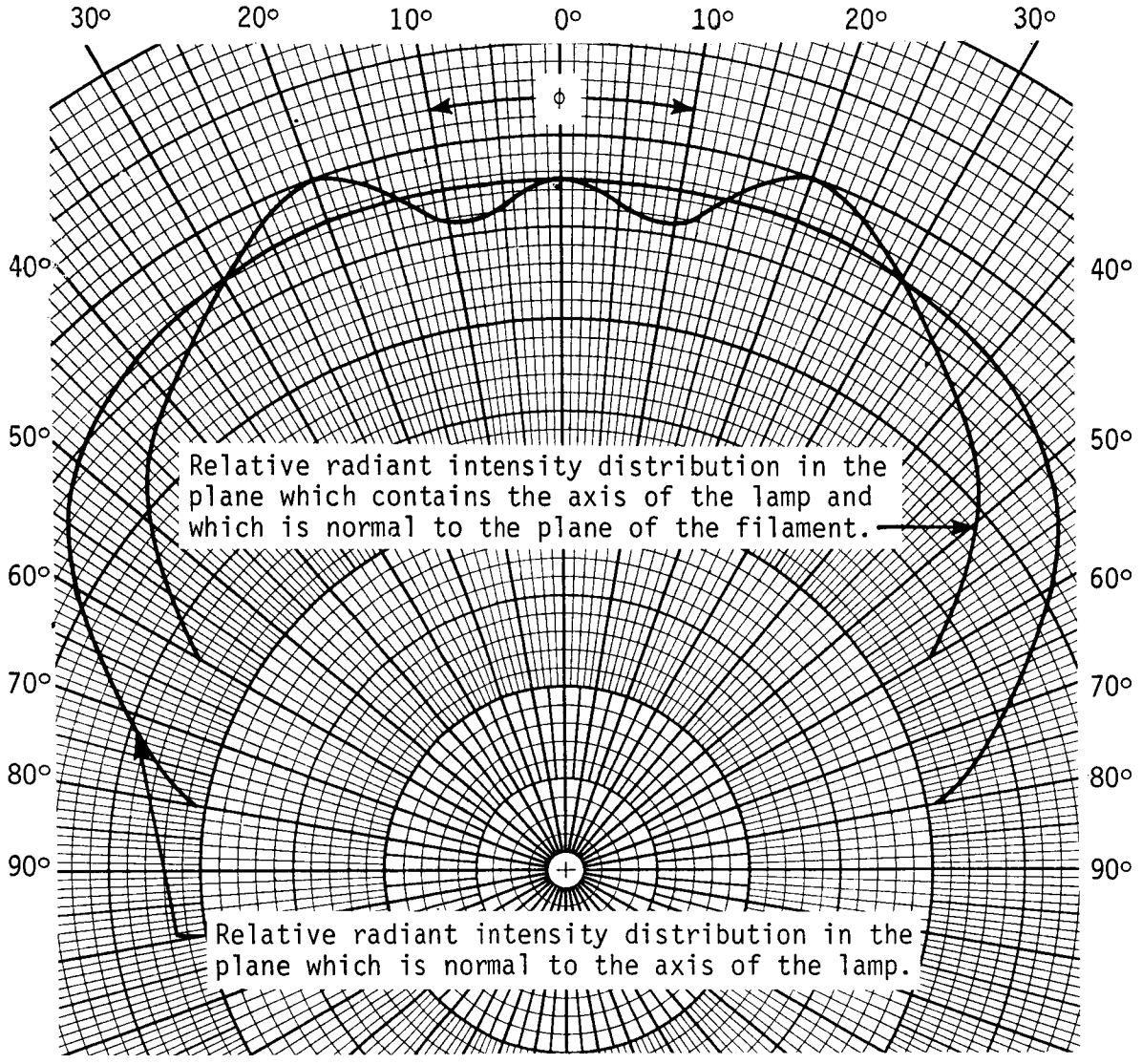

Data Source: Wallin Optical Systems, Inc.,
Chatsworth, California

Figure 4-29. Relative radiant intensity distribution of a C-13 tungsten filament projection lamp within a solid angle of 2π steradians (a hemisphere).

view to the further coils is increasingly obstructed by the nearer coils as ϕ increases to 90°. The irregularities in the distribution curve plotted from measurements taken in the plane which contains the axis of the lamp envelope and which is normal to the filament plane, are possibly the result of measuring inaccuracies but are more likely the result of reflection by components of the filament support structure. If the tolerance on the radiant intensity distribution of the radiant flux emanating from each module is not too restrictive, it may be possible to use the C-13 tungsten filament lamp with a hemispherical mirror. (The tolerance on the radiant intensity distribution of the radiant flux emanating from a module can only be established after the geometry of the array reference and the tolerance on the uniformity of the irradiance within the target volume have been specified.) Alternatively, the shape of the reflector to be used with this source can be defined using the techniques discussed in Appendix VI.

Finally, the module may consist of a lamp whose radiant intensity distribution approximates that of a cylindrical Lambertian radiator (e.g., a tungsten-iodine lamp with a coiled-coil filament) and which is located so that its axis is perpendicular to the axis of the module. Again, if the tolerance on the required radiant intensity distribution is not too restrictive, it may be possible to use the lamp with a hemispherical reflector. However, it is more probable that the tolerances will require the reflector shape to be defined in accordance with the techniques discussed in Appendix VI.

Irrespective of how the required radiant intensity distribution is achieved, each module must be equipped with a field mask to restrict the radiant flux emanating from the module to within an angle Φ with respect to the array field axis. (Φ is the field half-angle subtended by the simulated earth.) A convenient shape for the field mask would be a sphere with a circular area S removed. This area S is given by

$$S = 2\pi R^2 \left(1 - \cos \Phi_m\right) \tag{4-71}$$

where R is the radius of the sphere and Φ_m is the field half-angle subtended by the aperture area S at the center of the sphere. The field subtended by the simulated earth can be varied by displacing the center of curvature of the spherical masking surface away from the source (i.e., the position from which the radiant flux emitted by the module is apparently emanating) along the direction of the array field axis (i.e., the direction of the axis of the aperture of the field mask). Define Φ_{max} and Φ_{min} as the limits on the range of Φ for all orbits to be simulated. Specify that when $\Phi = \Phi_{max}$, the center of curvature of the spherical masking surface is displaced a distance d from the source position in the direction along the array field axis toward the target volume. Further, specify that when $\Phi = \Phi_{min}$, the center of curvature of the spherical masking surface is displaced a distance d from the source position in the direction along the array field axis away from the target volume. Therefore, the field half-angle Φ_m subtended by the aperture in the masking surface is given by

$$\Phi_m = \arctan \left[\frac{\sqrt{4 - \left(\cos \Phi_{max} + \cos \Phi_{min}\right)^2}}{\cos \Phi_{max} + \cos \Phi_{min}} \right] \tag{4-72}$$

The varying field subtended by the earth as seen by a spacecraft in an elliptic orbit can be simulated by varying the distance between source and the center of curvature of the spherical masking surface. Defining x as the displacement between the source and the center of curvature of the spherical masking surface at time t, then x is given by

$$x = R \sin \Phi_m \left(\cos \Phi_m - \cos \Phi\right) \tag{4-73}$$

where Φ is the field half-angle subtended by the earth at time t and is given by equation (4-31).

It has been shown that the angle Θ between the solar field axis and

the array field axis (see figure 4-28) must be varied in accordance with equation (4-42) If the array surface is a portion of a sphere, then the angle Θ can be varied by rotating the array reference surface about an axis which is perpendicular to the solar field axis and which passes through the center of curvature of the array reference surface. For most other reference surface shapes, the movement of the reference surface is physically restricted by the chamber walls and each module must be equipped with a field mask which can be rotated so that the angle Θ between the solar field axis and the axis of the aperture of the field mask (i.e., the direction of the array field axis) varies according to equation (4-42). The axes of rotation of all of the field masks must be mutually parallel and must be perpendicular to the solar field axis. If a circular orbit is to be simulated, the spherical masking surface is rotated about an axis which passes through the source position and which is displaced a distance x from the center of curvature of the spherical masking surface along the axis of the aperture in the masking surface, where x is given by equation (4-73) and Φ is constant. An elliptic orbit can be simulated by additionally displacing the axis of rotation a distance d away from the source position (toward the target volume) in the direction Θ for which the value of Φ is a maximum. To simulate an elliptic orbit, the displacement d between the source and the axis of rotation is

$$d = R \sin \Phi_m \left[\cos\left(\frac{\Phi_{max} + \Phi_{min}}{2} \right) - \cos \Phi_{max} \right] \qquad (4\text{-}74)$$

where Φ_{max} and Φ_{min} are respectively the maximum and minimum values of Φ for the orbit. The corresponding displacement x between the axis of rotation and the center of curvature of the spherical masking surface is

$$x = R \sin \Phi_m \left[\cos \Phi_m - \cos\left(\frac{\Phi_{max} - \Phi_{min}}{2} \right) \right] \qquad (4\text{-}75)$$

Because the direction Θ for which Φ is a maximum varies with time [see equations (4-31) and (4-42)], the direction of the displacement d

must be varied with time. This can be accomplished by rotating the axis of rotation of the spherical masking surface about a parallel axis which passes through the source position.

In order to simulate any given orbit, the input power to the modules must be varied, see equations (4-57) and (4-62). The maximum power input occurs when $\Theta = 180°$. The minimum power input occurs when $\Theta \leq \Phi$.

When an orbit is being simulated in the Space Environment Simulator, see figure 4-28, the field masks are rotated so that the angle Θ between the solar field axis and the array field axis varies, with time, within the range between $\Theta_{max} = 180°$ and $\Theta_{min} = \Phi$. Because of dimensional restrictions imposed by the presence of the Solar Radiation Simulator, it will probably not be possible to decrease Θ all the way to Φ and still maintain uniformity throughout the entire target volume. However, if the rotation of the field masks is halted at $\Theta \simeq 90°$ for that period of time when the value of Θ given by equation (4-42) is less than $90°$, it appears from the data plotted in figures 4-3 through 4-18 that the error thus introduced will be negligible. For that period of time when the value of Θ given by equation (4-42) is less than Φ , the Solar Radiation Simulator is turned off.

It is desirable, in order to reduce re-reflections and minimize the load on the cryogenic walls, that each module also be equipped with an additional mask, called the target mask. The aperture in the target mask is sized and positioned so that radiant flux can be emitted from the module only into the field subtended by the target volume at the module.

ERROR ANALYSIS

Error Introduced by Failure to Simulate the Smoothly Continuous Field Subtended by the Earth

Because the modules of the Planetary Radiation Environment Simulator are of finite size, there will be a finite distance between adjacent modules in the array. Thus, it is not possible to simulate the smoothly continuous field.

subtended by the earth. Further, because of the finite distance between adjacent modules in the array, the module density seen over that portion of the array reference surface contained within the field-of-view to the simulated earth [see equation (4-27)] will vary as the position-of-view varies within the target volume. This variation in the module density seen from various positions within the target volume results in a corresponding variation in the irradiance experienced by target surface elements located at these same positions, see equation (4-28).

For several reasons (primarily economic) it is desirable that the Planetary Radiation Environment Simulator consist of the fewest possible number of modules. Therefore, performance characteristics were calculated, for various arrangements of modules on array reference surfaces of various geometries, for what was opined to be the probable minimum module density. Densities of 0.180118 modules-per-square-foot and 0.158317 modules-per-square-foot were assumed; the corresponding values of the maximum radiant power output required per module are, approximately, 370 watts and 425 watts. The geometrical and operational parameters for the optimum array configurations determined for these module densities (denoted, respectively, as array configuration 1 and array configuration 2) are listed in table 4-1. A scale drawing of the Space Environment Simulator, including array configuration 1 , is shown in figure 4-30. The approximate boundary of the reference surface of array configuration 1 is indicated, for various orbital altitudes, by the dashed lines in figure 4-30.

Error Introduced by Failure to Simulate the Variable Irradiation of the Earth by the Sun

For economic reasons, it is not practical to provide each module with an identical graded field mask to simulate the variable irradiation of the earth by the sun. Therefore, the earth will be simulated as a spherical Lambertian radiator whose radiance is uniform and equal to the average radiance seen at the earth's surface. Although this will introduce no error in the irradiance experienced by surface elements whose normals lie in the direction toward the center of the simulated earth, there will be an error

Table 4-1. Geometrical and operational parameters of two proposed configurations for the Planetary Radiation Environment Simulator.

		ARRAY CONFIGURATION 1				ARRAY CONFIGURATION 2			
Geometric Parameters of the array reference surface (see Appendix IV, figure IV-2)	Radius of curvature $r_c = a_u = a_L$ of the cylinder and the hemispherical caps	144 inches				144 inches			
	Height h_c of the cylinder	201.166 inches				184.472 inches			
	Radius r_u of the centered hole in the upper hemispherical cap	127.752 inches				132.257 inches			
	Displacement Z_c between the centers of the target volume and the cylinder	100.583 inches				92.236 inches			
	Distance between adjacent modules	28.275 inches				30.159 inches			
	Total number of modules on the array reference surface	480				397			
Operational Parameters	Orbital altitude h	300 miles		600 miles		300 miles		600 miles	
	Field half-angle Φ subtended by the earth	136.732°		120.544°		136.732°		120.544°	
	Angle Θ between the directions to the sun and to the earth	180°	90°	180°	90°	180°	90°	180°	90°
	Axial radiant intensity of each module (watts-per-steradian)	116.446	39.598	116.541	41.129	134.517	45.389	133.344	46.941
	Average irradiance within the target volume (watts-per-square-foot)	57.318	19.265	49.756	17.505	57.318	19.265	49.756	17.505
	Maximum irradiance within the target volume (watts-per-square-foot)	66.103 (+15.33%)	21.954 (+13.96%)	62.529 (+25.67%)	21.786 (+24.45%)	67.119 (+17.10%)	23.848 (+23.79%)	66.534 (+33.72%)	22.344 (+27.64%)
	Minimum irradiance within the target volume (watts-per-square-foot)	49.395 (-13.82%)	16.833 (-12.62%)	39.056 (-21.50%)	14.580 (-16.71%)	39.652 (-30.82%)	16.378 (-14.99%)	29.629 (-40.45%)	13.948 (-20.32%)
	Probable error in the irradiance within the target volume (watts-per-square-foot)	1.072 (1.87%)	0.388 (2.01%)	2.019 (4.06%)	0.492 2.81%)	2.365 (4.13%)	0.518 (2.69%)	2.678 (5.38%)	0.583 (3.33%)
	Number of modules used	261	328	229	290	220	273	190	247

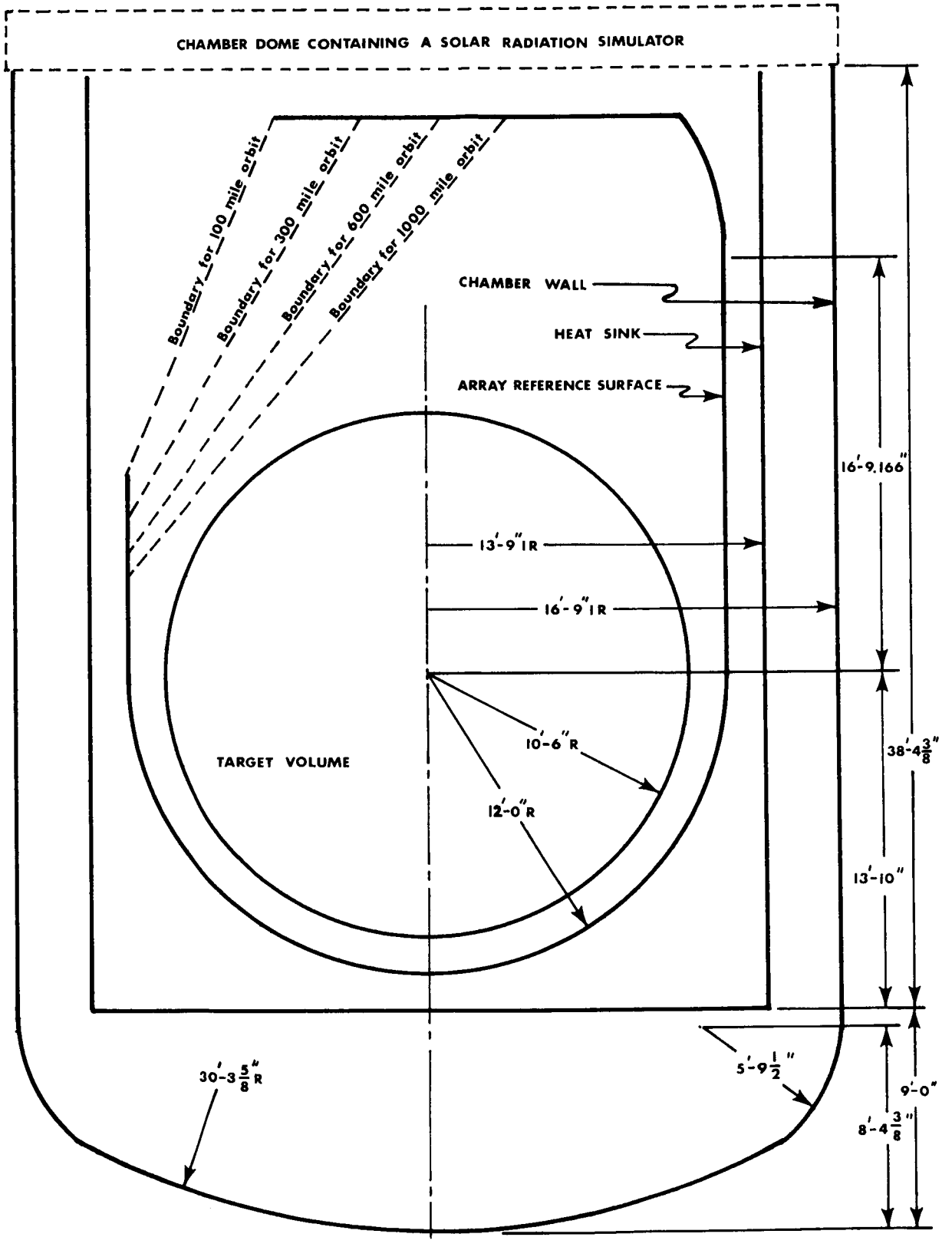

Figure 4-30. The Space Environment Simulator at NASA Goddard Space Flight Center.

in the irradiance experienced by target surface elements whose normals do not lie in this direction.

Define α and β as the direction angles of the normal to the target surface element with respect to the direction to the center of the earth, see figure 4-1. Defining E_e as the irradiance produced on a target surface element by radiant flux thermally emitted from the earth (assuming that the earth is a spherical Lambertian radiator) and defining $E_e + E_a$ as the total irradiance produced on the target surface element by both the reflected and emitted radiant flux emanating from the earth, the percent error S in the irradiance experienced by the target surface element, introduced by failure to simulate the variable irradiation of the earth by the sun, is given by

$$S = 100 \left[1 - \left(\frac{E_e}{E_{e_o}} \right) \left(\frac{E_{e_o} + E_{a_o}}{E_e + E_a} \right) \right] \text{ percent} \qquad (4\text{-}76)$$

where E_{e_o} and $E_{e_o} + E_{a_o}$ denote, respectively, the values of E_e and $E_e + E_a$ when $\alpha = 0$. The error S is a maximum when the angle γ, at the center of the earth, between the directions to the sun and to the target surface element is $90°$. The percent error S, introduced by failure to simulate the variable irradiation of the earth, was calculated using the computer program SPACE and is plotted versus γ, in figures 4-31 through 4-36, for $\gamma = 90°$ and for orbital altitudes h from 200 to 700 miles in 100-mile increments. From these figures, the error S becomes quite large as α increases; however, from figures 4-13 through 4-18, the total irradiance experienced by the target surface element decreases as α increases, thereby reducing the effect of the error to relative insignificance. For example, when $h = 400$ miles, $\gamma = 90°$, $\alpha = 90°$ and $\beta = 0°$, the irradiance error is 13.8% but in absolute terms is only 0.876 watt-per-square-foot. When $h = 400$ miles, $\gamma = 90°$, $\alpha = 135°$ and $\beta = 0°$, the irradiance error is 25.6% but in absolute terms is only 0.015 watt-per-square-foot. The insignificance of this error can also be seen by comparing figure 4-4 with figures 4-13 through 4-18.

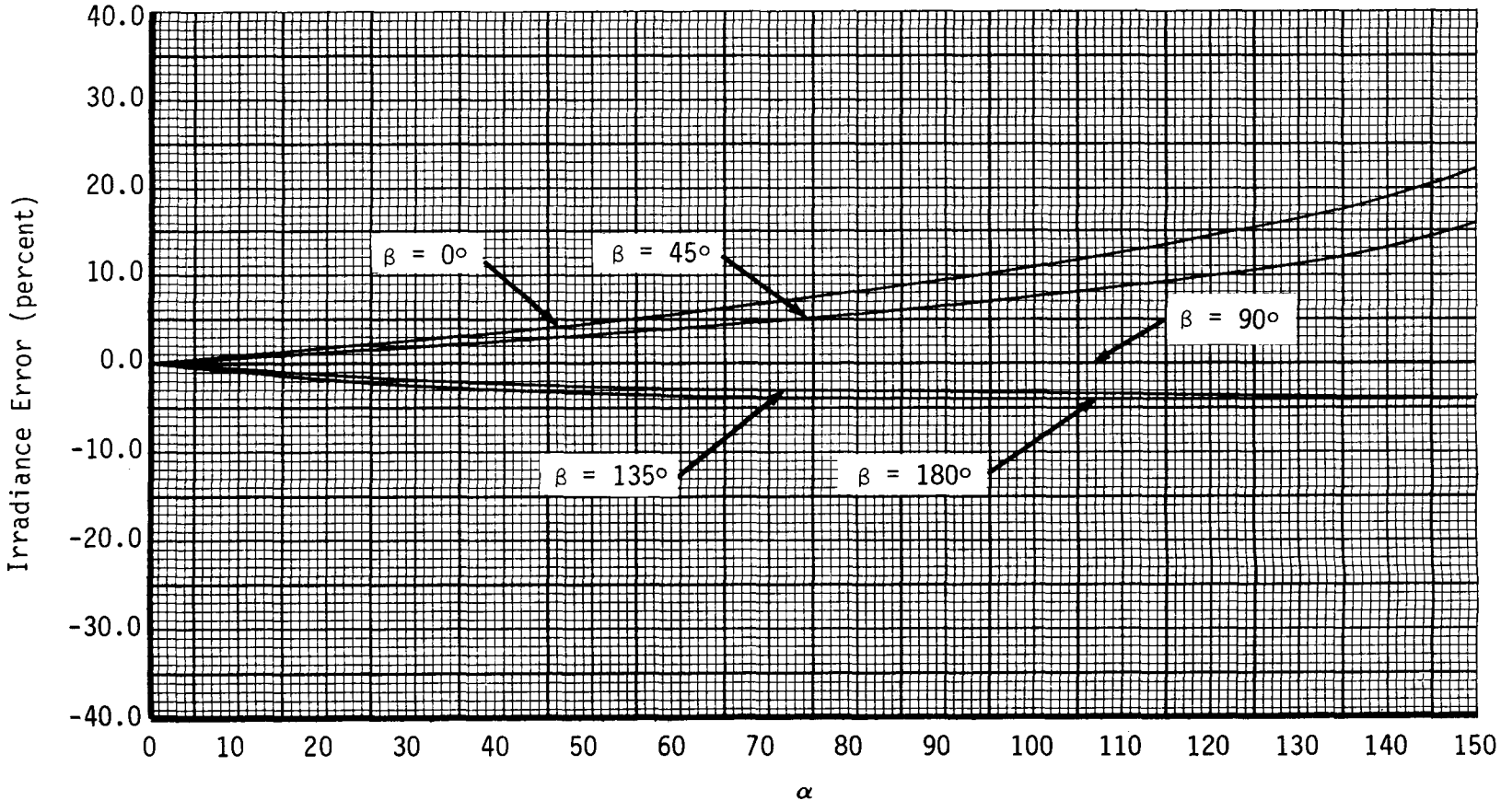

Figure 4-31. Irradiance error introduced by failure to simulate the variable irradiation of the earth versus α when $\gamma = 90°$ and h = 200 miles.

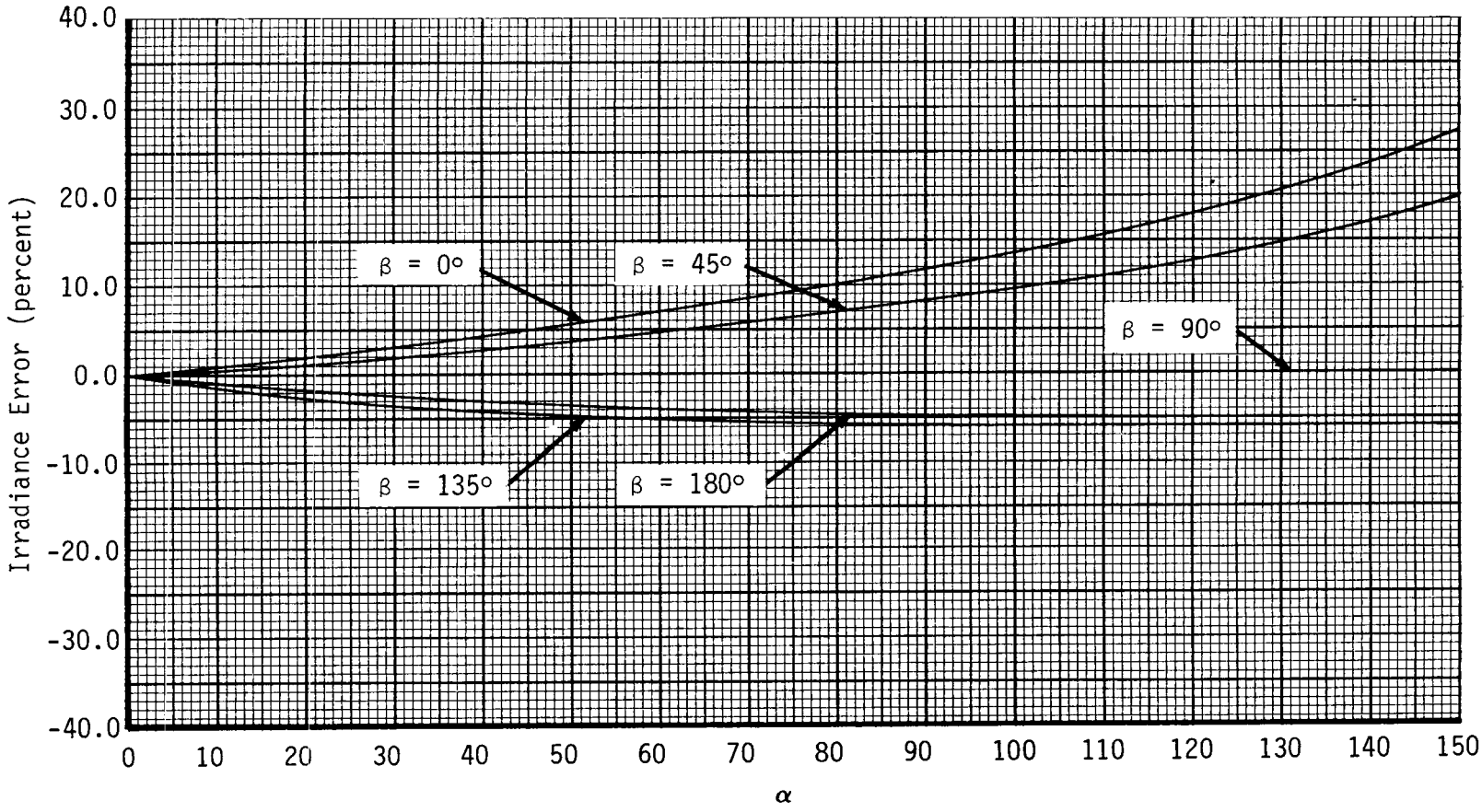

Figure 4-32. Irradiance error introduced by failure to simulate the variable irradiation of the earth versus α when $\gamma = 90°$ and $h = 300$ miles.

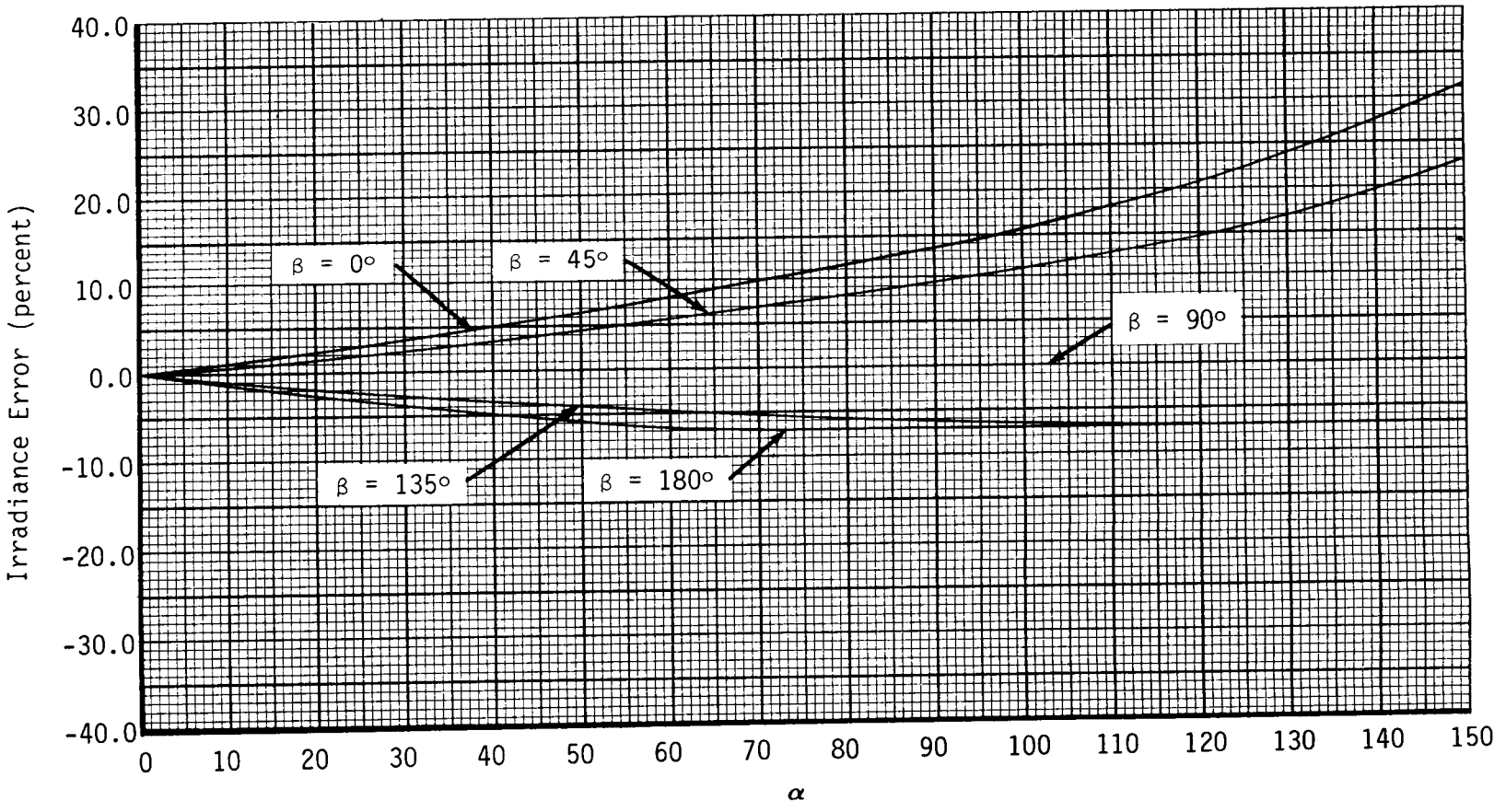

Figure 4-33. Irradiance error introduced by failure to simulate the variable irradiation of the earth versus α when $\gamma = 90°$ and $h = 400$ miles.

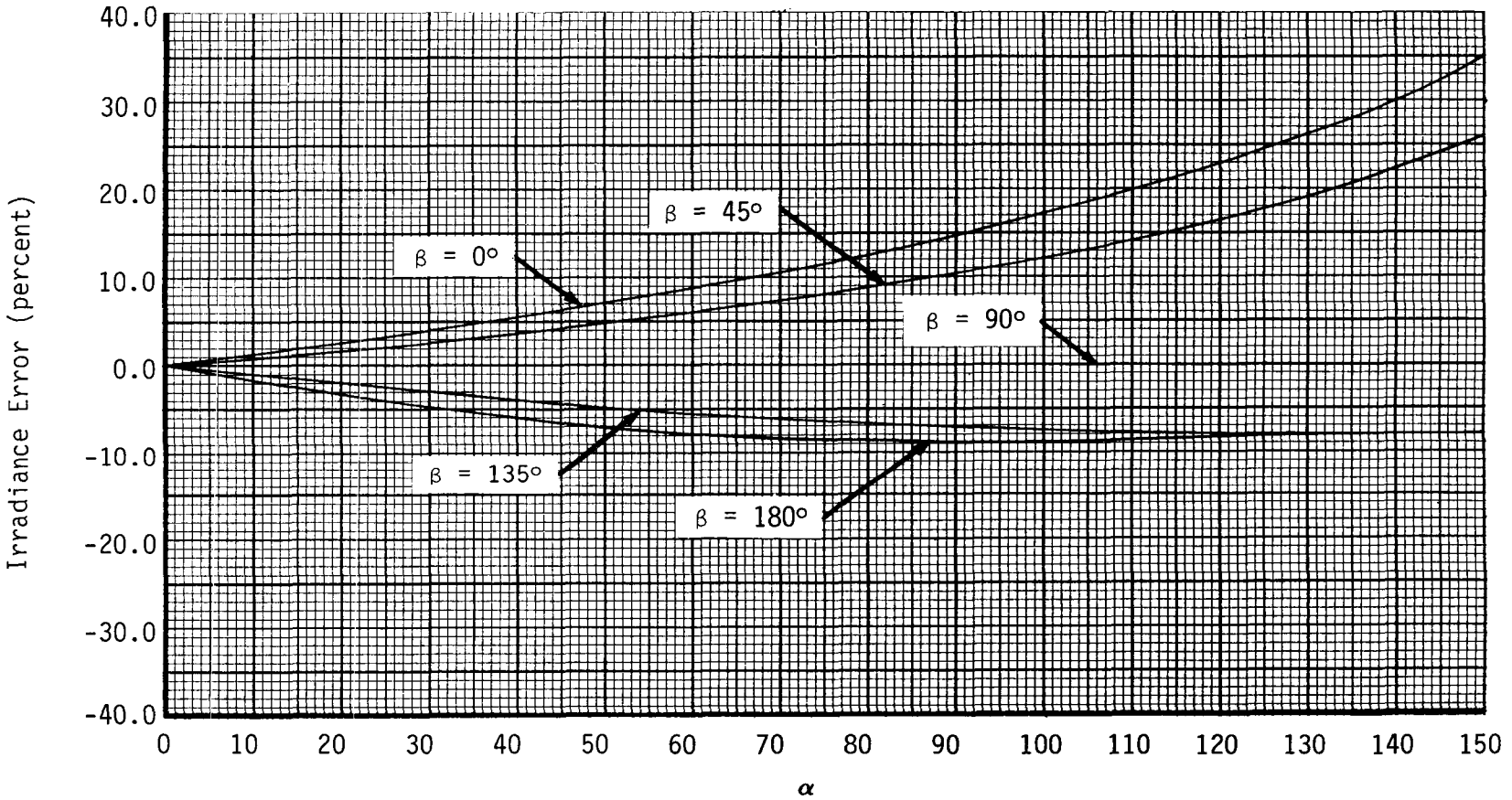

Figure 4-34. Irradiance error introduced by failure to simulate the variable irradiation of the earth versus α when $\gamma = 90°$ and $h = 500$ miles.

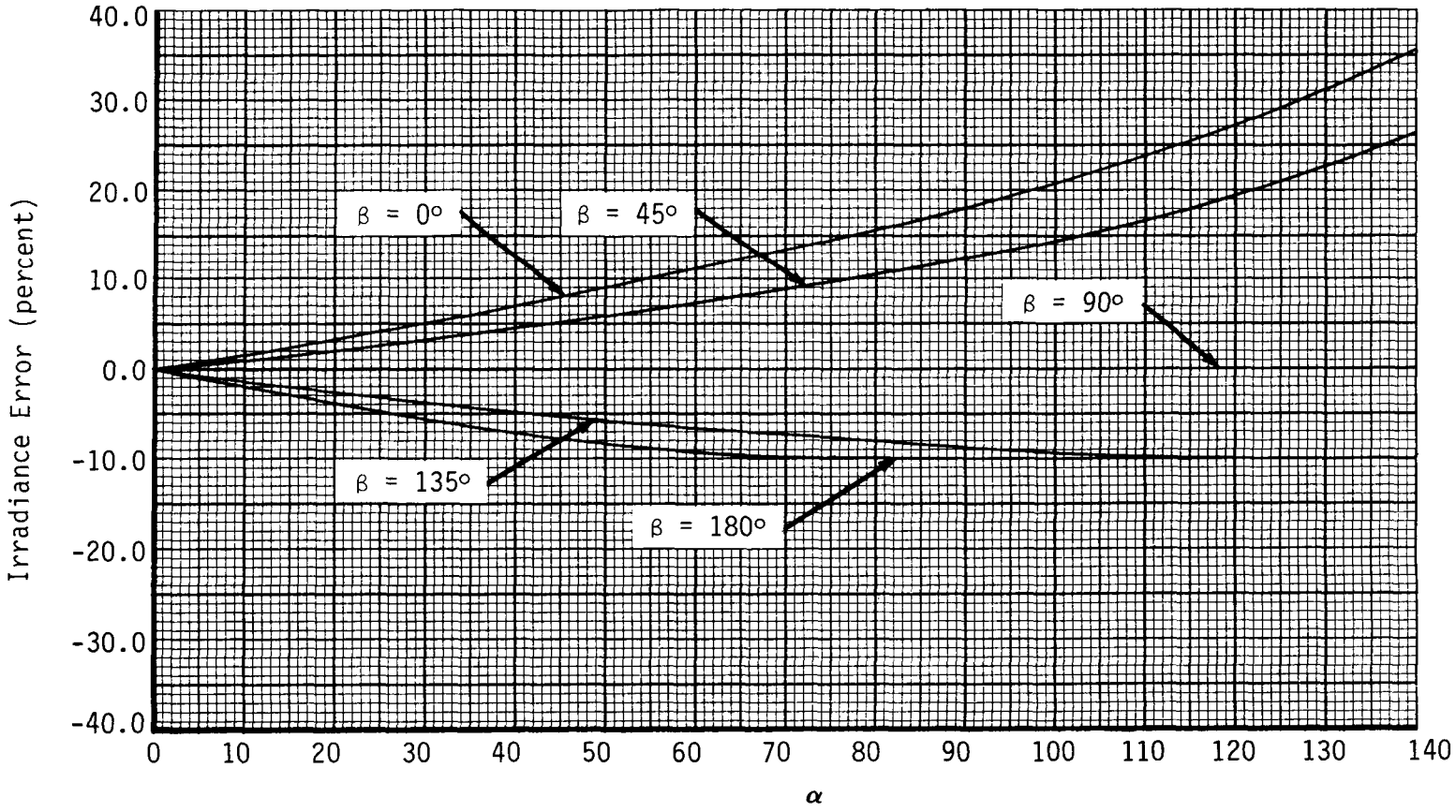

Figure 4-35. Irradiance error introduced by failure to simulate the variable irradiation of the earth versus α when $\gamma = 90°$ and $h = 600$ miles.

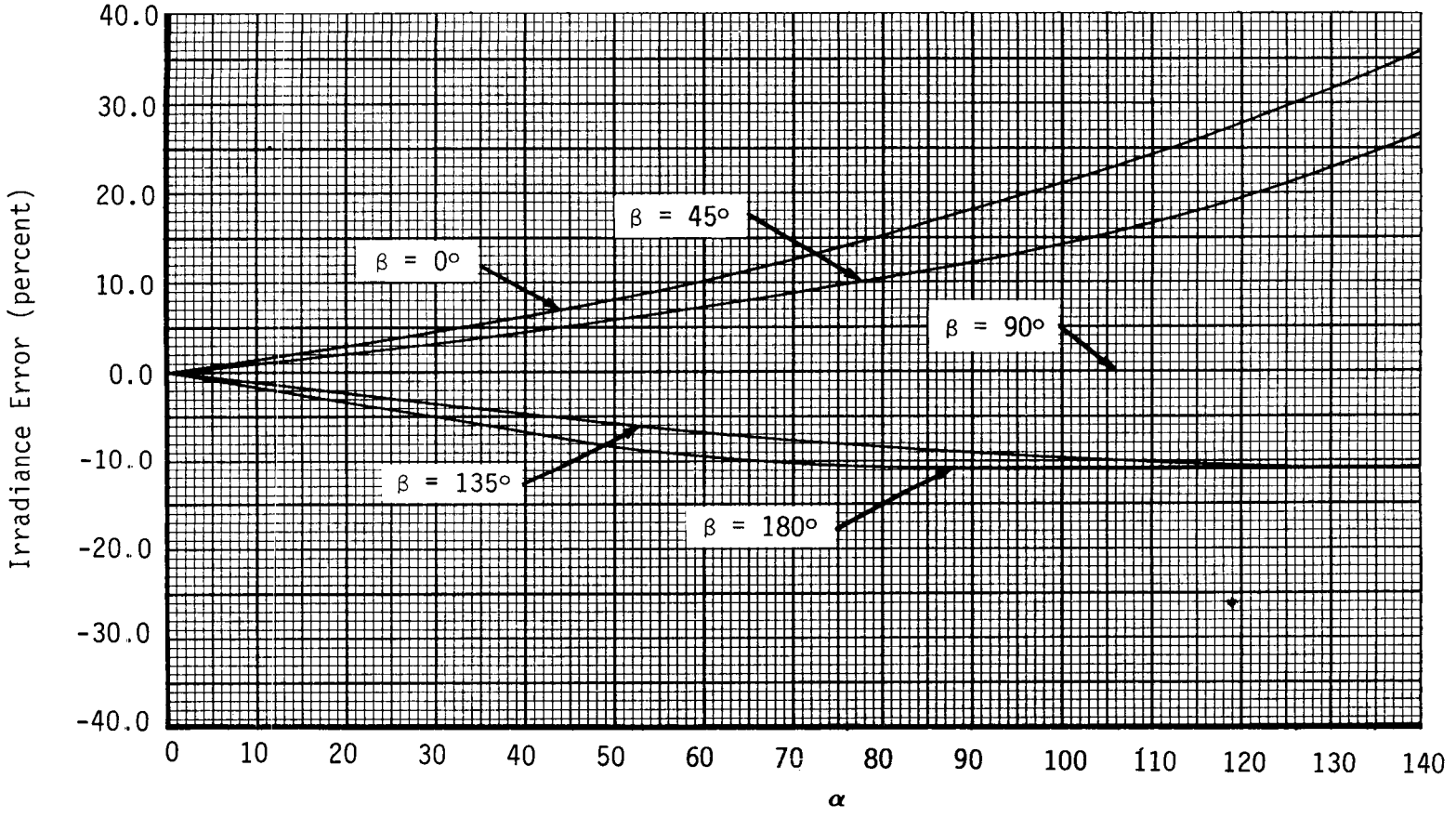

Figure 4-36. Irradiance error introduced by failure to simulate the variable irradiation of the earth versus α when $\gamma = 90°$ and $h = 700$ miles.

Error Introduced by Failure to Simulate the Field Subtended by the Earth

If the field subtended by the simulated earth is not correct, then in order to achieve the required irradiance on the target surface elements whose normals lie in the direction toward the center of the simulated earth, the axial intensity I_{o_e} of the radiant flux from each module must be [from equation (4-19)]

$$I_{o_e} = \frac{I_o \sin^2\Phi}{\sin^2\Phi_e} \tag{4-77}$$

where Φ is the field half-angle subtended by the earth at the orbit being simulated, Φ_e is the field half-angle subtended by the simulated earth, and I_o is the axial radiant intensity which would be required of each module if the simulated earth subtended the correct field half-angle Φ. From figure 4-4, the irradiance error experienced, by target surface elements whose normals do not lie in the direction toward the center of the earth, increases as the angle α (between the normal to the target surface element and the direction to the center of the simulated earth) increases. For example, if a 200 mile orbit is simulated with a field which corresponds to that of a 700 mile orbit, then (from figure 4-4) when $\alpha = 90°$, the irradiance is 73% of the correct value. When $\alpha = 120°$, the irradiance is 41% of the correct value. Defining E_{e_o} as the irradiance (watts-per-square-foot) experienced by the target surface element when $\alpha = 0°$; then (from figure 4-4) when $\alpha = 90°$, the irradiance error is $-0.09\ E_{e_o}$ watts-per-square-foot; when $\alpha = 120°$, the irradiance error is $-0.066\ E_{e_o}$ watts-per-square-foot.

Error Introduced by Failure of the Modules to Produce Radiant Flux with the Correct Spectrum

In order to compensate for the error introduced by the failure of the modules to produce radiant flux with the correct spectrum, the axial intensity I_{o_e} of the radiant flux emitted by each module must be

$$I_{e_o} = \left(\frac{P}{P_e}\right) I_o \tag{4-78}$$

where I_o is the axial intensity which would be required if the radiant flux emitted by each module had the correct spectrum, P is the absorptance of the material for the correct spectrum, and P_e is the absorptance of the material for the spectrum of the radiant flux emitted by the module. The correction factor $\frac{P}{P_e}$ can be determined for various materials using the data presented in Appendix V. If the spacecraft is coated with several materials and if the correction factor is different for each material, then it is not possible to totally compensate for spectral mismatch. However, by analyzing the geometry of the spacecraft and weighting the various correction factors (perhaps on an area basis), it is possible that a compromise correction factor can be determined.

SECTION 5
CONCLUSIONS

As a result of this study, it has been concluded that if the following requirements are satisfied, the Planetary Radiation Environment of the earth at a given location in space can be closely approximated by locating an array of modules on a reference surface of arbitrary shape.

1. The modules must be uniformly distributed over the array reference surface.

2. The array reference surface must be large enough and so located that its boundary cannot be seen, within the field subtended by the simulated earth, from any position within the target volume.

3. The number of modules used must be great enough that the density of the modules, over that portion of the array reference surface which is contained within the field subtended by the earth, as seen from all parts of the target volume, is uniform within the specified tolerance on the uniformity of the irradiance within the target volume.

4. Each module must be oriented so that its axis coincides with the local normal to the array reference surface.

5. The intensity of the radiant flux emanating from each module must be proportional to the cosine of the angle between the direction of emission and the axis of the module.

6. The axial intensity of the radiant flux emanating from each module must be the same for all modules.

7. Each module must be equipped with a field mask which restricts the angular divergence of the radiant flux emanating from each module to within an angle Φ with respect to the direction to the center of the simulated earth. (Φ is the field half-angle subtended by the earth at the location in space whose environment is being simulated.)

It has further been concluded that, in order to simulate any orbit in real time, the radiant power output, and the location and orientation of the field masks, must be varied in an identical manner for all of the modules.

Finally, it has been concluded that the simulation fidelity is more a function of economic rather than of technological factors. For example, the uniformity of the irradiance within the target volume of the simulator is a function, not only of the uniformity of the module density, but also of the module density itself. That is, the more modules that are used, the more uniform the irradiance within the target volume becomes. Also, the simulation fidelity could be increased by equipping all of the modules with identical filters (i.e., graded field masks) in order to simulate the variable irradiation of the earth by the sun and the local variations in the albedo and emissivity of the earth's surface.

APPENDIX I

RADIOMETRIC TERMS AND MATHEMATICAL SYMBOLS

TERMINOLOGY

Absorptance - The ratio of the absorbed flux to the flux incident on a surface. Also, the ratio of the flux absorbed by any substance to that absorbed under the same conditions by a blackbody. Also called absorptivity.

Absorptance, Spectral - Absorptance as a function of wavelength.

Albedo - The albedo of an object is the fraction of the incident energy (within the entire spectral band from the ultraviolet to the far infrared) which is reflected by the object.

Angle of Emission - The angle between the normal to a radiating surface and the emitted ray.

Angle of Incidence - The angle between the normal to a reflecting or refracting surface and the incident ray.

Angle of Reflection - The angle between the normal to a reflecting surface and the reflected ray.

Angle of Refraction - The angle between the normal to a refracting surface and the refracted ray.

Blackbody - A body which absorbs all the radiant energy which strikes it; a perfect radiator and a perfect absorber. A contraction of the term ideal blackbody. Also called ideal radiator, full radiator, complete radiator.

Flux - see Radiant Flux.

Irradiance - The incident radiant flux per unit area (this term is analogous to the photometric term illuminance).

Lambertian Radiator - A source whose radiance is independent of the angle of emission and whose radiant intensity is proportional to the cosine of the angle of emission.

Lambertian Reflector - Sometimes called a Lambert diffuse reflector. A surface which diffusely reflects all of the unabsorbed incident radiant flux such that the radiance of the surface is constant. (The Lambertian reflector serves as the apparent source of the reflected radiant flux.) The radiant intensity of the flux reflected from a Lambertian reflector is proportional to the cosine of the angle of reflection.

Normal - Sometimes called the "perpendicular." An imaginary line forming right angles with the plane tangent to a surface at a given point. It is used as a basis for determining angles of emission, incidence, reflection, and refraction.

Radiance - The radiant intensity per unit of the projected area of an extended source. (This term is analogous to the photometric term luminance, sometimes called brightness.)

Radiant Emittance - The radiant flux emitted per unit of area of a source. (This term is analogous to the photometric term luminous emittance.)

Radiant Flux - Radiant energy transferred per unit of time. (This term is analogous to the photometric term luminous flux.) Also called radiant power, the MKSA unit of radiant flux is the watt.

Radiant Intensity - Flux radiated per unit of solid angle about a specified direction. (This term is analogous to the photometric term luminous intensity.)

Reflectance - The ratio of the reflected flux to the incident flux. Unless qualified, this term applies to specular (regular) reflection. Also called reflectivity.

Reflectance, Diffuse - The ratio of the flux reflected diffusely in all directions to the total incident flux, specular reflection excluded.

Reflectance, Spectral - Reflectance as a function of wavelength.

Solar Constant - Irradiance on a surface, oriented normal to the direction from the surface to the sun, located outside the atmosphere at mean earth-sun distance. The solar constant has been variously measured from 1322 to 1430 watts-per-square-meter (122.82 to 132.85 watts-per-square-foot). For this study, the solar constant was taken as 130.00 watts-per-square-foot (1400 watts-per-square-meter).

Solid Angle - Measured by the ratio of an area on the surface of a sphere to the square of the radius of the sphere. The unit of solid angle is the steradian.

Steradian - The unit of solid angle. A solid angle of one steradian encloses an area on the surface of a sphere which is equivalent to the square of the radius of the sphere. A sphere subtends a solid angle of 4π steradians at its center.

Thermal Emission - The process whereby an object transfers heat to its surroundings in the form of radiant energy.

SYMBOLOGY

Symbols for the Radiometric Parameters:

Symbol	Radiometric Parameter
A	Albedo
B	Radiance
E	Irradiance
F	Radiant Flux
I	Radiant Intensity
W	Radiant Emittance

Vector Notation:

Unit vectors are identified by a circumflex (^) placed over an English or Greek letter symbol, e.g., $\hat{r}$.

General vectors are identified by an arrow (→) placed above an English or Greek letter symbol, e.g., $\vec{Q}$.

Scalars are any English or Greek letter symbols which are not identified as a vector by placing (^) or (→) above the letter symbol.

L, M, N designate the direction cosines of a vector.

$\hat{i}$, $\hat{j}$, $\hat{k}$ designate the unit orthogonal triad ($\hat{i}$, $\hat{j}$, and $\hat{k}$ are unit vectors in the x-direction, the y-direction, and the z-direction, respectively).

Equation of a unit vector:

$$\hat{r} = L_r\hat{i} + M_r\hat{j} + N_r\hat{k}$$

Equation of a general vector:

$$\vec{Q} = Q(L_Q\hat{i} + M_Q\hat{j} + N_Q\hat{k})$$

ϕ , θ designate the direction angles of a vector in a spherical coordinate system, where θ is the longitude and ϕ is the co-latitude. ϕ is measured from the z-direction and θ is measured in the xy-plane, counter-clockwise from the x-direction. Under these conditions, the following relationships exist between the direction cosines (L, M, N) and the direction angles (ϕ , θ):

$$L = \sin \phi \cos \theta$$

$$M = \sin \phi \sin \theta$$

$$N = \cos \phi$$

REFERENCES

1. Handbook of Geophysics, U. S. Air Force Research Directorate, Macmillan Co., New York, 1960.

2. Military Standard Optical Terms and Definitions, MIL-STD-1241, 30 September 1960, U.S. Government Printing Office, Washington, D. C., 20402.

3. The International Systems of Units, by E.A. Mechtly, NASA SP-7012, U. S. Government Printing Office, Washington, D. C., 20402.

4. Handbook of Chemistry and Physics, Chemical Rubber Publishing Co., 2310 Superior Avenue, N.E., Cleveland, Ohio.

5. Mathematical Tables and Formulas, 3rd Edition, by R. S. Burington, McGraw-Hill Book Company, New York.

APPENDIX II
IRRADIANCE PRODUCED ON A TARGET SURFACE ELEMENT BY RADIANT FLUX EMITTED BY A SPHERICAL LAMBERTIAN RADIATOR

The irradiance dE produced on a target surface element dT, by an element of radiant flux d^2F emitted by (or through) an element of area on the surface of a source to the target element, is equal to the product of the radiance B of the source element, the cosine of the angle of incidence ψ, and the element of solid angle $d\omega$ subtended by the source element at the target element. That is

$$dE = \frac{d^2F}{dT} = B \cos \psi \, d\omega \qquad \text{(II-1)}$$

Using this equation, it is possible to determine the irradiance on a surface which is being irradiated by a spherical Lambertian radiator (a source whose radiance B is independent of the angle of emission, see Appendix I). The pertinent geometrical relationships involved are schematically represented in figure II-1, where dT is an element of area on the target surface and dS is an element of area on the surface of a spherical Lambertian source. The coordinate system of this figure has been chosen so that (1) the target element and the center of spherical source lie on the z-axis and (2) the unit vector $\hat{n}$, normal to the target surface element, lies in the xz-plane and makes an angle α with the direction to the center of the spherical source (the z-axis). The unit vector $\hat{r}$ lies in the direction from dT to dS, ψ is the angle of incidence (the angle between $\hat{r}$ and $\hat{n}$), and ϕ is the field half-angle subtended by the spherical source at the target location.

The element of solid angle $d\omega$ subtended by the source element dS may be written, in terms of the direction angles ϕ and θ of a spherical coordinate system (see Appendix I) whose origin is at the target location and whose polar axis coincides with the z-axis, as

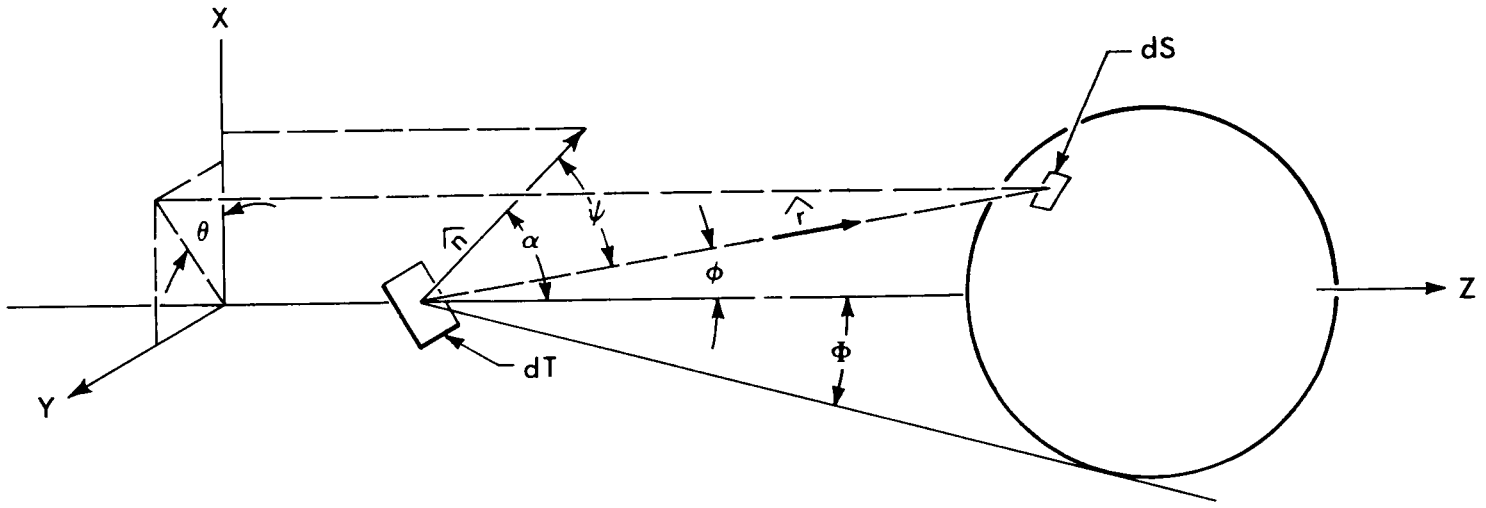

Figure II-1. Schematic representation of the geometrical relationships which govern the transfer of radiant flux from a spherical source to a target surface element.

$$d\omega = \sin \phi \, d\phi \, d\theta \tag{II-2}$$

where ϕ is the angle between $\hat{r}$ and the z-axis.

The unit vectors $\hat{n}$ and $\hat{r}$ may be expressed, in terms of the unit orthogonal vector triad (see Appendix I), as

$$\hat{n} = \hat{i} \sin \alpha + \hat{k} \cos \alpha \tag{II-3}$$

$$\hat{r} = \hat{i} \sin \phi \cos \theta + \hat{j} \sin \phi \sin \theta + \hat{k} \cos \phi \tag{II-4}$$

Thus, the angle of incidence ψ (the angle between $\hat{r}$ and $\hat{n}$) is given by

$$\cos \psi = \hat{n} \cdot \hat{r} = \sin \alpha \sin \phi \cos \theta + \cos \alpha \cos \phi \tag{II-5}$$

It was noted above that, by definition, the radiance B of a Lambertian radiator is constant (independent of the angle of emission). Therefore, if equations (II-2) and (II-5) are substituted into equation (II-1), and since B is independent of ϕ and θ , the expression for the irradiance E produced on the target element dT by the spherical Lambertian radiator is

$$E = B \int\int (\sin \alpha \sin^2 \phi \cos \theta + \cos \alpha \sin \phi \cos \phi) \, d\phi \, d\theta \tag{II-6}$$

Equation (II-6) must be integrated over those ϕ, θ directions which are not only within the field subtended by the source at the target location (i.e., the directions for which $0 \leq \phi \leq \Phi$), but which are also within the field-of-view from the front of the target surface element, i.e., the directions for which $0 \leq \psi \leq \frac{\pi}{2}$. If these two conditions are applied to the geometry of figure II-1 to determine the limits of integration for equation (II-6) as the target surface element is tilted with respect to the z-axis, discontinuities in these limits occur when $\alpha = \frac{\pi}{2} - \phi$; when $\alpha = \frac{\pi}{2}$; and when $\alpha = \frac{\pi}{2} + \phi$. These discontinuities require that the

integration of equation (II-6) be divided into four cases on the basis of the angle α between the z-axis and the normal to the target surface element or, equivalently, on the basis of what fraction of the field subtended by the source at the target element location lies within the field-of-view from the front of the target surface element. The three non-trivial cases, for which all or part of the source lies within the field-of-view from the front of the target surface element, are discussed in detail below.

Case 1. $0 \leq \alpha \leq (\frac{\pi}{2} - \Phi)$

This condition obtains when the target surface element is not tilted so that the plane of the target surface element intersects the spherical source. Therefore, the entire source lies within the field-of-view from the front of the target surface element. The simple constant limits of integration apply and equation (II-6) may be written, by inspection, as

$$E = B \int_0^{\Phi} d\phi \int_{-\pi}^{\pi} d\theta \, (\sin \alpha \sin^2 \phi \cos \theta + \cos \alpha \sin \phi \cos \phi) \qquad \text{(II-7)}$$

which, when integrated, yields the result

$$E = \pi B \sin^2 \Phi \cos \alpha \qquad \text{(II-8)}$$

The principal fact to be observed from this result is that the irradiance on the target surface is directly proportional to $\cos \alpha$ so long as $0 \leq \alpha \leq (\frac{\pi}{2} - \Phi)$

Case 2. $(\frac{\pi}{2} - \Phi) < \alpha \leq \frac{\pi}{2}$

From the geometry of figure II-1, it can be seen that, when $\alpha \leq \frac{\pi}{2}$, at least half of the spherical Lambertian source can be seen within the

field-of-view from the front of the target surface element. Further, within the solid angle defined by $0 \leq \phi \leq (\frac{\pi}{2} - \alpha)$, the integration of equation (II-6) with respect to θ is uninterrupted from $-\pi$ to $+\pi$. Therefore, by defining BJ_1 as the irradiance on the target surface element produced by that portion of the spherical Lambertian source which can be seen within the solid angle defined by these limits on ϕ and θ; then from equation (II-6), equation (II-9) can be written for J_1.

$$J_1 = \int_0^{\frac{\pi}{2}-\alpha} d\phi \int_{-\pi}^{\pi} d\theta \, (\sin \alpha \sin^2\phi \cos \theta + \cos \alpha \sin \phi \cos \phi) \qquad \text{(II-9)}$$

When equation (II-9) is integrated it yields

$$J_1 = \pi \sin^2 (\tfrac{\pi}{2} - \alpha) \cos \alpha = \pi \cos^3 \alpha \qquad \text{(II-10)}$$

When $(\frac{\pi}{2} - \alpha) < \phi \leq \Phi$, the range of θ has variable limits defined by the condition that $\psi = \frac{\pi}{2}$, which occurs when $\hat{n}$ and $\hat{r}$ are perpendicular, $\hat{r}$ lying in the plane of the target surface element dT. Defining Γ as the upper limit on θ when $\phi > (\frac{\pi}{2} - \alpha)$, it can be seen from the geometry of figure II-1 that $\frac{\pi}{2} \leq \Gamma \leq \pi$ and that the lower limit on θ is $-\Gamma$. The value of Γ can be determined, by substituting Γ for θ in equation (II-5) as follows:

$$\cos (\tfrac{\pi}{2}) = \sin \alpha \sin \phi \cos \Gamma + \cos \alpha \cos \phi = 0 \qquad \text{(II-11)}$$

Therefore:

$$\cos \Gamma = -\text{ctn } \alpha \, \text{ctn } \phi \qquad \text{(II-12)}$$

$$\sin \Gamma = \sqrt{1 - \text{ctn}^2 \alpha \, \text{ctn}^2 \phi} \qquad \text{(II-13)}$$

$$\Gamma = \arctan\left(\frac{\sin \Gamma}{\cos \Gamma}\right) \tag{II-14}$$

If J_2 is now defined such that the total irradiance E on the target surface element is given by

$$E = B\,(J_1 + J_2) \tag{II-15}$$

then

$$J_2 = \int_{\frac{\pi}{2}-\alpha}^{\Phi} d\phi \int_{-\Gamma}^{\Gamma} (\sin\alpha \sin^2\phi \cos\theta + \cos\alpha \sin\phi \cos\phi)\, d\theta \tag{II-16}$$

Since Γ is a function of ϕ, then equation (II-16) must first be integrated with respect to θ, which yields

$$J_2 = 2 \int_{\frac{\pi}{2}-\alpha}^{\Phi} (\sin\alpha \sin^2\phi \sin\Gamma + \Gamma \cos\alpha \sin\phi \cos\phi)\, d\phi \tag{II-17}$$

For convenience, J_2 may be split into two terms such that

$$J_2 = (P_1 + P_2) \tag{II-18}$$

where

$$P_1 = 2 \int_{\frac{\pi}{2}-\alpha}^{\Phi} (\sin\alpha \sin^2\phi \sin\Gamma)\, d\phi \tag{II-19}$$

and

$$P_2 = 2 \int_{\frac{\pi}{2}-\alpha}^{\Phi} (\Gamma \cos\alpha \sin\phi \cos\phi)\, d\phi \tag{II-20}$$

Substituting equation (II-13) into equation (II-19) and simplifying yields

$$P_1 = 2 \int_{\frac{\pi}{2} - \alpha}^{\Phi} \sin \phi \sqrt{\sin^2\alpha - \cos^2\phi} \, d\phi \tag{II-21}$$

Letting

$$\chi = \cos \phi$$

$$d\chi = -\sin \phi \, d\phi$$

then equation (II-21) may be written as

$$P_1 = -2 \int_{\cos(\frac{\pi}{2} - \alpha)}^{\cos \Phi} \sqrt{\sin^2\alpha - \chi^2} \, d\chi \tag{II-22}$$

which, when integrated yields

$$P_1 = (\tfrac{\pi}{2} - \xi) \sin^2\alpha - G \cos \Phi \tag{II-23}$$

where

$$G = \sqrt{\sin^2\alpha - \cos^2\Phi} \tag{II-24}$$

$$\xi = \arctan\left(\frac{\cos \Phi}{G}\right) \tag{II-25}$$

The integration of equation (II-20) for P_2 proceeds, by parts, as follows.

Letting

$$dV = \cos \alpha \sin \phi \cos \phi \, d\phi \tag{II-26}$$

then

$$V = \int dV = \frac{\cos \alpha \sin^2 \phi}{2} \tag{II-27}$$

Using these parameters, equation (II-20) may be written as

$$P_2 = 2 \int_{\frac{\pi}{2} - \alpha}^{\Phi} \Gamma \, dV = 2 \, \Gamma \, V \Big|_{\frac{\pi}{2} - \alpha}^{\Phi} - 2 \int_{\frac{\pi}{2} - \alpha}^{\Phi} V \, d\Gamma \tag{II-28}$$

Separating the terms of this equation such that

$$P_2 = Q_1 + Q_2 \tag{II-29}$$

then the first term is

$$Q_1 = 2 \, \Gamma \, V \Big|_{\frac{\pi}{2} - \alpha}^{\Phi} = \Gamma \cos \alpha \sin^2 \phi \Big|_{\frac{\pi}{2} - \alpha}^{\Phi} \tag{II-30}$$

Defining δ as the value of Γ when $\phi = \Phi$ and ζ as the value of Γ when $\phi = \frac{\pi}{2} - \alpha$, then from equations (II-12),(II-13) and (II-14)

$$\cos \delta = -\text{ctn} \, \alpha \, \text{ctn} \, \Phi \tag{II-31}$$

$$\sin \delta = \sqrt{1 - \text{ctn}^2 \alpha \, \text{ctn}^2 \Phi} \tag{II-32}$$

$$\delta = \arctan \left(\frac{\sin \delta}{\cos \delta} \right) \tag{II-33}$$

$$\cos \zeta = -\text{ctn} \, \alpha \, \text{ctn} \left(\frac{\pi}{2} - \alpha \right) = -1 \tag{II-34}$$

$$\sin \zeta = 0 \tag{II-35}$$

$$\zeta = \arctan\left(\frac{0}{-1}\right) = \pi \tag{II-36}$$

Since $\alpha \leq \frac{\pi}{2}$ for Case 2, then from these equations it can be seen that $\pi \leq \delta \leq \frac{\pi}{2}$. Therefore, Q_1 is given by

$$Q_1 = \delta \cos \alpha \sin^2\Phi - \pi \cos^3\alpha \tag{II-37}$$

The second term Q_2 is

$$Q_2 = -2 \int_{\frac{\pi}{2}-\alpha}^{\Phi} V \, d\Gamma = \int_{\frac{\pi}{2}-\alpha}^{\Phi} \frac{\cos \alpha \operatorname{ctn} \alpha \, d\phi}{\sqrt{1 - \operatorname{ctn}^2\phi \operatorname{ctn}^2\alpha}} \tag{II-38}$$

Letting

$$\operatorname{ctn} \phi = \tan \alpha \sin \tau \tag{II-39}$$

$$d\phi = \frac{-\tan \alpha \cos \tau \, d\tau}{1 + \tan^2\alpha \sin^2\tau} \tag{II-40}$$

$$\tau = \arcsin(\operatorname{ctn} \alpha \operatorname{ctn} \phi) \tag{II-41}$$

then the equation for Q_2 may be written as

$$Q_2 = \int_{\tau_1}^{\tau_2} \frac{-\cos \alpha \, d\tau}{1 + \tan^2\alpha \sin^2\tau} = \int_{\tau_1}^{\tau_2} \frac{-\cos \alpha \, d\tau}{\cos^2\tau + \sec^2\alpha \sin^2\tau} \tag{II-42}$$

where the limits, τ_1 and τ_2, are

$$\tau_1 = \arcsin\left[\operatorname{ctn}\alpha \operatorname{ctn}\left(\frac{\pi}{2} - \alpha\right)\right] = \frac{\pi}{2} \tag{II-43}$$

$$\tau_2 = \arcsin\left(\operatorname{ctn}\alpha \operatorname{ctn}\Phi\right) = \delta - \frac{\pi}{2} \tag{II-44}$$

Therefore,

$$Q_2 = \cos^2\alpha \left\{ \frac{\pi}{2} - \arctan\left[\frac{\tan\left(\delta - \frac{\pi}{2}\right)}{\cos\alpha} \right] \right\} \tag{II-45}$$

From equations (II-15), (II-18) and (II-29)

$$E = B\left(J_1 + P_1 + Q_1 + Q_2\right) \tag{II-46}$$

Substituting equations (II-10), (II-23), (II-37) and (II-45) into this equation and simplifying yields the desired equation for the irradiance E produced on the target surface element by a spherical Lambertian radiator when $\left(\frac{\pi}{2} - \Phi\right) < \alpha \leq \frac{\pi}{2}$. This equation is

$$E = B\left[U \sin^2\alpha - G\cos\Phi + \left(\frac{\pi}{2} + H\right)\cos\alpha \sin^2\alpha + C\cos^2\alpha\right] \tag{II-47}$$

where

$$G = \sqrt{\sin^2\alpha - \cos^2\Phi} \tag{II-48}$$

$$U = \frac{\pi}{2} - \xi = \arctan\left(\frac{G}{\cos\Phi}\right) \tag{II-49}$$

$$H = \delta - \frac{\pi}{2} = \arctan\left(\frac{\operatorname{ctn}\alpha \operatorname{ctn}\Phi}{\sqrt{1 - \operatorname{ctn}^2\alpha \operatorname{ctn}^2\Phi}}\right) \tag{II-50}$$

$$C = \arctan\left(\sin\alpha \sqrt{\tan^2\Phi - \operatorname{ctn}^2\alpha}\right) \tag{II-51}$$

Case 3. $\frac{\pi}{2} < \alpha < (\frac{\pi}{2} + \Phi)$

From the geometry of figure II-1, it can be seen that, when $\alpha > \frac{\pi}{2}$, less than half of the spherical source can be seen within the field-of-view from the front of the target surface element. Therefore, for all values of ϕ, the range of θ is limited by the condition that $\psi = \frac{\pi}{2}$. Furthermore, if Γ is again defined as the upper limit on θ, then $0 \leq \Gamma < \frac{\pi}{2}$ and the lower limit on θ is $-\Gamma$. The value of Γ is given by equation (II-14). Therefore, the irradiance E produced on a target surface element by a spherical Lambertian radiator is

$$E = B \int_{\alpha - \frac{\pi}{2}}^{\Phi} d\phi \int_{-\Gamma}^{\Gamma} (\sin \alpha \sin^2\phi \cos \theta + \cos \alpha \sin \phi \cos \phi)\, d\theta \quad \text{(II-52)}$$

Since the form of this equation is identical with that of equation (II-16), this equation may be integrated using the same techniques as were applied to integrate equation (II-16). Letting P_1', Q_1', and Q_2' represent quantities which correspond to the quantities P_1, Q_1 and Q_2 defined for Case 2, then, because $\cos (\alpha - \frac{\pi}{2}) = \cos (\frac{\pi}{2} - \alpha) = \sin \alpha$

$$P_1' = P_1 = (\tfrac{\pi}{2} - \xi) \sin^2\alpha - G \cos \phi \quad \text{(II-53)}$$

Defining ζ' as the value of Γ when $\Phi = \alpha - \frac{\pi}{2}$

$$\cos \zeta' = - \operatorname{ctn} \alpha \operatorname{ctn} (\alpha - \tfrac{\pi}{2}) = 1 \quad \text{(II-54)}$$

then $\zeta' = 0$ and

$$Q_1' = \delta \cos \alpha \sin^2\Phi \quad \text{(II-55)}$$

Correspondingly,

$$Q_{\hat{2}} = - \cos^2\alpha \left\{ \frac{\pi}{2} + \arctan \left[\frac{\tan (\delta - \frac{\pi}{2})}{\cos \alpha} \right] \right\} \qquad \text{(II-56)}$$

Combining these terms so that the irradiance E is given by

$$E = B (P_{\hat{1}} + Q_{\hat{1}} + Q_{\hat{2}}) \qquad \text{(II-57)}$$

yields an expression which is identical to equation (II-47).

SUMMARY

The irradiance produced on a target surface element by a spherical Lambertian radiator can be determined, for any orientation of the target surface element for which $0 \leq \alpha \leq (\frac{\pi}{2} - \Phi)$, by using equation (II-8). For those orientations of the target surface element for which $(\frac{\pi}{2} - \Phi) < \alpha < (\frac{\pi}{2} + \Phi)$, the field-of-view to the source is partially obstructed due to the tilt of the target surface element, in which case equation (II-47) applies. When $(\frac{\pi}{2} + \Phi) \leq \alpha \leq \pi$, the source cannot be seen.

APPENDIX III
IRRADIANCE PRODUCED ON A TARGET SURFACE ELEMENT BY RADIANT FLUX REFLECTED FROM A SPHERICAL LAMBERTIAN REFLECTOR

The irradiance dE produced on a target surface element dT, by an element of radiant flux d^2F reflected from an element of area on a reflecting surface to the target element, is equal to the product of the radiance B of the reflecting element, the cosine of the angle of incidence ψ, and the element of solid angle $d\Omega$ subtended by the reflecting element at the target element. That is

$$dE = \frac{d^2F}{dT} = B \cos \psi \, d\Omega \qquad \text{(III-1)}$$

If the reflecting surface is a Lambertian reflector then, by definition, the radiance B of an element of area on the reflecting surface is given by (see Appendix I)

$$B = \frac{A E_s}{\pi} \qquad \text{(III-2)}$$

where E_s is the irradiance produced on the reflecting element by the source and A is the diffuse reflectance (the albedo) of the Lambertian reflector. Combining these equations, the irradiance dE produced on a target surface element by radiant flux reflected from an element of area on the surface of a Lambertian reflector is given by

$$dE = \frac{A E_s}{\pi} \cos \psi \, d\Omega \qquad \text{(III-3)}$$

Using this expression, it is possible to determine the irradiance produced on a target surface by radiant flux reflected from a spherical Lambertian reflector to the target surface. The pertinent geometrical

relationships involved are schematically represented in figure III-1, where dT is an element of area on the target surface and dS is an element of area on the surface of a spherical Lambertian reflector. The coordinate systems of this figure have been chosen so that (1) X and X' are parallel, (2) Y and Y' are parallel, and (3) the centers of the source, the spherical Lambertian reflector, and the target surface element all lie in the XZ-plane (and thus the $X'Z$-plane). The unit vector $\hat{n}$ is normal to the target element dT. The unit vector $\hat{m}$ is normal to reflecting element dS. The unit vector $\hat{r}$ lies in the direction from dT to dS. The unit vector $\hat{p}$ lies in the direction from dS to the center of the source. The unit vector $\hat{u}$ lies in the XZ-plane in the direction from the center of the spherical Lambertian reflector to the center of the source. The unit vectors $\hat{n}$, $\hat{m}$, $\hat{r}$ and $\hat{u}$ may be expressed, in terms of the unit orthogonal triad $\hat{i}$, $\hat{j}$, $\hat{k}$ (see Appendix I) and the angles shown in figure III-1 as follows:

$$\hat{n} = \hat{i} \sin\alpha \cos\beta + \hat{j} \sin\alpha \sin\beta + \hat{k} \cos\alpha \qquad \text{(III-4)}$$

$$\hat{m} = \hat{i} \sin T \cos\theta + \hat{j} \sin T \sin\theta - \hat{k} \cos T \qquad \text{(III-5)}$$

$$\hat{r} = \hat{i} \sin\phi \cos\theta + \hat{j} \sin\phi \sin\theta + \hat{k} \cos\phi \qquad \text{(III-6)}$$

$$\hat{u} = \hat{i} \sin\gamma - \hat{k} \cos\gamma \qquad \text{(III-7)}$$

By definition, the cosine of the angle of incidence (the angle ψ between $\hat{n}$ and $\hat{r}$) is

$$\cos\psi = \hat{n}\cdot\hat{r} = \sin\alpha \sin\phi \cos(\theta - \beta) + \cos\alpha \cos\phi \qquad \text{(III-8)}$$

The element of solid angle $d\Omega$ subtended by the reflecting element dS may be written in terms of the direction angles ϕ and θ of the unit vector $\hat{r}$ (see Appendices I and II) as

$$d\Omega = \sin\phi \, d\phi \, d\theta \qquad \text{(III-9)}$$

The irradiance E_s produced by the source on the reflecting element dS is a function of the geometry, the location, and the radiance of the

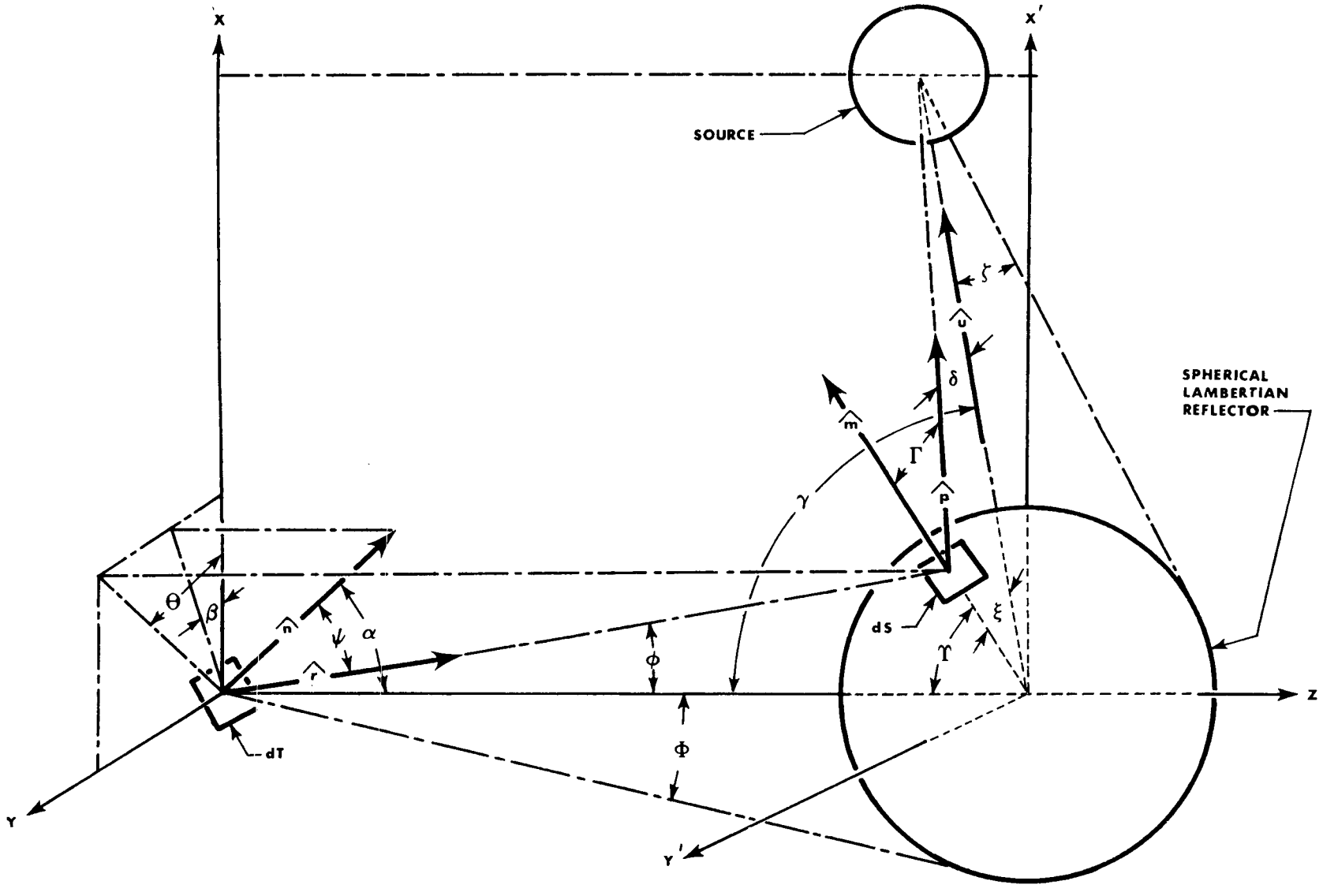

Figure III-1. Schematic representation of the geometrical relationships which govern the reflection of radiant flux from a spherical Lambertian reflector to a target surface element.

source. If it is now assumed that the source is a spherical Lambertian radiator of radiance B_s, it is possible to express E_s in terms of the parameters of figure III-1. Defining ρ as the field half-angle subtended by the source at dS, then (see Appendix II) when $0 \leq \Gamma \leq \frac{\pi}{2} - \rho$ (see equation II-8)

$$E_s = \pi B_s \sin^2\rho \cos \Gamma \tag{III-10}$$

and when $\frac{\pi}{2} - \rho < \Gamma < \frac{\pi}{2} + \rho$ (see equation II-47)

$$E_s = B_s \left[U \sin^2\Gamma - G \cos \rho + (\tfrac{\pi}{2} + H) \cos \Gamma \sin^2\Gamma + C \cos^2\Gamma \right] \tag{III-11}$$

where

$$G = \sqrt{\sin^2\Gamma - \cos^2\rho} \tag{III-12}$$

$$U = \arctan \left(\frac{G}{\cos \rho} \right) \tag{III-13}$$

$$H = \arctan \left(\frac{\operatorname{ctn} \Gamma \operatorname{ctn} \rho}{\sqrt{1 - \operatorname{ctn}^2\Gamma \operatorname{ctn}^2\rho}} \right) \tag{III-14}$$

$$C = \arctan \left(\sin \Gamma \sqrt{\tan^2\rho - \operatorname{ctn}^2\Gamma} \right) \tag{III-15}$$

When $\frac{\pi}{2} + \rho \leq \Gamma \leq \pi$

$$E_s = 0 \tag{III-16}$$

If equations (III-8) and (III-9) are now substituted into equation (III-3), the expression for the irradiance E on the target surface element, produced by the radiant flux reflected from the spherical Lambertian reflector to the target surface element, may be written as

$$E = \frac{A}{\pi} \iint E_s \left[\sin \alpha \sin^2\phi \cos (\theta - \beta) + \cos \alpha \cos \phi \sin \phi \right] d\phi \, d\theta \tag{III-17}$$

As was the case with equation (II-6) for the irradiance produced on a target surface element by a spherical Lambertian source (see Appendix II), this equation must be integrated over those ϕ , θ directions which are not only within the field subtended by the source at the target location (the directions for which $0 \leq \phi \leq \Phi$), but which are also within the field-of-view from the front of the target surface element (the directions for which $0 \leq \psi \leq \frac{\pi}{2}$). However, the irradiance E_s seen at the surface of the spherical Lambertian reflector is a variable (and thus is a function of both ϕ and θ) and there is an additional condition which must be applied to determine the limits of integration for equation (III-17). This third condition requires that equation (III-17) be integrated only over those ϕ , θ directions which intersect that portion of the surface of the spherical Lambertian reflector which is being irradiated by the source; i.e., the directions for which $E_s > 0$.

Since equation (III-17) is to be integrated in ϕ and θ , it is necessary that E_s (and thus Γ and ρ) be expressed as functions of these two independent variables. Defining R as the radius of the reflector and D as the distance between the center of the source and the center of the reflector, then from the geometry of figure III-1

$$\Gamma = \delta + \xi \tag{III-18}$$

$$R \sin \xi = (D - R \cos \xi) \tan \delta \tag{III-19}$$

$$\cos \xi = \hat{m} \cdot \hat{u} = \sin \gamma \sin \Upsilon \cos \theta + \cos \gamma \cos \Upsilon \tag{III-20}$$

$$R \sin \Upsilon = \left[\left(\frac{R}{\sin \Phi} \right) - R \cos \Upsilon \right] \tan \phi \tag{III-21}$$

From equation (III-21)

$$\sin \Upsilon = \frac{\sin \phi \cos \phi}{\sin \Phi} - \sin \phi \sqrt{1 - \frac{\sin^2 \phi}{\sin^2 \Phi}} \tag{III-22}$$

$$\cos \Upsilon = \frac{\sin^2\phi}{\sin \Phi} + \cos \phi \sqrt{1 - \frac{\sin^2\phi}{\sin^2\Phi}} \qquad \text{(III-23)}$$

From equation (III-19) and figure III-1 (ζ is the field half-angle subtended by the spherical reflector at the center of the source)

$$\delta = \arctan \left(\frac{R \sin \xi}{D - R \cos \xi} \right) = \arctan \left(\frac{\sin \xi}{\csc \zeta - \cos \xi} \right) \qquad \text{(III-24)}$$

From equation (III-18)

$$\cos \Gamma = \cos (\delta + \xi) = \cos \delta \cos \xi - \sin \delta \sin \xi \qquad \text{(III-25)}$$

Using trigonometric identities, equation (III-24) can be substituted into equation (III-25) to eliminate δ. Thus

$$\cos \Gamma = \frac{\cos \xi - \sin \zeta}{\sqrt{1 - 2 \cos \xi \sin \zeta + \sin^2\zeta}} \qquad \text{(III-26)}$$

Substitution of equations (III-22) and (III-23) into equation (III-20) yields

$$\cos \xi = \csc \Phi \Big[(\sin \gamma \cos \theta \cos \phi + \cos \gamma \sin \phi) \sin \phi - (\sin \gamma \cos \theta \sin \phi - \cos \gamma \cos \phi) \sqrt{\sin^2\Phi - \sin^2\phi} \Big] \qquad \text{(III-27)}$$

which, if substituted into equation (III-26), would yield an expression for Γ in terms of the two independent variables ϕ and θ.

From the geometry of figure III-1, the distance D_s from the reflecting element dS to the center of the source is

$$D_s = \frac{(D - R \cos \xi)}{\cos \delta} = D \sqrt{1 - 2 \cos \xi \sin \zeta + \sin^2\zeta} \qquad \text{(III-28)}$$

Letting R_s be the radius of the source and ε be the field half-angle

subtended by the source at the center of the spherical reflector, then the field half-angle ρ subtended by the source at dS is given by

$$\sin \rho = \frac{R_s}{D_s} = \frac{\sin \varepsilon}{\sqrt{1 - 2 \cos \xi \sin \zeta + \sin^2 \zeta}} \qquad \text{(III-29)}$$

$$\rho = \arctan \left(\frac{\sin \varepsilon}{\sqrt{\sin^2 \zeta - 2 \cos \xi \sin \zeta + \cos^2 \varepsilon}} \right) \qquad \text{(III-30)}$$

If equation (III-27) was substituted into equations (III-29) and (III-30), the resulting expressions for $\sin \rho$ and for ρ would be in terms of the two independent variables ϕ and θ.

From the preceding, it can be seen that it is possible to obtain expressions for E_s in terms of the two independent variables ϕ and θ by substituting equations (III-26), (III-27), (III-29) and (III-30) into equations (III-10) through (III-16), using trigonometric identities as appropriate. However, if these expressions are substituted into equation (III-17), it will be seen that the complexity of the resulting expressions, coupled with the complicated limits of integration, makes it extremely difficult (if not impossible) to integrate to obtain a general and exact expression (or set of expressions) for the irradiance E produced on a target surface element by the radiant flux emitted by a spherical Lambertian radiator and reflected from a spherical Lambertian reflector to the target surface element. The irradiance E, however, can be closely approximated by applying the following numerical integration procedure.

If the field subtended by the spherical Lambertian reflector is divided into many small elements of solid angle and if these elements of solid angle are sufficiently small, then it can be assumed that (1) the irradiance E_s produced by the source is a constant over that portion of the surface of the spherical Lambertian reflector which can be seen through a given element of solid angle, and (2) all of the radiant flux, which is

reflected from the spherical Lambertian reflector and which is contained within a given element of solid angle, strikes the target surface element at the same angle of incidence ψ. If $\Delta\Omega_{ij}$ is defined as the element of solid angle which is centered about the direction $\left(\phi_i , \theta_j\right)$, then, from equation (III-9)

$$\Delta\Omega_{ij} = \int_{\phi_i - \frac{\Delta\phi}{2}}^{\phi_i + \frac{\Delta\phi}{2}} \sin\phi \, d\phi \int_{\theta_j - \frac{\Delta\theta}{2}}^{\theta_j + \frac{\Delta\theta}{2}} d\theta \qquad \text{(III-31)}$$

Integrating yields

$$\Delta\Omega_{ij} = 2\left[\sin\phi_i \sin\left(\frac{\Delta\phi}{2}\right)\right]\Delta\theta \qquad \text{(III-32)}$$

Thus, the irradiance E produced on the target surface element by the radiant flux reflected from the spherical Lambertian reflector to the target surface element is, from equations (III-3) and (III-31) and assumptions (1) and (2) above,

$$E = \frac{A}{\pi} \sum_{i=1}^{n} \sum_{j=1}^{m} E_{s_{ij}} \cos\psi_{ij} \, \Delta\Omega_{ij} \qquad \text{(III-33)}$$

where A is the diffuse reflectance (the albedo) of the spherical Lambertian reflector. From equation (III-8)

$$\cos\psi_{ij} = \sin\alpha \sin\phi_i \cos(\theta_j - \beta) + \cos\alpha \cos\phi_i \qquad \text{(III-34)}$$

where α and β are the direction angles which define the orientation of the target surface element as shown in figure III-1. (When $\cos\psi_{ij} < 0$,

the radiant flux contained within the element of solid angle $\Delta\Omega_{ij}$ does not strike the front of the target surface element. To avoid erroneous calculation either this term of the series must be omitted or, alternatively, $\cos \psi_{ij}$ must be set equal to zero.)

Before the irradiance $E_{s_{ij}}$ seen on the front surface of the spherical Lambertian reflector through the element of solid angle $\Delta\Omega_{ij}$ can be determined, the following calculations must be made:

From equations (III-22), (III-23) and (III-20)

$$\sin T_i = \frac{\sin \phi_i \left(\cos \phi_i - \sqrt{\sin^2\Phi - \sin^2\phi_i}\right)}{\sin \Phi} \tag{III-35}$$

$$\cos T_i = \frac{\sin^2\phi_i + \cos \phi_i \sqrt{\sin^2\Phi - \sin^2\phi_i}}{\sin \Phi} \tag{III-36}$$

$$\cos \xi_{ij} = \sin \gamma \sin T_i \cos \theta_j + \cos \gamma \cos T_i \tag{III-37}$$

where Φ is the field half-angle subtended by the spherical Lambertian reflector at the target location and γ is the angle, at the center of the reflector, between the directions to the target and to the center of the spherical Lambertian source. From equation (III-26) and the trigonometric identities

$$\Gamma_{ij} = \arctan \left(\frac{\sin \xi_{ij}}{\cos \xi_{ij} - \sin \zeta}\right) \tag{III-38}$$

where ζ is the field half-angle subtended by the spherical Lambertian reflector at the center of the source. From equation (III-30)

$$\rho_{ij} = \arctan\left(\frac{\sin\varepsilon}{\sqrt{\sin^2\zeta - 2\cos\xi_{ij}\sin\zeta + \cos^2\varepsilon}}\right) \qquad \text{(III-39)}$$

where ε is the field half-angle subtended by the spherical Lambertian source at the center of the reflector.

After making the calculations defined by equations (III-35) through (III-39), the value of $E_{s_{ij}}$ is determined as follows: (B_s is the radiance of the spherical Lambertian source.)

When $0 \leq \Gamma_{ij} \leq \frac{\pi}{2} - \rho_{ij}$ (see equation III-10)

$$E_{s_{ij}} = \pi B_s \sin^2\rho_{ij} \cos\Gamma_{ij} \qquad \text{(III-40)}$$

When $\frac{\pi}{2} - \rho_{ij} < \Gamma_{ij} < \frac{\pi}{2} + \rho_{ij}$ (see equations III-11 through III-15)

$$E_{s_{ij}} = B_s\left[\left(U_{ij} + V_{ij}\cos\Gamma_{ij}\right)\sin^2\Gamma_{ij} - G_{ij}\cos\rho_{ij} + C_{ij}\cos^2\Gamma_{ij}\right] \qquad \text{(III-41)}$$

where

$$G_{ij} = \sqrt{\sin^2\Gamma_{ij} - \cos^2\rho_{ij}} \qquad \text{(III-42)}$$

$$U_{ij} = \arctan\left(\frac{G_{ij}}{\cos\rho_{ij}}\right) \qquad \text{(III-43)}$$

$$V_{ij} = \frac{\pi}{2} + \arctan\left(\frac{\operatorname{ctn}\Gamma_{ij}\operatorname{ctn}\rho_{ij}}{\sqrt{1 - \operatorname{ctn}\Gamma_{ij}\operatorname{ctn}\rho_{ij}}}\right) \qquad \text{(III-44)}$$

$$C_{ij} = \arctan\left(\sin\Gamma_{ij}\sqrt{\tan^2\rho_{ij} - \operatorname{ctn}^2\Gamma_{ij}}\right) \qquad \text{(III-45)}$$

When $\frac{\pi}{2} + \rho_{ij} \leq \Gamma_{ij} \leq \pi$ (see equation III-16)

$$E_{s_{ij}} = 0 \qquad \text{(III-46)}$$

SUMMARY

The irradiance produced on a target surface element by radiant flux emitted by a spherical Lambertian source and reflected from a spherical Lambertian reflector to the target surface element can be determined, to a close approximation, using the numerical integration process defined by equation (III-33). In performing the numerical integration, equation (III-32) and equations (III-34) through (III-45) are utilized.

APPENDIX IV
COMPUTER PROGRAMS

Several computer programs were written for and utilized in this study of the characteristics and the simulation of the Planetary Radiation Environment. A brief description of each computer program, including a list of the basic equations utilized to generate each program, is given below.

Program - SPACE

For each specified location in the vicinity of the earth, this computer program calculates the irradiance components and the total irradiance experienced by a target surface element at that location as a function of the orientation of the target surface element. In making the calculations, it is assumed that: (1) the sun is a spherical Lambertian radiator; (2) the earth is in a state of thermal equilibrium; (3) the earth emits radiant flux as a spherical Lambertian radiator; and (4) the earth reflects radiant flux as a spherical Lambertian reflector. The geometrical relationships involved are illustrated in figure IV-1 where: α and β are the direction angles (see Appendix I) of the unit vector $\hat{n}$ normal to the target surface element and define the orientation of the target surface element; γ is the angle, at the center of the earth, between the directions to the sun and to the target element; h is the distance between the target surface element and the earth's surface (the orbital altitude); ε is the field half-angle subtended by the assumed spherical sun at the center of the earth; R is the radius of the assumed spherical earth; and D is the distance between the centers of the sun and the earth. Before making any calculations, the computer program assigns values to ε, R, and D as follows:

$\varepsilon = 0°16'$ (Field half-angle subtended by the sun)

$R = 3958.89$ miles (Radius of a sphere having the same volume as the earth)

$D = 92{,}900{,}000$ miles (Mean radius of the earth's orbit)

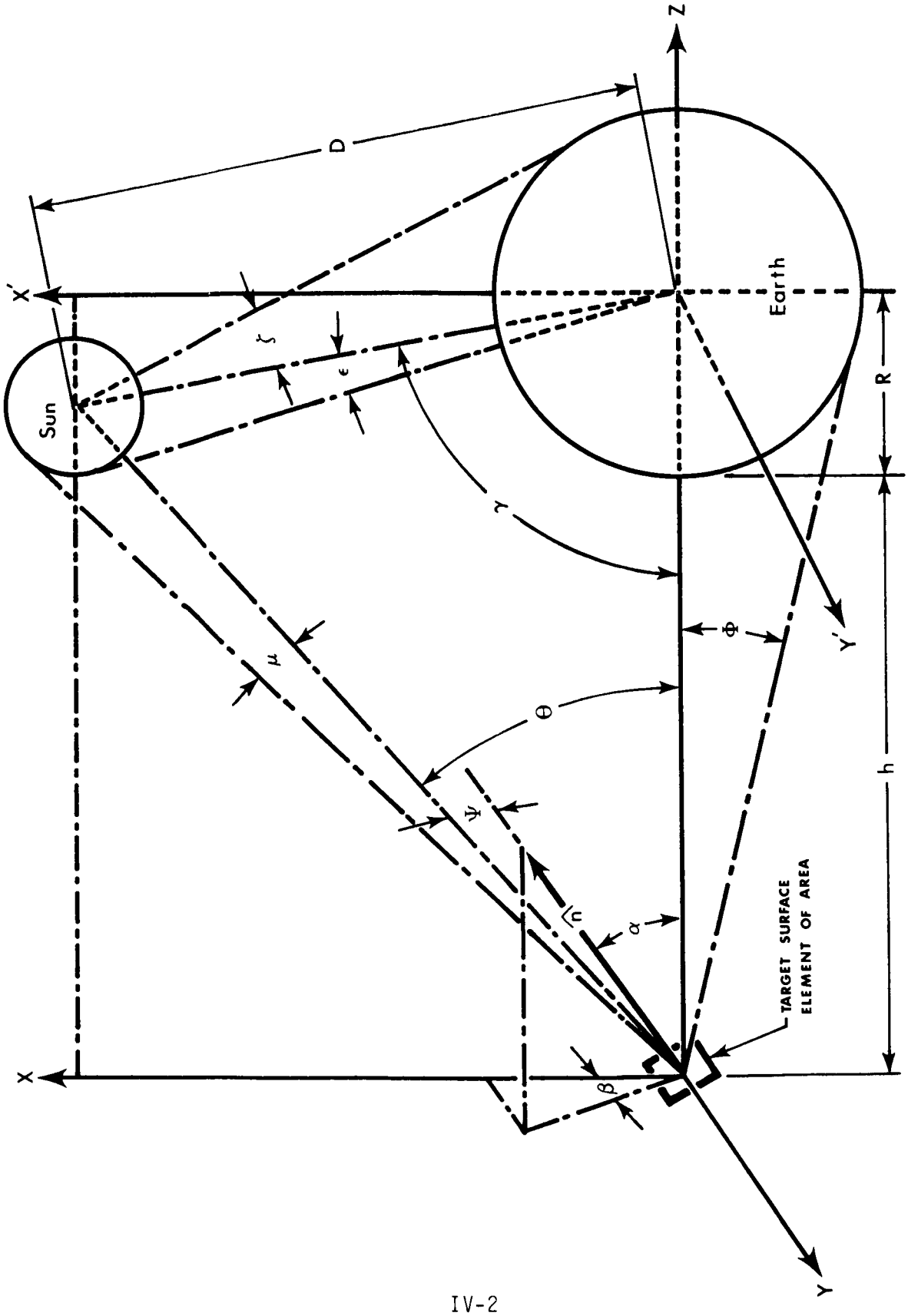

Figure IV-1. Schematic representation of the geometrical relationships which affect the irradiance experienced by a target surface element in space.

$$E_{s_o} = 130 \text{ watts-per-square-foot (the solar constant)}$$

The parameters h, γ and A (the average albedo of the earth) must be included in the input data to the computer program.

Equations Utilized to Calculate the Irradiance Due to Radiant Flux Emitted by the Sun

The following equations, which define the irradiance E_s on a target surface element due to radiant flux emitted by the sun in terms of the geometrical relationships of figure IV-1, were determined by making parametric substitutions into the equations of Appendix II.

From the geometry of figure IV-1

$$\Theta = \arctan \left[\frac{D \sin \gamma}{(R + h) - D \cos \gamma} \right] \tag{IV-1}$$

$$\mu = \arctan \left(\frac{\sin \varepsilon \sin \Theta}{\sqrt{\sin^2 \gamma - \sin^2 \varepsilon \sin^2 \Theta}} \right) \tag{IV-2}$$

$$\cos \Psi = \sin \alpha \cos \beta \sin \Theta + \cos \alpha \cos \Theta \tag{IV-3}$$

Given that E_{s_o} is the solar constant and assuming that the sun is a spherical Lambertian radiator, the radiance B_s of the sun is, from equation (II-8)

$$B_s = \frac{E_{s_o}}{\pi \sin^2 \varepsilon} \tag{IV-4}$$

Therefore, when $0 \leq \Psi \leq \frac{\pi}{2} - \mu$

$$E_s = \pi B_s \sin^2 \mu \cos \Psi \tag{IV-5}$$

When $\frac{\pi}{2} - \mu < \Psi < \frac{\pi}{2} + \mu$, then

$$E_s = B_s \left[(U + V \cos \Psi) \sin^2 \Psi - G \cos \mu + C \cos^2 \Psi \right] \qquad \text{(IV-6)}$$

where

$$G = \sqrt{\sin^2 \Psi - \cos^2 \mu} \qquad \text{(IV-7)}$$

$$U = \arctan \left(\frac{G}{\cos \mu} \right) \qquad \text{(IV-8)}$$

$$V = \frac{\pi}{2} + \arctan \left(\frac{\operatorname{ctn} \Psi \operatorname{ctn} \mu}{\sqrt{1 - \operatorname{ctn}^2 \Psi \operatorname{ctn}^2 \mu}} \right) \qquad \text{(IV-9)}$$

$$C = \arctan \left(\sin \Psi \sqrt{\tan^2 \mu - \operatorname{ctn}^2 \Psi} \right) \qquad \text{(IV-10)}$$

When $\frac{\pi}{2} + \Phi \leq \Psi \leq \pi$,the target surface element faces away from the sun and thus,

$$E_s = 0 \qquad \text{(IV-11)}$$

Equations Utilized to Calculate the Irradiance Due to Radiant Flux Thermally Emitted from the Earth

If the earth is assumed to be in a state of thermal equilibrium, then the average radiant emittance W_e of the earth is, from equation (4-5)

$$W_e = \frac{(1 - A) E_{s_o}}{4} \qquad \text{(IV-12)}$$

where E_{s_o} is the solar constant and A is the average albedo of the earth. If the earth is assumed to be a spherical Lambertian radiator of uniform radiance, then the radiance B_e of the earth is given by

$$B_e = \frac{W_e}{\pi} \tag{IV-13}$$

The irradiance E_e produced by radiant flux emitted by the earth is calculated as follows.

From the geometry of figure IV-1,

$$\Phi = \arcsin\left(\frac{R}{R + h}\right) = \arctan\left(\frac{R}{\sqrt{2Rh + h^2}}\right) \tag{IV-14}$$

The irradiance E_e produced by radiant flux emitted by the earth is calculated as follows, using the equations from Appendix II, when $0 \leq \alpha \leq \frac{\pi}{2} - \Phi$

$$E_e = \pi B_e \sin^2\Phi \cos\alpha \tag{IV-15}$$

When $\frac{\pi}{2} - \Phi < \alpha < \frac{\pi}{2} + \Phi$

$$E_e = B_e \left[(U + V \cos\alpha) \sin^2\Phi - G \cos\Phi + C \cos^2\alpha\right] \tag{IV-16}$$

where

$$G = \sqrt{\sin^2\alpha - \cos^2\Phi} \tag{IV-17}$$

$$U = \arctan\left(\frac{G}{\cos\Phi}\right) \tag{IV-18}$$

$$V = \frac{\pi}{2} + \arctan\left(\frac{\operatorname{ctn}\alpha \operatorname{ctn}\Phi}{\sqrt{1 - \operatorname{ctn}^2\alpha \operatorname{ctn}^2\Phi}}\right) \tag{IV-19}$$

$$C = \arctan\left(\sin\alpha \sqrt{\tan^2\Phi - \operatorname{ctn}^2\alpha}\right) \tag{IV-20}$$

When $\frac{\pi}{2} + \Phi \leq \alpha \leq \pi$, the target surface element faces away from the earth and thus

$$E_e = 0 \tag{IV-21}$$

Equations Utilized to Calculate the Irradiance Due to Radiant Flux Reflected from the Earth

If the earth is assumed to be a spherical Lambertian reflector whose albedo A is uniform over the entire surface, then the irradiance E_a produced by radiant flux reflected from the earth is calculated using the equations from Appendix III. Thus

$$E_a = \frac{A}{\pi} \sum_{i=1}^{n} \sum_{j=1}^{m} E_{s_{ij}} \cos \psi_{ij} \, \Delta\Omega_{ij} \tag{IV-22}$$

where

$$\cos \psi_{ij} = \sin \alpha \sin \phi_i \cos (\theta_j - \beta) + \cos \alpha \cos \phi_i \tag{IV-23}$$

When the calculated value of $\cos \psi_{ij}$ is negative, the computer program sets $\cos \psi_{ij} = 0$.

The parameter $E_{s_{ij}}$ is calculated as follows. From equations (III-35) through (III-46)

$$\sin \tau_i = \frac{\sin^2 \phi_i \left(\cos \phi_i - \sqrt{\sin^2 \Phi - \sin^2 \phi_i} \right)}{\sin \Phi} \tag{IV-24}$$

$$\cos T_i = \frac{\sin^2\phi_i + \cos\phi_i \sqrt{\sin^2\phi - \sin^2\phi_i}}{\sin\Phi} \tag{IV-25}$$

$$\cos\xi_{ij} = \sin\gamma \sin T_i \cos\theta_j + \cos\gamma \cos T_i \tag{IV-26}$$

$$\sin\zeta = \frac{R}{D} \tag{IV-27}$$

$$\Gamma_{ij} = \arctan\left(\frac{\sin\xi_{ij}}{\cos\xi_{ij} - \sin\zeta}\right) \tag{IV-28}$$

$$\rho_{ij} = \arctan\left(\frac{\sin\varepsilon}{\sqrt{\sin^2\zeta - 2\cos\xi\sin\zeta + \cos^2\varepsilon}}\right) \tag{IV-29}$$

When $0 \leq \Gamma_{ij} \leq \frac{\pi}{2} - \rho_{ij}$

$$E_{s_{ij}} = \pi B_s \sin^2\rho_{ij} \cos\Gamma_{ij} \tag{IV-30}$$

Again, B_s is the radiance of the sun and is given by equation (IV-4).

When $\frac{\pi}{2} - \rho_{ij} < \Gamma_{ij} < \frac{\pi}{2}$

$$E_{s_{ij}} = B_s \left[\left(U_{ij} + V_{ij}\cos\Gamma_{ij}\right)\sin^2\Gamma_{ij} - G_{ij}\cos\rho_{ij} + C_{ij}\cos^2\Gamma_{ij}\right] \tag{IV-31}$$

where

$$G_{ij} = \sqrt{\sin\Gamma_{ij} - \cos^2\rho_{ij}} \tag{IV-32}$$

$$U_{ij} = \arctan\left(\frac{G_{ij}}{\cos\rho_{ij}}\right) \tag{IV-33}$$

$$V_{ij} = \frac{\pi}{2} + \arctan\left(\frac{\text{ctn}\,\Gamma_{ij}\,\text{ctn}\,\rho_{ij}}{\sqrt{1 - \text{ctn}^2\Gamma_{ij}\,\text{ctn}^2\rho_{ij}}}\right) \qquad \text{(IV-34)}$$

$$C_{ij} = \arctan\left(\sin\Gamma_{ij}\sqrt{\tan^2\rho_{ij} - \text{ctn}^2\Gamma_{ij}}\right) \qquad \text{(IV-35)}$$

When $\frac{\pi}{2} + \rho_{ij} \leq \Gamma_{ij} \leq \pi$, the element of area on the earth which lies in the direction ϕ_i , θ_j from the target element location, is facing away from the sun and thus

$$E_{s_{ij}} = 0 \qquad \text{(IV-36)}$$

Before equations (IV-22) through (IV-36) can be utilized to calculate E_a , it is necessary to define the parameters $\Delta\Omega_{ij}$, ϕ_i , θ_j , n and m . This is accomplished, in the computer program, through the following procedure.

In the input data to the computer program, it is specified that the solid angle Ω subtended by the earth at the target element location is to be divided into approximately N elements $\Delta\Omega_{ij}$. Therefore, as the first step in this procedure, set

$$\phi_1 = 0 \qquad \text{(IV-37)}$$

$$\Delta\Omega_{11} = \frac{\Omega}{N} = \frac{2\pi\,(1 - \cos\,\Phi)}{N} \qquad \text{(IV-38)}$$

If δ is now defined so that

$$\Delta\Omega_{11} = 2\pi\,(1 - \cos\,\delta) \qquad \text{(IV-39)}$$

the equations (IV-38) and (IV-39) can be solved for δ , which yields

$$\delta = \arctan \left[\frac{(1 - \cos \Phi)\sqrt{2N - (1 - \cos \Phi)}}{N - (1 - \cos \Phi)} \right] \qquad \text{(IV-40)}$$

The parameter n (the upper limit on i) is given by

$$n = \left(\frac{\Phi}{\sqrt{\Delta\Omega_{11}}} + 1.75 \right)^{*} \qquad \text{(IV-41)}$$

[In this and the following equations, an asterisk (*) in the exponent position indicates that the computed value is truncated to an integer before proceeding with the calculation.]

Given the value of n, then

$$\Delta\phi = \frac{\Phi - \delta}{n} \qquad \text{(IV-42)}$$

$$\phi_2 = \delta + \frac{\Delta\phi}{2} \qquad \text{(IV-43)}$$

$$\phi_{i+1} = \phi_i + \Delta\phi \qquad \text{if } i \geq 2 \qquad \text{(IV-44)}$$

If, using equation (III-32), m is defined so that

$$m\ \Delta\Omega_{ij} = 4\pi \left[\sin \phi_i \sin \left(\frac{\Delta\phi}{2} \right) \right] \qquad \text{(IV-45)}$$

and since it is desirable that $\Delta\Omega_{ij}$ be approximately equal to $\Delta\Omega_{11}$, then from equations (IV-38) and (IV-45) m is given by

$$m = \left[\frac{2N \sin \phi_i \sin \left(\frac{\Delta\phi}{2} \right)}{1 - \cos \Phi} + 0.5 \right]^{*} \qquad \text{(IV-46)}$$

Therefore, when $i \geq 2$

$$\Delta\theta_i = \frac{2\pi}{m} \tag{IV-47}$$

$$\theta_1 = \frac{\Delta\theta_i}{2} \tag{IV-48}$$

$$\theta_{j+1} = \theta_j + \Delta\theta_i \quad \text{if} \quad j \geq 1 \tag{IV-49}$$

$$\Delta\Omega_{ij} = 2 \left[\sin \phi_i \sin\left(\frac{\Delta\phi}{2}\right)\right] \Delta\theta_i \tag{IV-50}$$

Information Provided by the Computer Program

The location of the target surface element is defined by the input values specified for γ and h. The orientation of the target surface element is defined by the direction angles (α and β) of the target element surface normal. Defining

$$n_\alpha = \left(\frac{\Phi + \frac{\pi}{2}}{\Delta\alpha}\right) + 1 \tag{IV-51}$$

$$n_\beta = \left(\frac{\pi}{\Delta\beta}\right) + 1 \tag{IV-52}$$

where the values of $\Delta\alpha$ and $\Delta\beta$ are specified in the input data, the values of α and β are varied for each specified target location, in accordance with the expressions:

$$\alpha_i = (i - 1)\,\Delta\alpha \tag{IV-53}$$

where i varies from 1 to n_α, and

$$\beta_j = (j - 1)\,\Delta\beta \tag{IV-54}$$

where j varies from 1 to n_β. The following parameters are calculated

and tabulated for each orientation (α_i , β_j) of the target surface element:

E_s = Irradiance produced, on the target surface element, by the radiant flux emitted by the sun [see equations (IV-1) through (IV-11)] .

E_e = Irradiance produced, on the target surface element, by the radiant flux thermally emitted from the earth [see equations (IV-12) through (IV-21)] .

E_a = Irradiance produced, on the target surface element, by the radiant flux reflected by the earth [see equations (IV-22) through (IV-50)] .

$E = E_s + E_e + E_a$ = Total irradiance experienced by the target surface element.

$E_p = E_e + E_a$ = Total irradiance produced, on the target surface element, by the radiant flux emanating from the earth.

$\overline{E}_p = \frac{E_p}{E_{p_o}} = \frac{E_e + E_a}{E_{e_o} + E_{a_o}}$ = Normalized irradiance produced, on the target surface element, by the radiant flux emanating from the earth.

$\overline{E}_e = \frac{E_e}{E_{e_o}}$ = Normalized irradiance produced, on the target surface element, by the radiant flux thermally emitted from the earth.

$Q = \frac{E_a}{E_e}$ = ratio between the two spectral components of the irradiance produced, on the target surface element, by the radiant flux emanating from the earth.

$$S = 100\left(1 - \frac{\overline{E}_e}{\overline{E}_p}\right) = 100\left[1 - \frac{E_e\left(E_{e_o} + E_{a_o}\right)}{E_{e_o}\left(E_e + E_a\right)}\right] = \text{percent}$$

error in the irradiance produced, on the target surface element, by the radiant flux emanating from the simulated earth if the earth is simulated as a spherical Lambertian radiator of uniform radiance.

In the above parametric definitions, the quantities E_{e_o}, E_{a_o} and E_{p_o} refer to the values calculated for E_e, E_a, and E_p, respectively, when $\alpha = 0$.

Program - ORBVAR

This program calculates, as a function of orbital position, the irradiance E_{e_o} produced by radiant flux thermally emitted from the earth and the irradiance E_{a_o} produced by radiant flux reflected from the earth, on a target surface element whose normal lies in the direction toward the center of the earth. The equations utilized for these calculations are essentially equations (IV-12) through (IV-50) with those simplifications incorporated that result from setting $\alpha = 0$. Define n_γ so that

$$n_\gamma = \left(\frac{\pi}{\Delta\gamma}\right) + 1 \qquad \text{(IV-55)}$$

where the value of $\Delta\gamma$ is specified in the input data. The angle γ,

at the center of the earth between the directions to the sun and to the orbital position of the target surface element, is varied in accordance with the expression

$$\gamma_i = (i - 1)\ \Delta\gamma \qquad \text{(IV-56)}$$

where i varies from 1 to n_γ. For each specified value of the orbital altitude h, the computer program calculates the following parameters and tabulates them as a function of γ_i:

E_{e_o} = Irradiance produced, by the radiant flux thermally emitted from the earth, on a target surface element oriented so that $\alpha = 0$.

E_{a_o} = Irradiance produced, by the radiant flux reflected by the earth, on a target surface element oriented so that $\alpha = 0$.

$E_{p_o} = E_{e_o} + E_{a_o}$ = Total irradiance produced, by the radiant flux emanating from the earth, on a target surface element oriented so that $\alpha = 0$.

$Q = \dfrac{E_{a_o}}{E_{e_o}}$ = ratio between the two spectral components of the irradiance produced, on the target surface element, by the radiant flux emanating from the earth.

$W_{ave} = \dfrac{E_{p_o}}{\sin^2\Phi} = \dfrac{E_{e_o} + E_{a_o}}{\sin^2\Phi}$ = average radiant emittance of the earth's surface as seen from the target surface element.

Program - SUBROUTINE AREA

Given a set of n points (x_i, y_i) which lie on an arbitrary curve which represents the function

$$y = f(x) \tag{IV-57}$$

this subroutine numerically evaluates the expression

$$A = \int_{x_1}^{x_n} y \, dx \tag{IV-58}$$

using a parabolic approximation technique. The integration is accomplished as follows.

Given three adjacent points $\left(x_i , y_i\right)$, $\left(x_{i+1} , y_{i+1}\right)$, $\left(x_{i+2} , y_{i+2}\right)$ on the curve, the function may be approximated between these points with the parabola given by

$$4\rho_i \, (y - k_i) = (x - h_i)^2 \tag{IV-59}$$

where ρ_i is the focal length of the parabola and $\left(h_i , k_i\right)$ locate the apex of the parabola with respect to the origin of the coordinate system. If the coordinates of the three adjacent points are substituted into equation (IV-59), the resulting three equations can be solved simultaneously to determine expressions for ρ_i , h_i , and k_i . Thus,

$$h_i = \frac{P_i \, x_i^2 + S_i \, x_{i+1}^2 + T_i \, x_{i+2}^2}{2\left(P_i \, x_i + S_i \, x_{i+1} + T_i \, x_{i+2}\right)} = \frac{Q}{R} \tag{IV-60}$$

where

$$P_i = y_{i+1} - y_{i+2} \tag{IV-61}$$

$$S_i = y_{i+2} - y_i \tag{IV-62}$$

$$T_i = y_i - y_{i+1} \tag{IV-63}$$

and

$$k_i = \frac{G_i\, y_{i+1} - y_i}{G_i} \tag{IV-64}$$

where

$$G_i = \left(\frac{x_i - h_i}{x_{i+1} - h_i} \right)^2 \tag{IV-65}$$

and

$$V_i = \frac{1}{4\rho_i} = \frac{y_i - k_i}{\left(x_i - h_i\right)^2} \tag{IV-66}$$

If equation (IV-59) is written as

$$y = V_i\, (x - h_i)^2 + k_i \tag{IV-67}$$

and substituted into the equation

$$a_{i,j} = \int_{x_{i+j-1}}^{x_{i+j}} y\, dx \tag{IV-68}$$

the resulting expression can be integrated to yield

$$a_{i,j} = V_i \left[\left(\frac{x_{i+j}^3 - x_{i+j-1}^3}{3}\right) - h\left(x_{i+j}^2 - x_{i+j-1}^2\right)\right] + \left[\left(k_i + V_i h_i^2\right)\left(x_{i+j} - x_{i+j-1}\right)\right] \qquad \text{(IV-69)}$$

Thus, when $j = 1$, the quantity $a_{i,1}$ represents the integral of equation (IV-68) between x_i and x_{i+1}; when $j = 2$, the quantity $a_{i,2}$ represents the integral of equation (IV-68) between x_{i+1} and x_{i+2}.

As the curve between x_i and x_{i+2} approaches a straight line, the above equations become indeterminate. Therefore, if the denominator R of equation (IV-60) is zero or if $G_i \leq 0.0001$, the quantities $a_{i,j}$ are calculated using the equation

$$a_{i,j} = \frac{\left(x_{i+j} - x_{i+j-1}\right)\left(y_{i+j} + y_{i+j-1}\right)}{2} \qquad \text{(IV-70)}$$

Further, if $a_{i,j}$ is calculated using the linear approximation represented by equation (IV-70), the computer sets $a_{i-1,2} = a_{i,1}$ and $a_{i+1,1} = a_{i,2}$. [This provision was incorporated in an effort to minimize the error introduced by slight inaccuracies in the values specified for the (x_i, y_i).]

If quantities $a_{i,j}$ are determined for each of the $n-2$ sets of three adjacent points on the curve, then A, the integral of the function between x_i and x_n, is given by

$$A = a_{1,1} + a_{n,2} + \sum_{i=2}^{n-2}\left(\frac{a_{i,1} + a_{i,2}}{2}\right) \qquad \text{(IV-71)}$$

Program - ABSORB, SUBROUTINE AREA

The absorptance P of a material, for a given source spectrum, is given by

$$P = \frac{\int_{\lambda_1}^{\lambda_n} \alpha_\lambda \, S_\lambda \, d\lambda}{\int_{\lambda_1}^{\lambda_n} S_\lambda \, d\lambda} \qquad \text{(IV-72)}$$

where α_λ is the spectral absorptivity of the material and S_λ is the spectral intensity of the source. Given n values of the spectral absorptivity α_{λ_i} of the material, this computer program uses SUBROUTINE AREA to calculate values for G and K, where

$$G = \int_{\lambda_1}^{\lambda_n} S_\lambda \, d\lambda \qquad \text{(IV-73)}$$

and

$$K = \int_{\lambda_1}^{\lambda_n} y_\lambda \, d\lambda \qquad \text{(IV-74)}$$

$$y_{\lambda_i} = \alpha_{\lambda_i} \, S_{\lambda_i} \qquad \text{(IV-75)}$$

The absorptance P of the material, therefore, is given by

$$P = \frac{K}{G} \qquad \text{(IV-76)}$$

As alternative input data, the spectral emissivity ε_{λ_i} (rather than the spectral intensity S_{λ_i}) of the source and the source temperature T may be specified, or the source may be specified as being a blackbody of temperature T. If the spectral emissivity of the source is specified, then the spectral intensity of the source is calculated using the equation

$$S_{\lambda_i} = \varepsilon_{\lambda_i} I_{\lambda_i} \tag{IV-77}$$

where I_{λ_i} is the normalized intensity at wavelength λ_i in the spectrum of a blackbody whose temperature is T. The normalized intensity I_{λ_i} at wavelength λ_i in the blackbody spectrum is calculated using Planck's Radiation Law. Thus,

$$I_{\lambda_i} = \frac{N}{\lambda_i^5 \left(e^x - 1\right)} \tag{IV-78}$$

where

$$x = \frac{c\ h}{\lambda_i\ k\ T} \tag{IV-79}$$

T is the absolute temperature of the blackbody, c is the speed of light, h is Planck's constant, k is Boltzmann's constant, and N is the normalization factor. The parameter N, defined so that the calculated intensity values are normalized with respect to the maximum intensity in the blackbody spectrum, is given by

$$N = \left(\frac{b}{T}\right)^5 \left(e^n - 1\right) \tag{IV-80}$$

where

$$n = \frac{ch}{bk} \tag{IV-81}$$

and b is the Wien displacement constant. The wavelength λ_m, at which the maximum intensity in the blackbody spectrum occurs, is given by

$$\lambda_m = \frac{b}{T} \tag{IV-82}$$

If λ_i is expressed in centimeters and T in degrees Kelvin, then

$c = 2.997925 \times 10^{10}$ centimeters/second

$h = 6.6256 \times 10^{-27}$ erg·second

$k = 1.38054 \times 10^{-16}$ erg/Kelvin degree

$b = 0.28978$ centimeter·Kelvin degree

$n = 4.9651064$

$T^5N = 0.29081685$ centimeters^5

Program - ORBHOT, SUBROUTINE AREA

The absorptance P of a material located in the Planetary Radiation Environment is given by

$$P = \frac{\int_{\lambda_1}^{\lambda_n} \alpha_\lambda S_\lambda \, d\lambda}{\int_{\lambda_1}^{\lambda_n} S_\lambda \, d\lambda} \tag{IV-83}$$

where α_λ is the spectral absorptivity of the material and S_λ is the

spectral intensity of the radiant flux incident upon the material. Given n values of the spectral intensity U_{λ_i} of the radiant flux reflected by the earth and corresponding values of the spectral intensity V_{λ_i} of the radiant flux thermally emitted from the earth, the relative spectral intensity S_{λ_i} of the radiant flux incident on the material is given, at each wavelength λ_i, by

$$S_{\lambda_i} = Q\, U_{\lambda_i} + V_{\lambda_i} \tag{IV-84}$$

where Q is given by

$$Q = \frac{E_a}{E_e} \tag{IV-85}$$

and is the ratio of the irradiance E_a, produced on the target surface element by the radiant flux reflected by the earth, to the irradiance E_e produced by the radiant flux thermally emitted from the earth. Thus, given n values of the spectral absorptivity of the material, this computer program uses SUBROUTINE AREA to calculate values for G and K, where

$$G = \int_{\lambda_1}^{\lambda_n} S_\lambda \, d\lambda \tag{IV-86}$$

and

$$K = \int_{\lambda_1}^{\lambda_n} y_\lambda \, d\lambda \tag{IV-87}$$

$$y_{\lambda_i} = \alpha_{\lambda_i} S_{\lambda_i} = \alpha_{\lambda_i} \left(Q\, U_{\lambda_i} + V_{\lambda_i} \right) \qquad \text{(IV-88)}$$

The absorptance P of the material, therefore, is given by

$$P = \frac{K}{G} \qquad \text{(IV-89)}$$

The flux per unit area H absorbed by the material as heat is then calculated using the expression

$$H = P\, E_e\, (1 + Q) \qquad \text{(IV-90)}$$

The values of P and H are then tabulated as a function of Q and the corresponding values of h (the orbital altitude) and γ (the angle at the center of the earth between the directions to the sun and to the target location) that define the position at which the values of Q and E_e were calculated using the computer programs ORBVAR or SPACE.

Program - ARRAY, SUBROUTINE MODULE

This computer program evaluates the performance characteristics of an arbitrarily specified Planetary Radiation Environment Simulator array configuration. In order to make this evaluation, it is first assumed that each module is designed so that there is a well-defined position from which emanates all of the radiant flux produced by the module. This apparent source of the radiant flux (hereinafter referred to as the pseudo-source) may be the real source, an image of the source, or a superimposition of the real source and an image of the source. It is further assumed that the distribution of the radiant flux emanating from each pseudo-source, at an angle γ with respect to the optic axis of the module, is a linear function of $\cos \gamma$ between any two specified intensity values I_i and I_{i+1} in directions γ_i and γ_{i+1}, respectively. That is, when

$\gamma_i \leq \gamma \leq \gamma_{i+1}$,

$$I = \left[\left(\frac{I_{i+1} - I_i}{\cos \gamma_{i+1} - \cos \gamma_i}\right) \left(\cos \gamma - \cos \gamma_i\right)\right] + I_i \qquad \text{(IV-91)}$$

The array configuration is generated by locating the pseudo-source of each module on an arbitrarily specified reference surface so that the optic axis of each module is perpendicular to the reference surface at the position of the pseudo-source. The reference surface may be specified as being any reasonable combination of the quadric surfaces illustrated in figure IV-2. (The various geometrical parameters identified on this figure are also those which must be specified in the input data to the computer program in order to generate the reference surface.)

As the first step in locating the pseudo-sources on the reference surface, the intersections between the reference surface and an appropriate number of xy-planes is determined. These xy-planes are defined, beginning with an initially specified xy-plane, so that the distance between adjacent parallel planes, as measured along the reference surface, is equal to S, the spacing parameter. The intersection of each xy-plane with the reference surface defines a circular ring which is centered about the z-axis. The pseudo-sources are then located along this ring so that the arc length between adjacent pseudo-sources, as measured along the ring, is also equal to S, the spacing parameter. The pseudo-sources are symmetrically located, with respect to the plane containing the x- and z-axes, on that portion of the reference surface which lies in the +x direction from some arbitrarily specified yz-plane.

A target surface element of area may be specified by defining its coordinates x_t, y_t, z_t, and its orientation angles, α and β. (α is the angle between the target element surface normal and the x-axis; β is the angle between the z-axis and the projection of the surface normal into the yz-plane.) The direction of the array field axis (the direction to the center of the simulated earth, i.e., the nadir direction) about which the field of each pseudo source is masked, is defined by specifying the angle ψ of figure IV-2. The field half-angle subtended by the

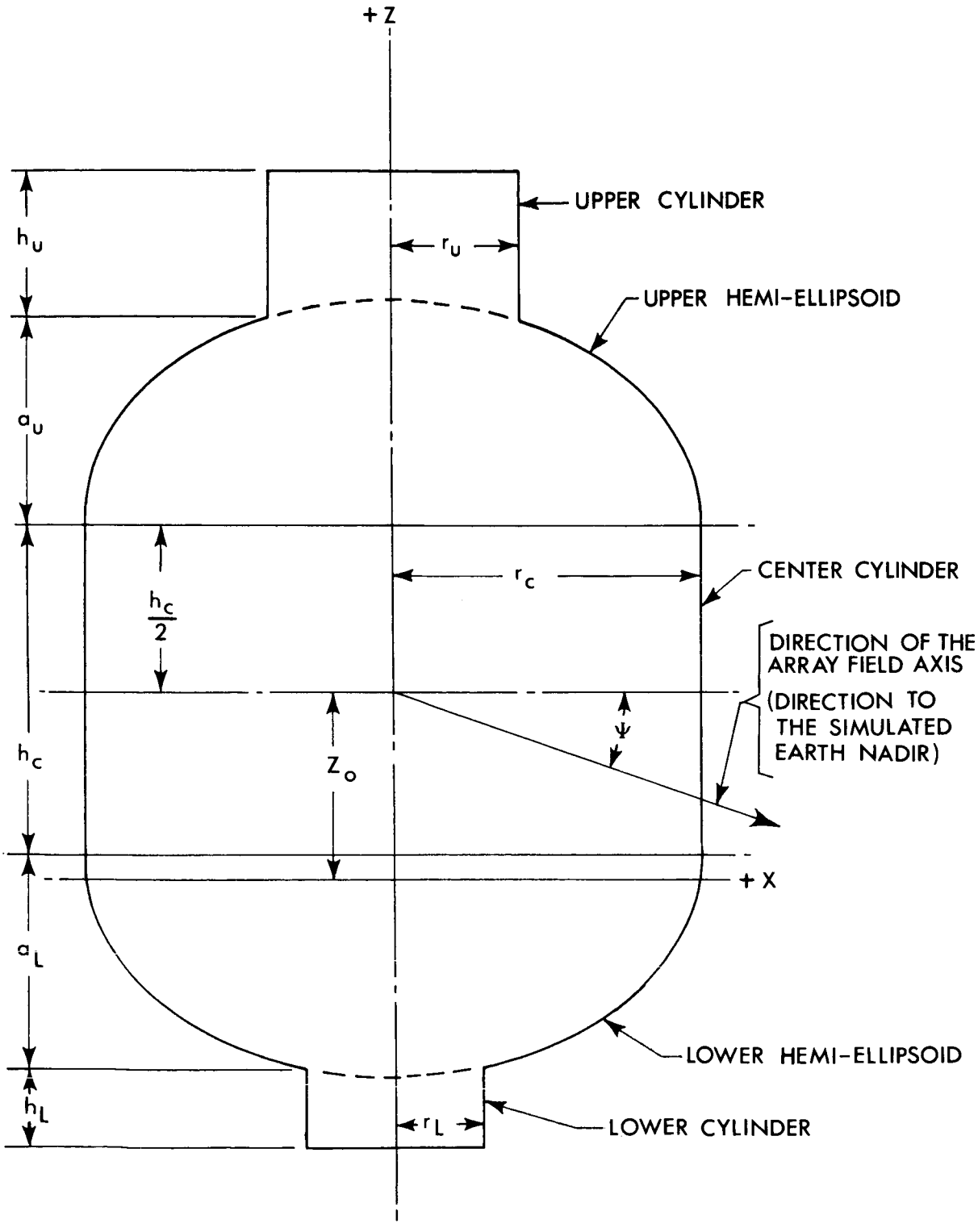

Figure IV-2. Geometry of a reference surface

simulated earth is defined by specifying Φ . Defining n as the number of modules in the array, then the irradiance E on the specified target surface element is determined by evaluating the equation

$$E = \sum_{j=1}^{n} \Delta E_j \qquad \text{(IV-92)}$$

where ΔE_j is the irradiance produced on the target surface element by radiant flux from the $j^{\underline{th}}$ module. The optic axis of the $j^{\underline{th}}$ module intersects the reference surface at x_j , y_j , z_j , and has direction cosines L_j , M_j , N_j with respect to the x-, y-, and z-axes, respectively.

The cosine of the angle T_j (the angle between the array field axis and the direction from the target element to the $j^{\underline{th}}$ module) is

$$\cos T_j = \frac{\left(x_j - x_t\right) \cos \psi + \left(z_j - z_t\right) \sin \psi}{\sqrt{\left(x_j - x_t\right)^2 + \left(y_j - y_t\right)^2 + \left(z_j - z_t\right)^2}} \qquad \text{(IV-93)}$$

If $\cos \Phi > \cos T_j$, then $\Delta E_j = 0$. If $\cos \Phi < \cos T_j$, then the computation proceeds as follows. Defining L_t , M_t , and N_t as the direction cosines of the normal to the target surface element, then the cosine of the angle ζ_j (the angle of incidence of the radiant flux from the $j^{\underline{th}}$ module) is

$$\cos \zeta_j = \frac{L_t \left(x_j - x_t\right) + M_t \left(y_j - y_t\right) + N_t \left(z_j - z_t\right)}{\sqrt{\left(x_j - x_t\right)^2 + \left(y_j - y_t\right)^2 + \left(z_j - z_t\right)^2}} \qquad \text{(IV-94)}$$

where

$$L_t = \sin \alpha \cos \beta \tag{IV-95}$$

$$M_t = \sin \alpha \sin \beta \tag{IV-96}$$

$$N_t = \cos \alpha \tag{IV-97}$$

If $\cos \zeta \leq 0$, then $\Delta E_j = 0$. If $\cos \zeta > 0$, then the computation proceeds as follows. Defining γ_j as the angle between the optic axis of the $j^{\underline{th}}$ module and the direction from the $j^{\underline{th}}$ pseudo-source to the target surface element, then

$$\cos \gamma_j = \frac{L_j \left(x_j - x_t\right) + M_j \left(y_j - y_t\right) + N_j \left(z_j - z_t\right)}{\sqrt{\left(x_j - x_t\right)^2 + \left(y_j - y_t\right)^2 + \left(z_j - z_t\right)^2}} \tag{IV-98}$$

Defining i such that $\gamma_i \leq \gamma_j \leq \gamma_{i+1}$, then the intensity I_j of the radiant flux from the $j^{\underline{th}}$ module in the direction of the target element is, from equation (IV-91),

$$I_j = \left[\left(\frac{I_{i+1} - I_i}{\cos \gamma_{i+1} - \cos \gamma_i}\right)\left(\cos \gamma_j - \cos \gamma_i\right)\right] + I_i \tag{IV-99}$$

where I_i and I_{i+1} are known values of the radiant intensity at angles γ_i and γ_{i+1}, respectively, from the optic axis of the module. The irradiance contribution from the $j^{\underline{th}}$ module is, therefore,

$$\Delta E_j = \frac{I_j \cos \zeta_j}{\left(x_j - x_t\right)^2 + \left(y_j - y_t\right)^2 + \left(z_j - z_t\right)^2} \tag{IV-100}$$

In addition to calculating the irradiance on each specified target surface element, the computer program also provides complete information concerning: the array geometry, the number of modules which irradiate each target surface element, how many of the specified target surface elements are irradiated (and the associated field half-angle required) by each module, and the total number of modules required to irradiate all of the specified target surface elements. The computer program also determines (using the irradiance values calculated for those target surface elements whose normals are in the direction of the array field axis) the average, the maximum, and the minimum irradiance within the target volume; the probable error in the irradiance at any position within the target volume; and the standard deviation.

APPENDIX V
ABSORPTANCE OF VARIOUS MATERIALS

Given a 1000-watt tungsten-iodine coiled-coil filament tubular lamp with a quartz envelope, the sun, a 6000°K blackbody, a 1000°K blackbody, and a 250°K blackbody, as sources of incident radiant flux (the spectrums of these sources are plotted in figures V-1 through V-5, respectively); the absorptance of each of the following materials was calculated, between 0.30 micron and 30.00 microns, using the computer program ABSORB (see Appendix IV).

1. Freshly evaporated gold, see figure V-6.
2. Freshly evaporated aluminum, see figure V-7.
3. Evaporated aluminum after atmospheric exposure, see figure V-8.
4. Leaf aluminum paint, see figure V-9.
5. Aluminized mylar with no protective coating, see figure V-10.
6. ALZAC, see figure V-11.
7. White paint (titanium dioxide pigment in a silicone vehicle), see figure V-12.
8. Black paint (CAT-A-LAC, sample 1), see figure V-13.

The absorptance values thus determined are listed in table V-1.

If radiant flux from two different sources is incident on a material, the total absorptance P of the material is given by

$$P = \frac{E_1 P_1 + E_2 P_2}{E_1 + E_2} \qquad (V\text{-}1)$$

where P_1 is the absorptance of the material for the spectrum of source #1, P_2 is the absorptance of the material for source #2, E_1 is the irradiance produced by the incident radiant flux from source #1, and E_2

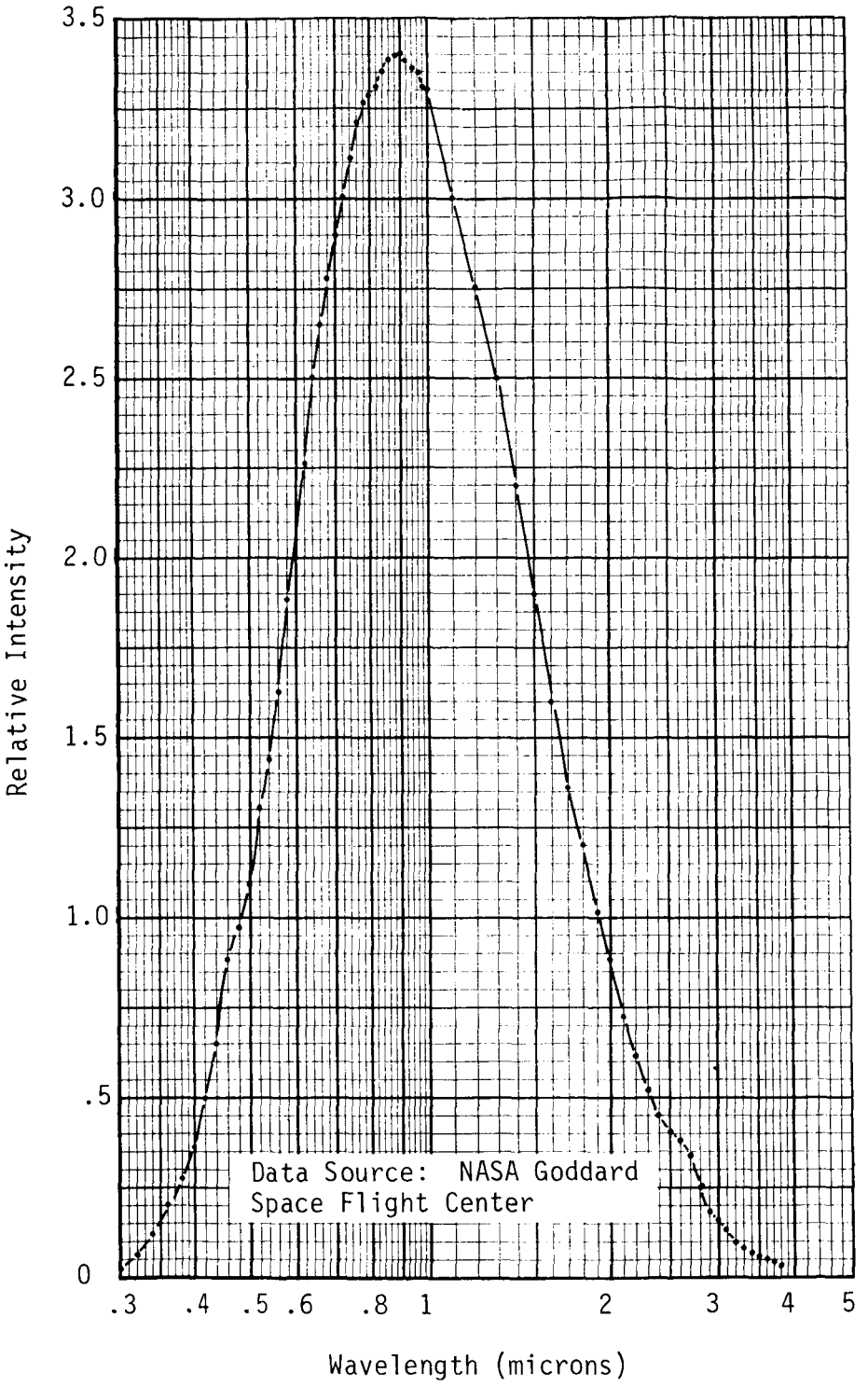

Figure V-1. Spectrum of a 1000-watt tungsten-iodine coiled-coil filament tubular lamp with a quartz envelope.

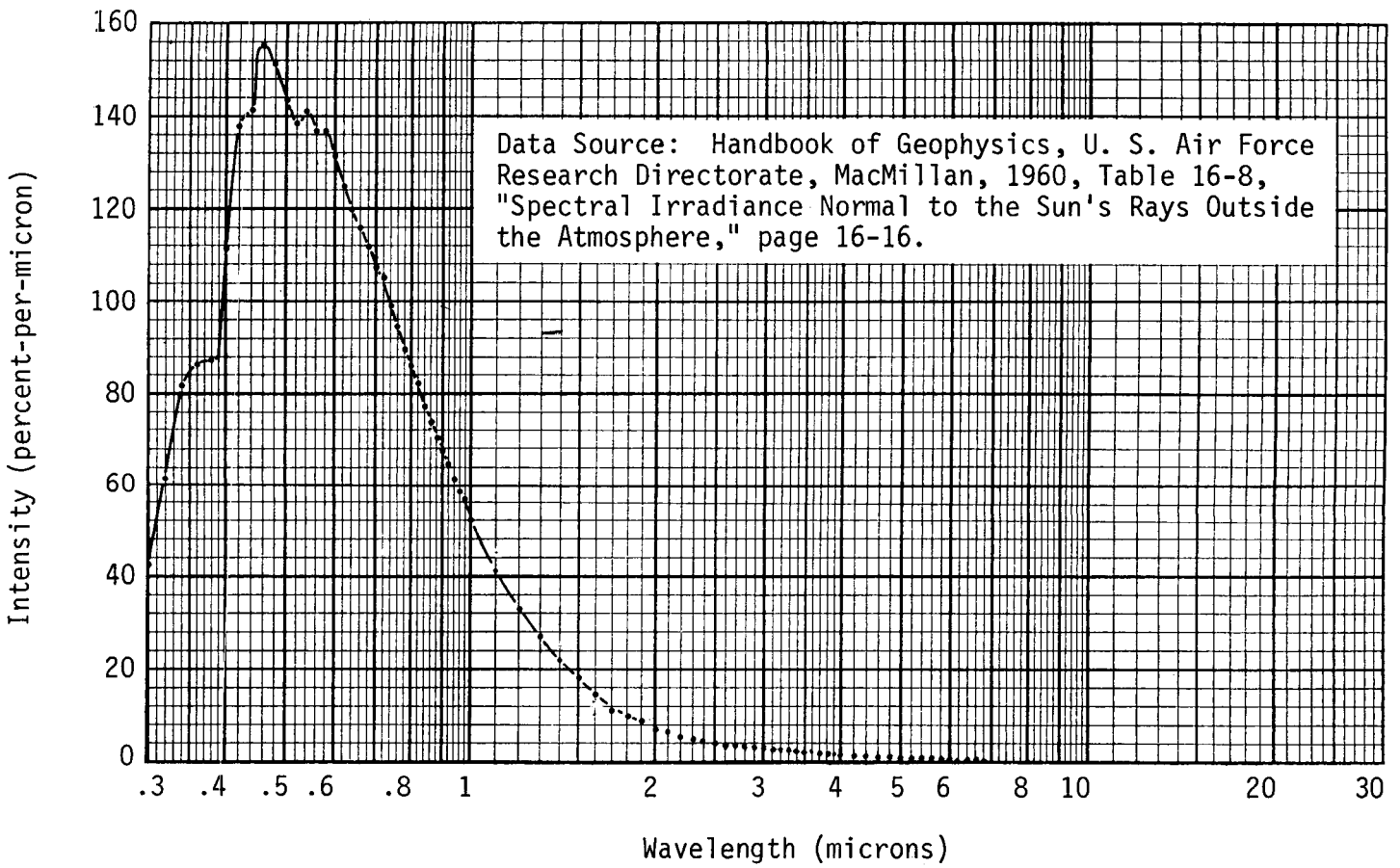

Figure V-2. The solar spectrum

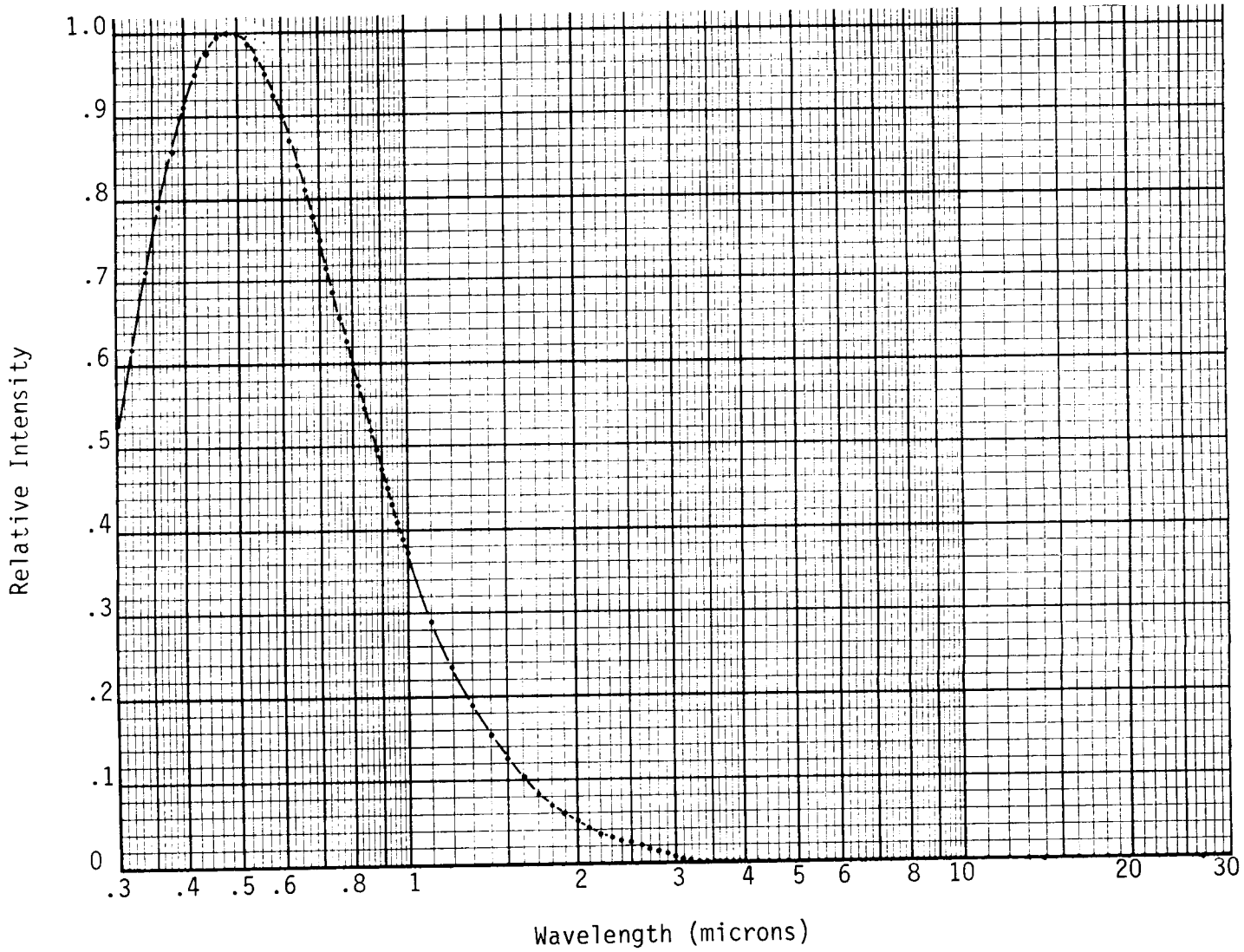

Figure V-3. Spectrum of a 6000°K blackbody

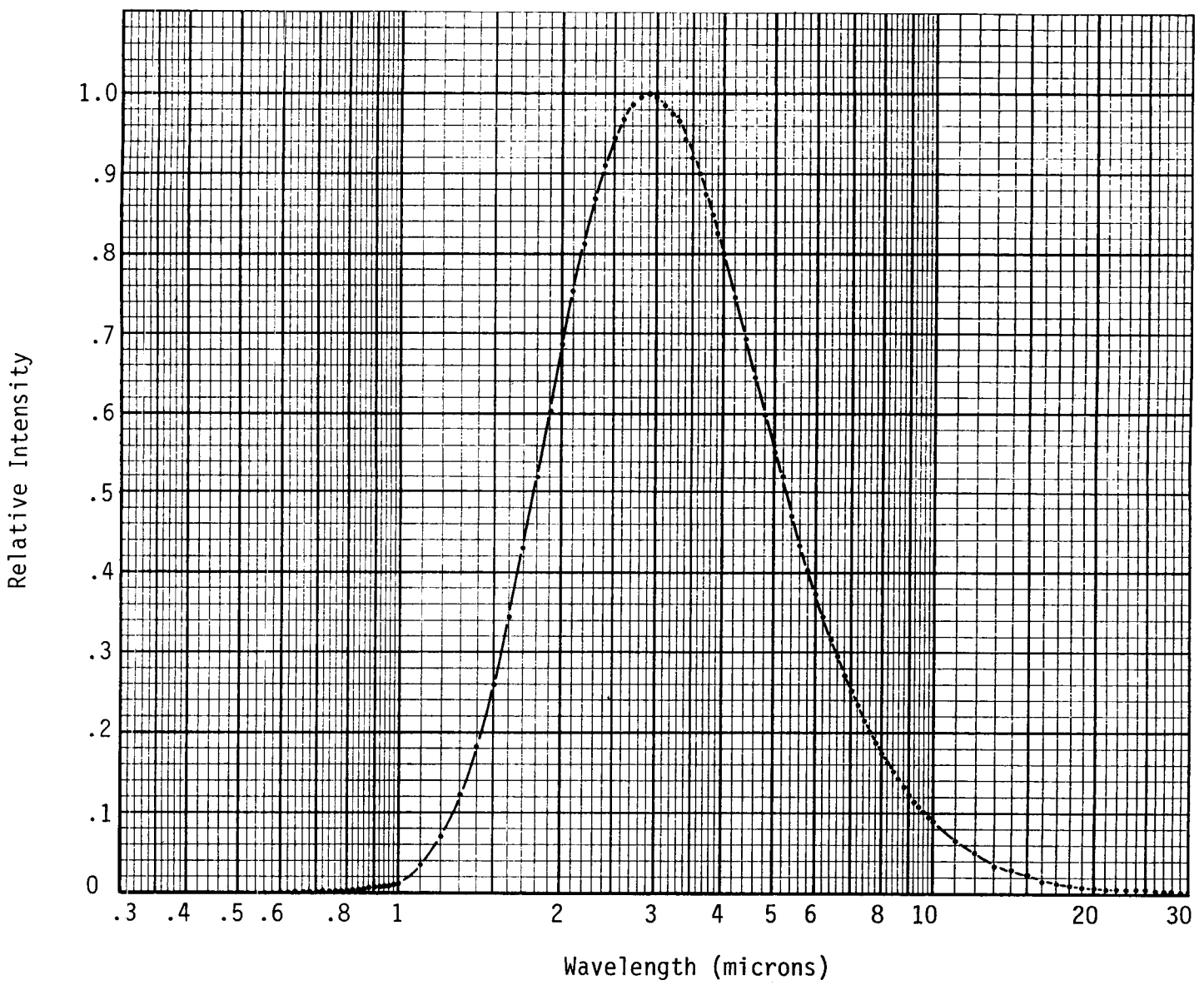

Figure V-4. Spectrum of a 1000°K blackbody

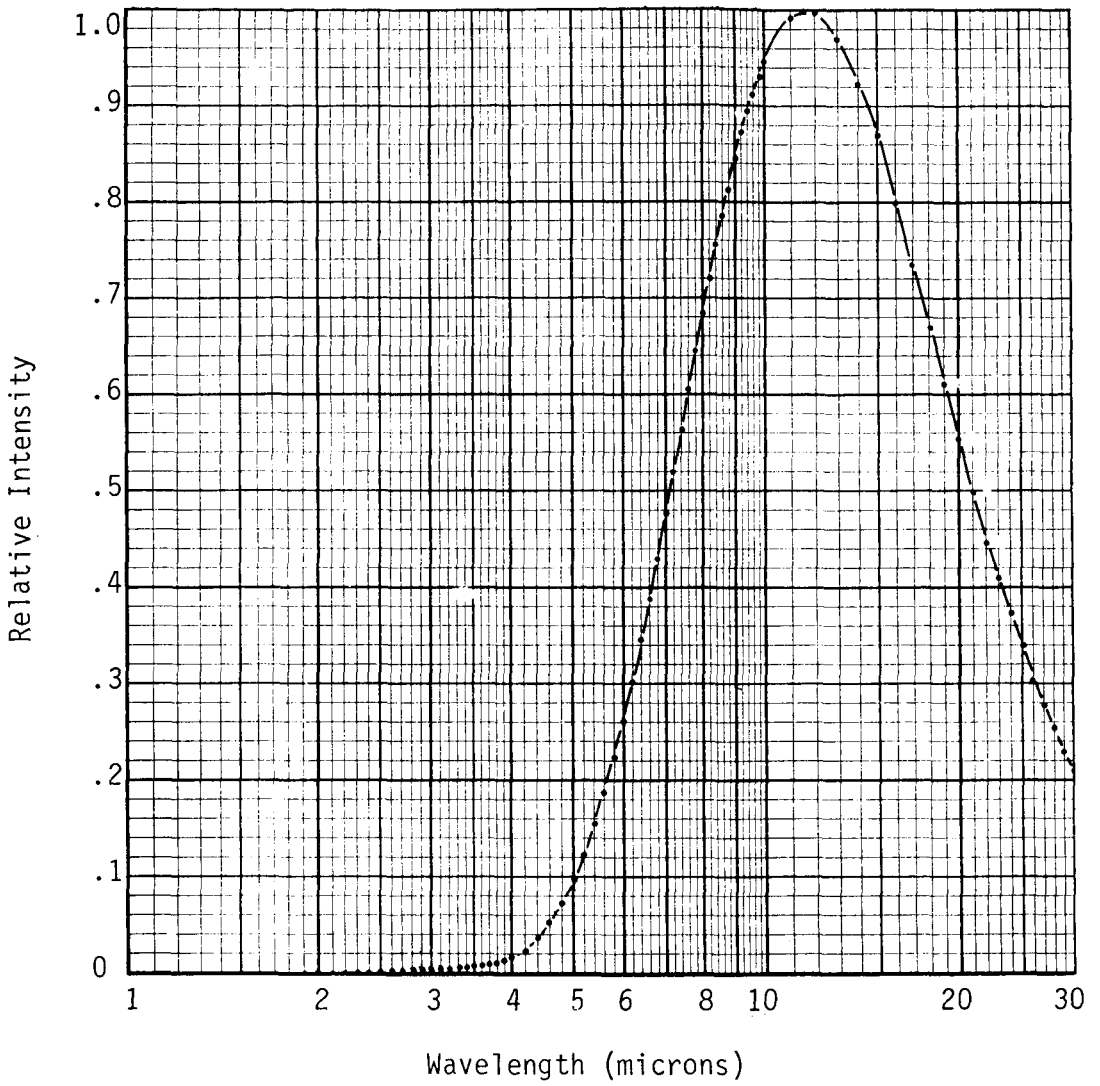

Figure V-5. Spectrum of a 250°K blackbody

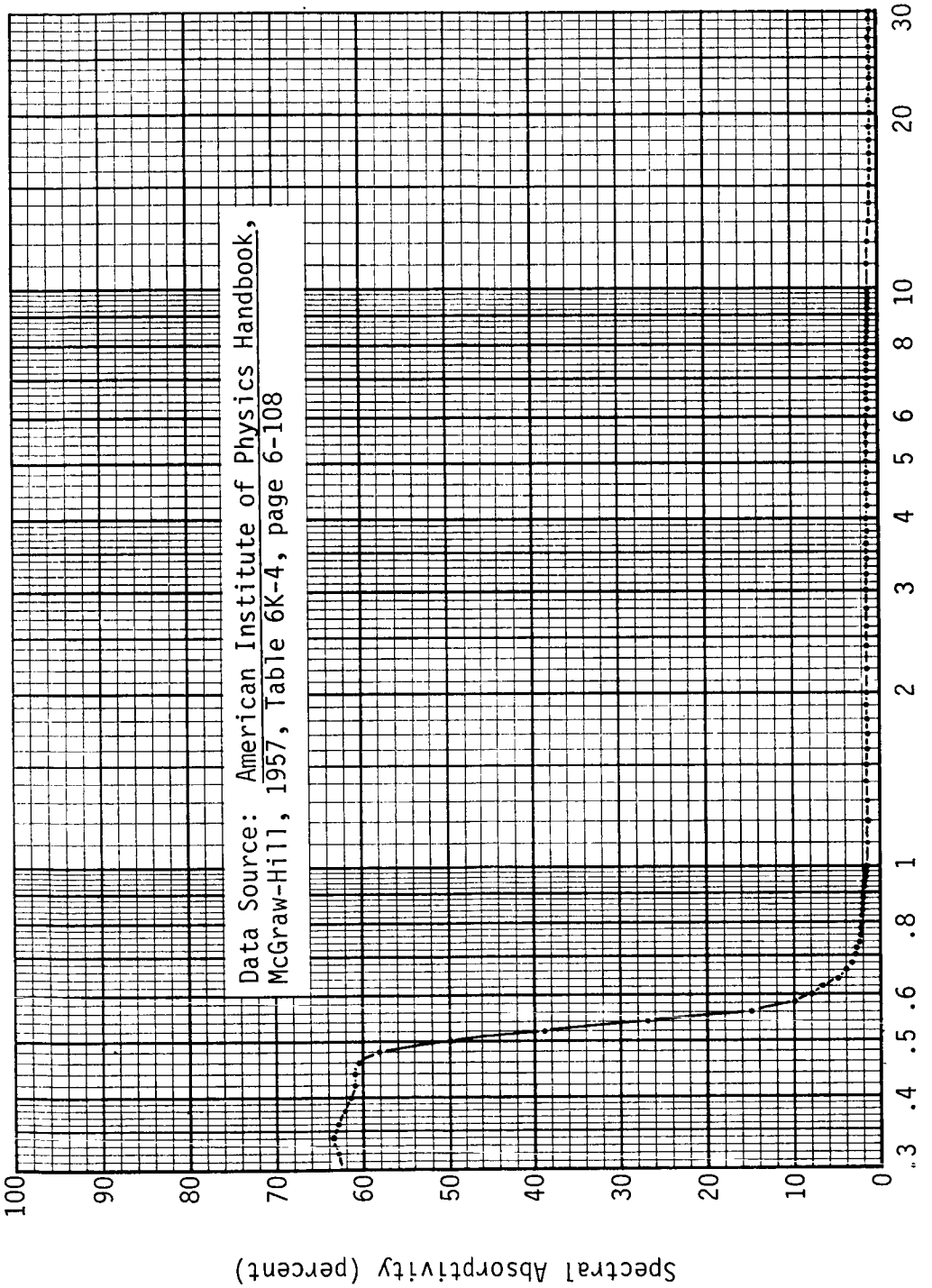

Figure V-6. Spectral absorptivity of freshly evaporated gold

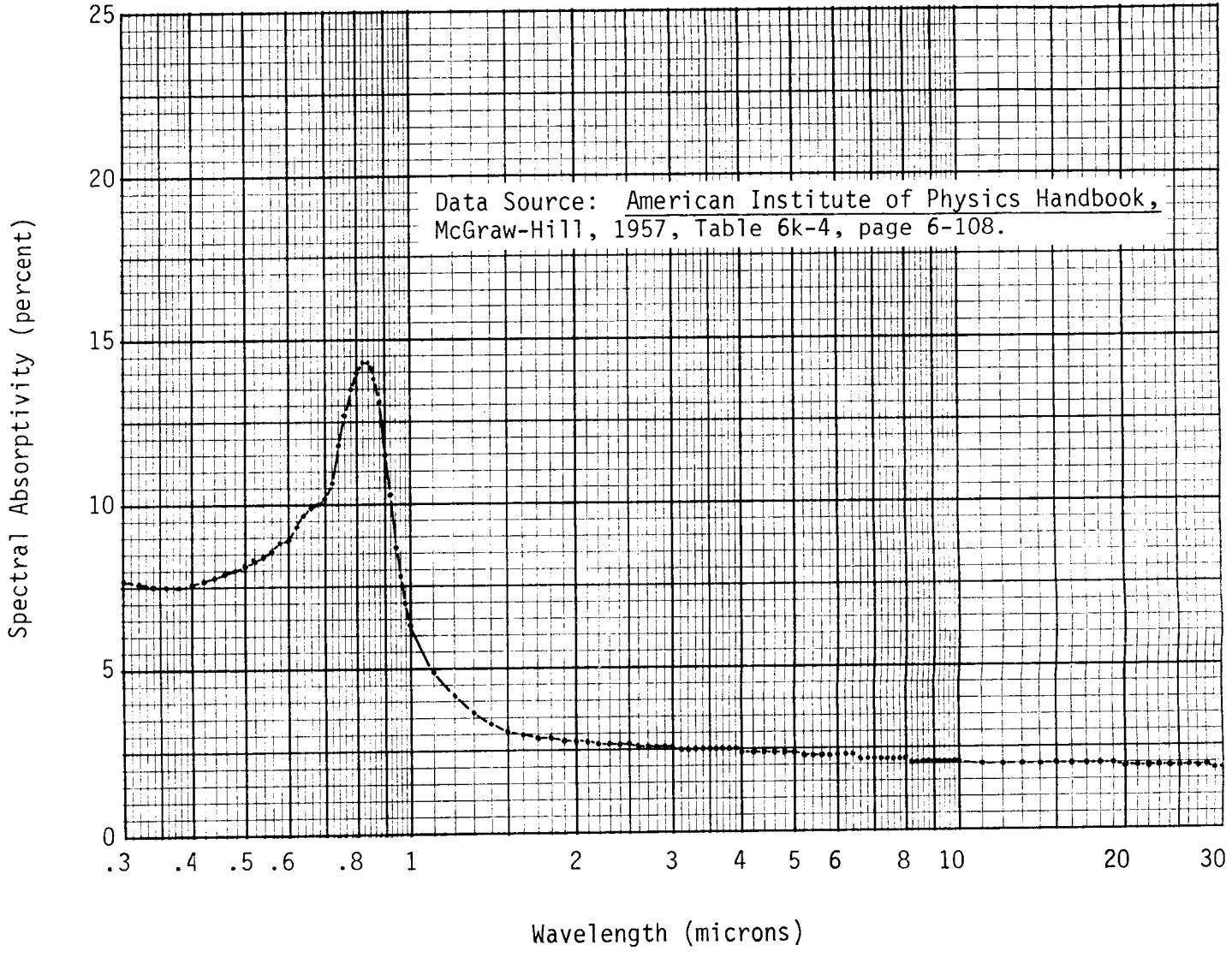

Figure V-7. Spectral absorptivity of freshly evaporated aluminum

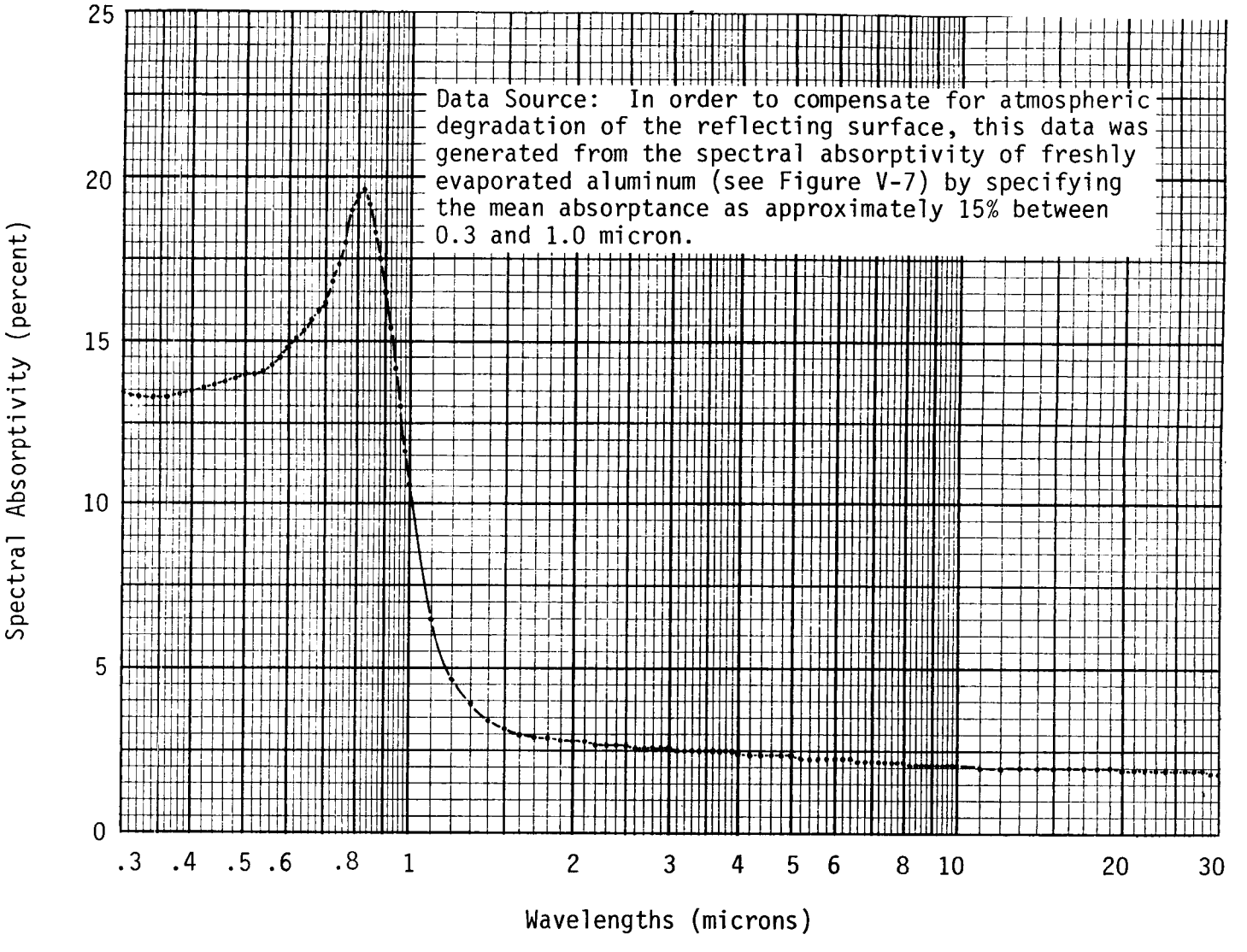

Figure V-8. Spectral absorptivity of evaporated aluminum which has been exposed to the atmosphere

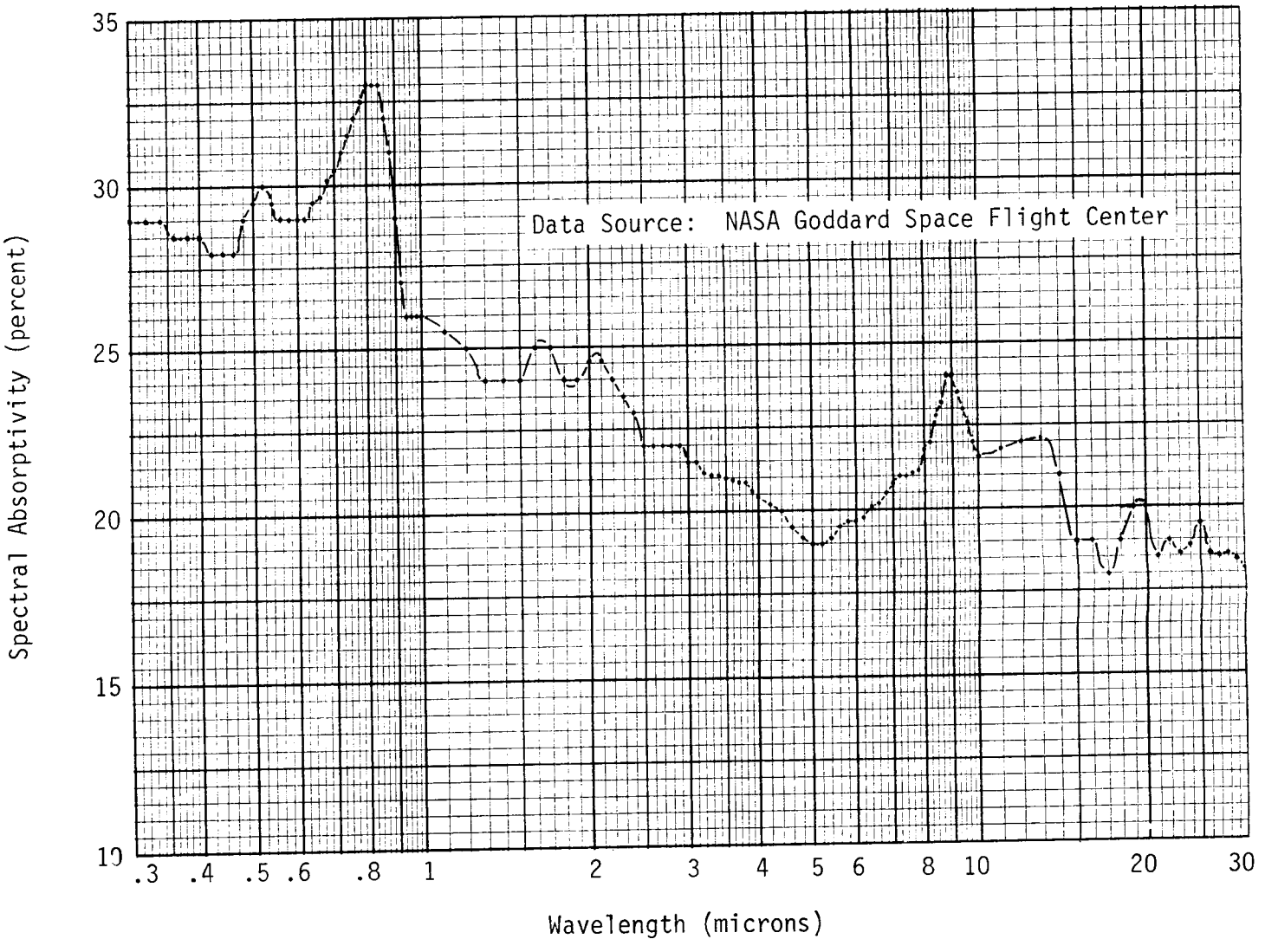

Figure V-9. Spectral absorptivity of leaf aluminum paint

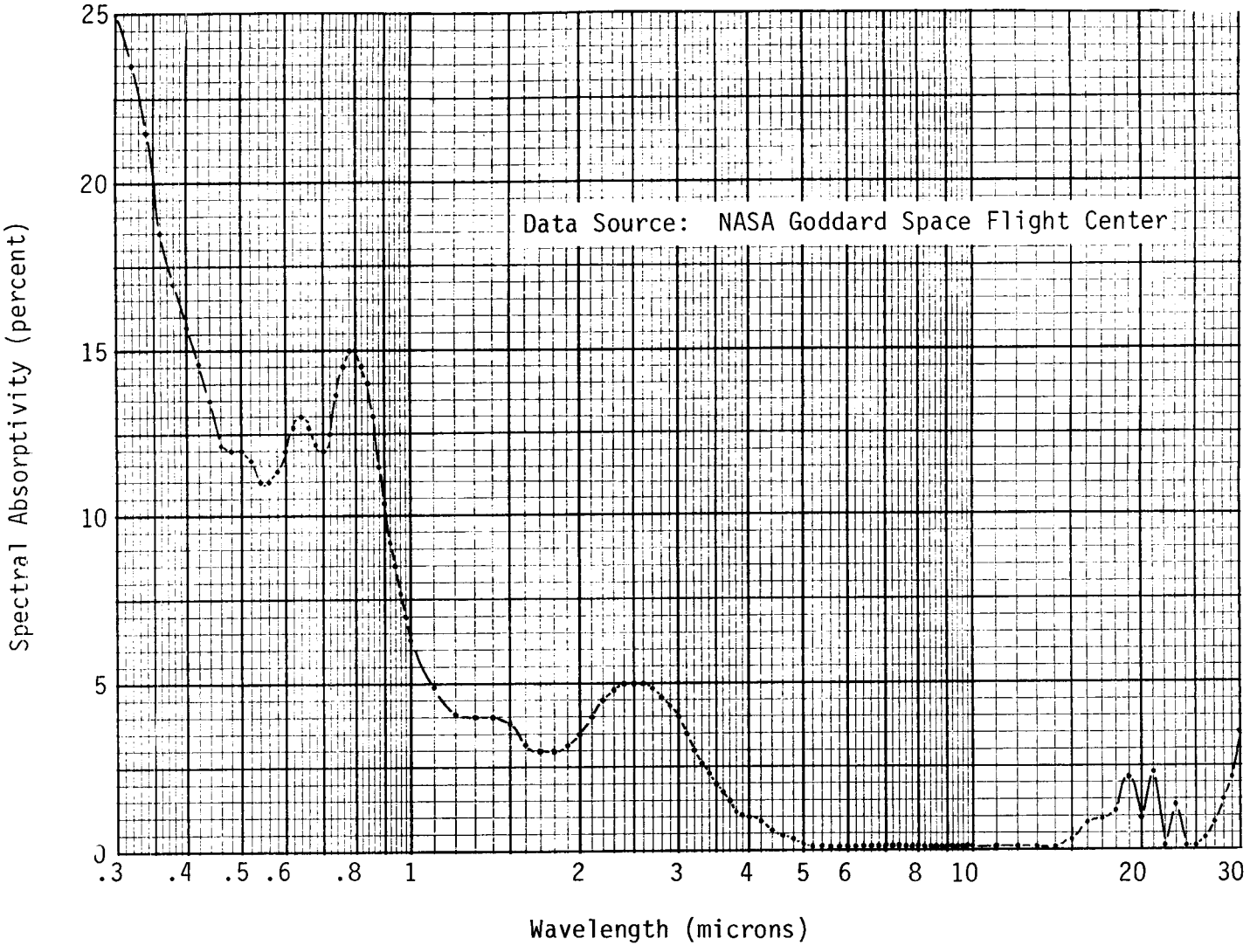

Figure V-10. Spectral absorptivity of aluminized mylar with no protective coating.

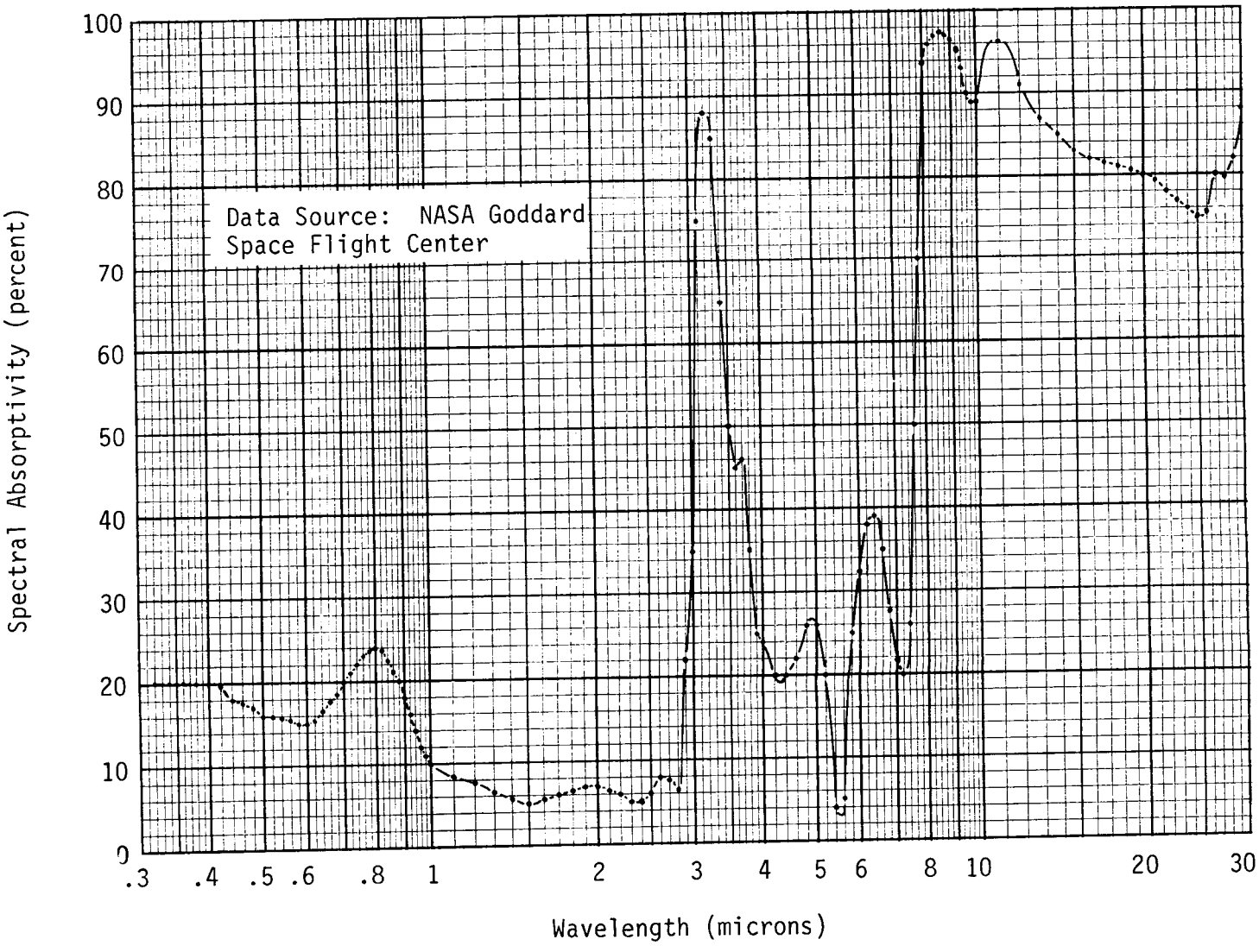

Figure V-11. Spectral absorptivity of ALZAC

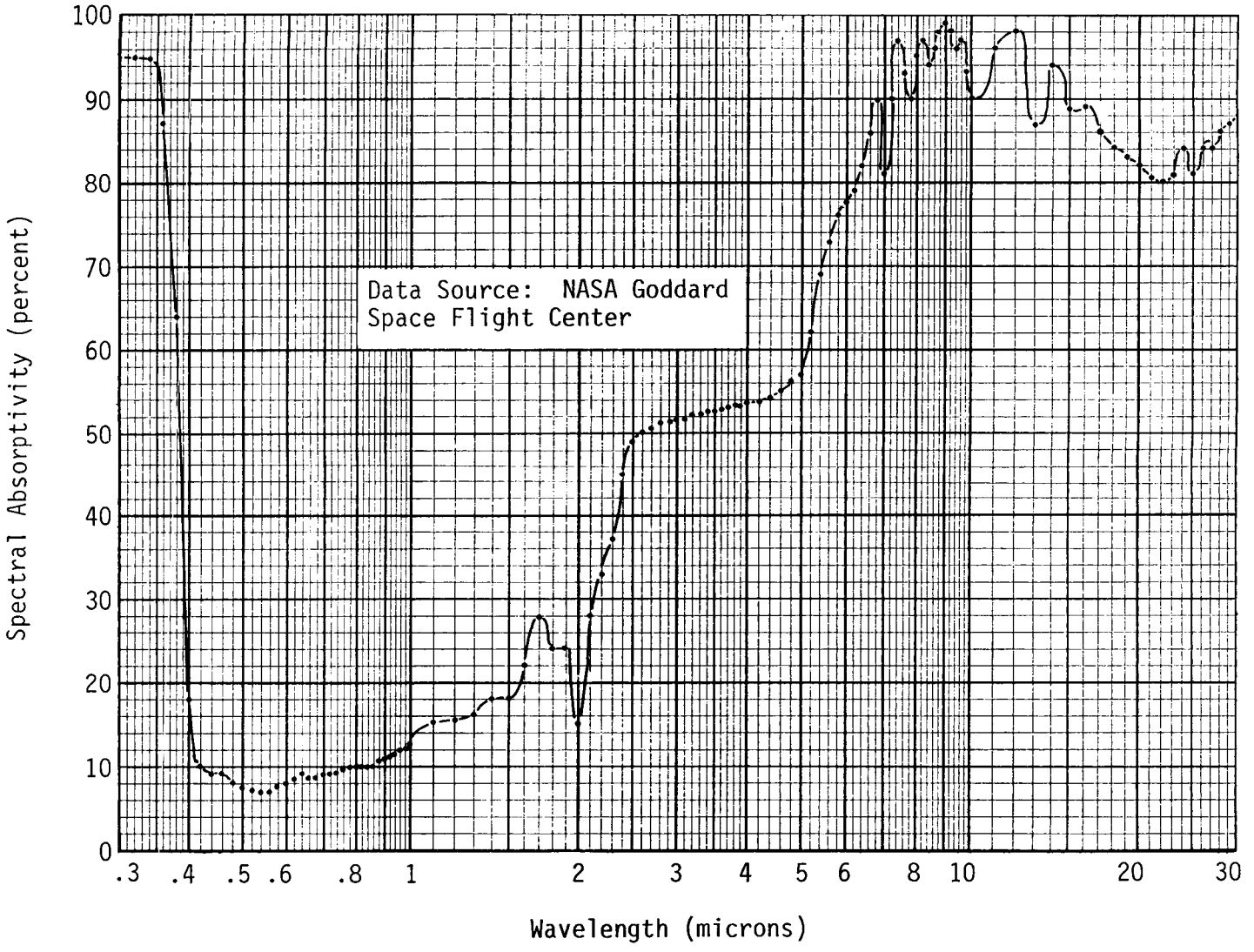

Figure V-12. Spectral absorptivity of white paint (titanium dioxide pigment in a silicone vehicle).

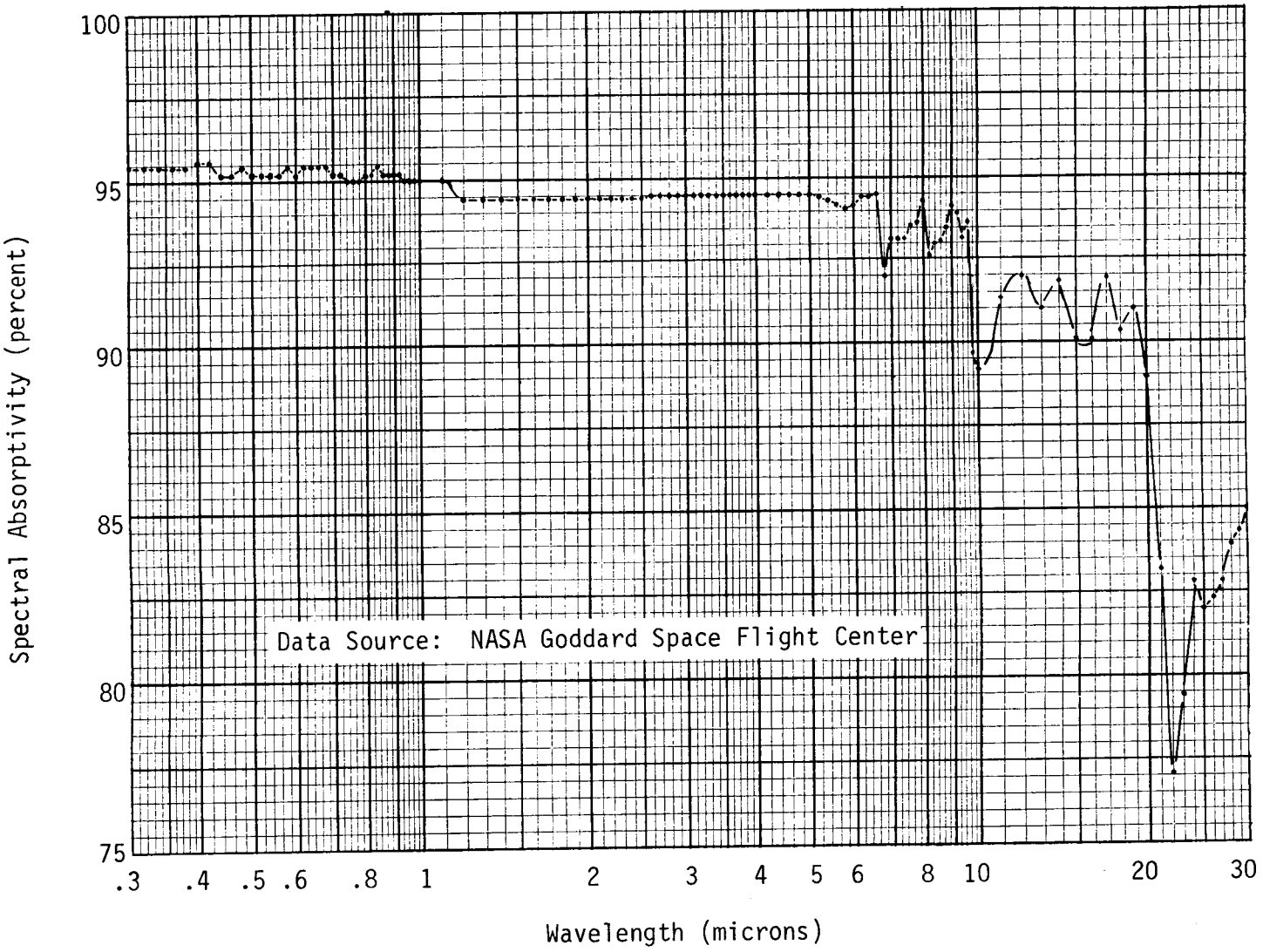

Figure V-13. Spectral absorptivity of black paint (CAT-A-LAC, sample 1)

Table V-1. Absorptance of various materials between 0.30 microns and 30.00 microns.

Source of the incident radiant flux	ABSORPTANCE BETWEEN 0.30 and 30.00 MICRONS							
	Freshly Evaporated Gold	Freshly Evaporated Aluminum	Evaporated Aluminum After Atmospheric Exposure	Leaf Aluminum Paint	Aluminized Mylar With No Protective Coating	ALZAC	White Paint (Titanium Dioxide Pigment in Silicone Vehicle)	Black Paint (CAT-A-LAC, Sample 1)
1000 watt Tungsten-Iodine Quartz Lamp	3.78%	5.52%	7.60%	27.75%	6.21%	10.86%	16.24%	89.17%
Sun	18.53%	7.87%	12.11%	27.96%	10.53%	15.35%	18.27%	95.34%
6000^{o} K Blackbody	19.67%	7.88%	12.17%	28.06%	10.81%	15.64%	20.15%	95.07%
1000^{o} K Blackbody	1.67%	2.44%	2.45%	21.25%	1.79%	36.18%	60.30%	93.90%
250^{o} K Blackbody	1.52%	2.01%	2.01%	20.36%	0.53%	81.03%	88.35%	89.35%
Radiant Flux from the Earth $\frac{E_a}{E_e} = 0.0$	1.52%	2.01%	2.01%	20.36%	0.53%	81.03%	88.35%	89.35%
Radiant Flux from the Earth $\frac{E_a}{E_e} = 0.5$	7.19%	3.96%	5.38%	22.89%	3.86%	59.14%	64.99%	91.35%
Radiant Flux from the Earth $\frac{E_a}{E_e} = 1.0$	10.03%	4.94%	7.06%	24.16%	5.53%	48.19%	53.31%	92.35%
Radiant Flux from the Earth $\frac{E_a}{E_e} = 1.5$	11.73%	5.53%	8.07%	24.92%	6.53%	41.62%	46.30%	92.94%
Radiant Flux from the Earth $\frac{E_a}{E_e} = 2.0$	12.86%	5.92%	8.74%	25.43%	7.20%	37.24%	41.63%	93.34%

is the irradiance produced by the incident radiant flux from source #2. Defining E_a as the irradiance produced, on a surface, by radiant flux reflected from the earth and E_e as the irradiance produced, on the same surface, by the radiant flux thermally emitted by the earth, then from equation (V-1)

$$P = \frac{\left(\frac{E_a}{E_e}\right) P_a + P_e}{\left(\frac{E_a}{E_e}\right) + 1} \qquad \text{(V-2)}$$

If it is assumed that the spectrum of the radiant flux reflected from the earth is identical to the solar spectrum, and if it is assumed that the spectrum of the radiant flux thermally emitted by the earth is identical to that of a 250°K blackbody, then the absorptance of the various materials can be calculated, for various values of $\frac{E_a}{E_e}$, using equation (V-2). The absorptance values thus determined are listed in table V-1.

Defining E_{a_o} and E_{e_o}, respectively, as the values of E_a and E_e when the normal to the target surface is in the direction toward the center of the earth, the quantity Q, where

$$Q = \frac{E_{a_o}}{E_{e_o}} \qquad \text{(V-3)}$$

was calculated, using the computer program ORBVAR (see Appendix IV), for various values of h (the orbital altitude) and γ (the angle, at the center of the earth, between the directions to the sun and to the target surface). These values of Q, the corresponding values of h and γ, the data for the assumed spectrums of the radiant flux reflected by the earth (the solar spectrum) and of the radiant flux thermally emitted by

the earth (the spectrum of a 250°K blackbody), and the spectral absorptivity data for the various materials, were then processed using the computer program ORBHOT (see Appendix IV) to obtain a tabulation of the absorptance of each of the materials at each location defined by h and γ. The absorptance values thus determined for each material are plotted versus the ratio $\frac{E_a}{E_e}$ between the two spectral components of the irradiance produced by the radiant flux emanating from the earth, in figures V-14 through V-21. (The ratio $\frac{E_{a_o}}{E_{e_o}}$, as calculated using the computer program ORBVAR, is plotted versus γ, for h = 100 miles and h = 1000 miles, in figure 4-19.

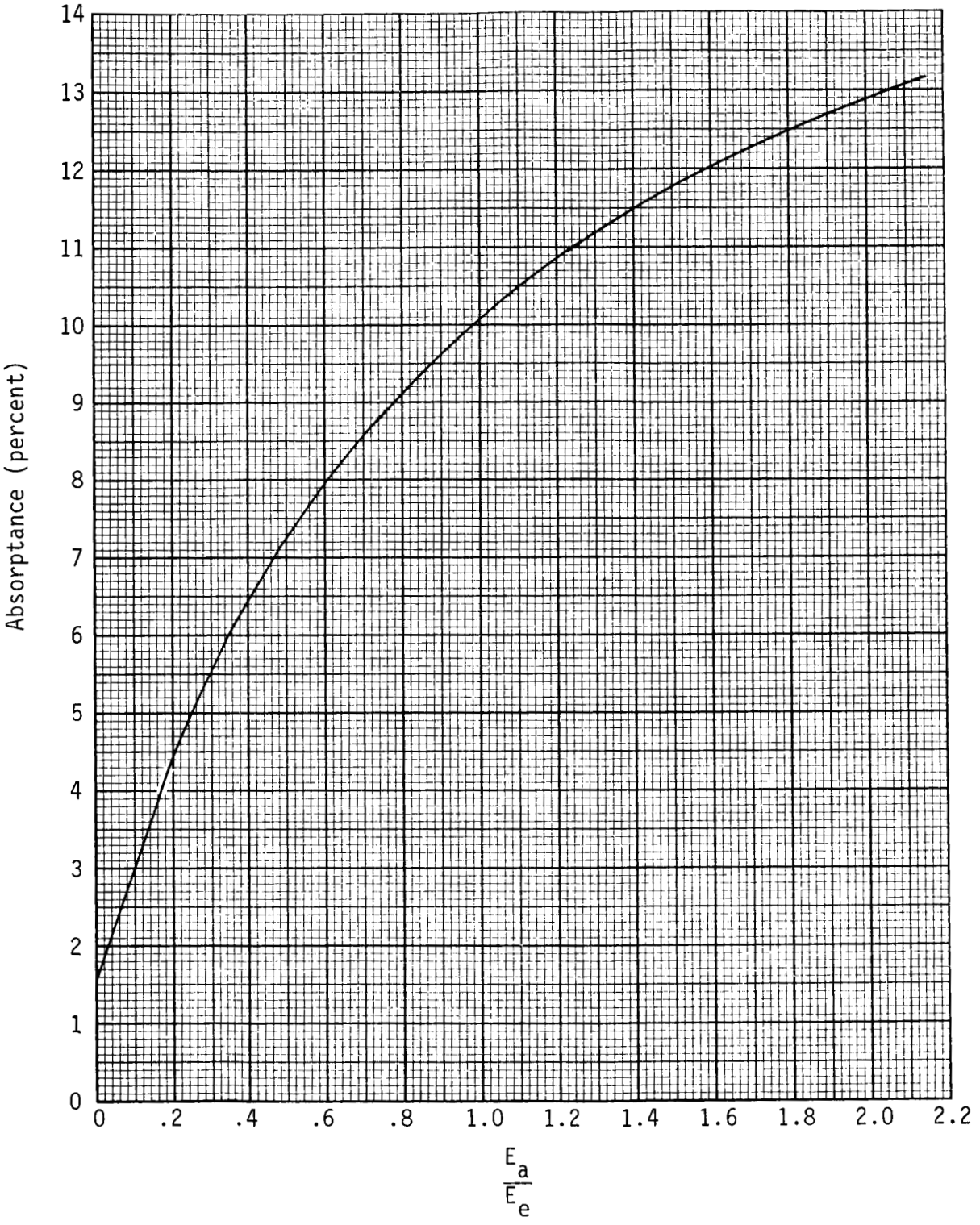

Figure V-14. Absorptance of freshly evaporated gold versus $\frac{E_a}{E_e}$

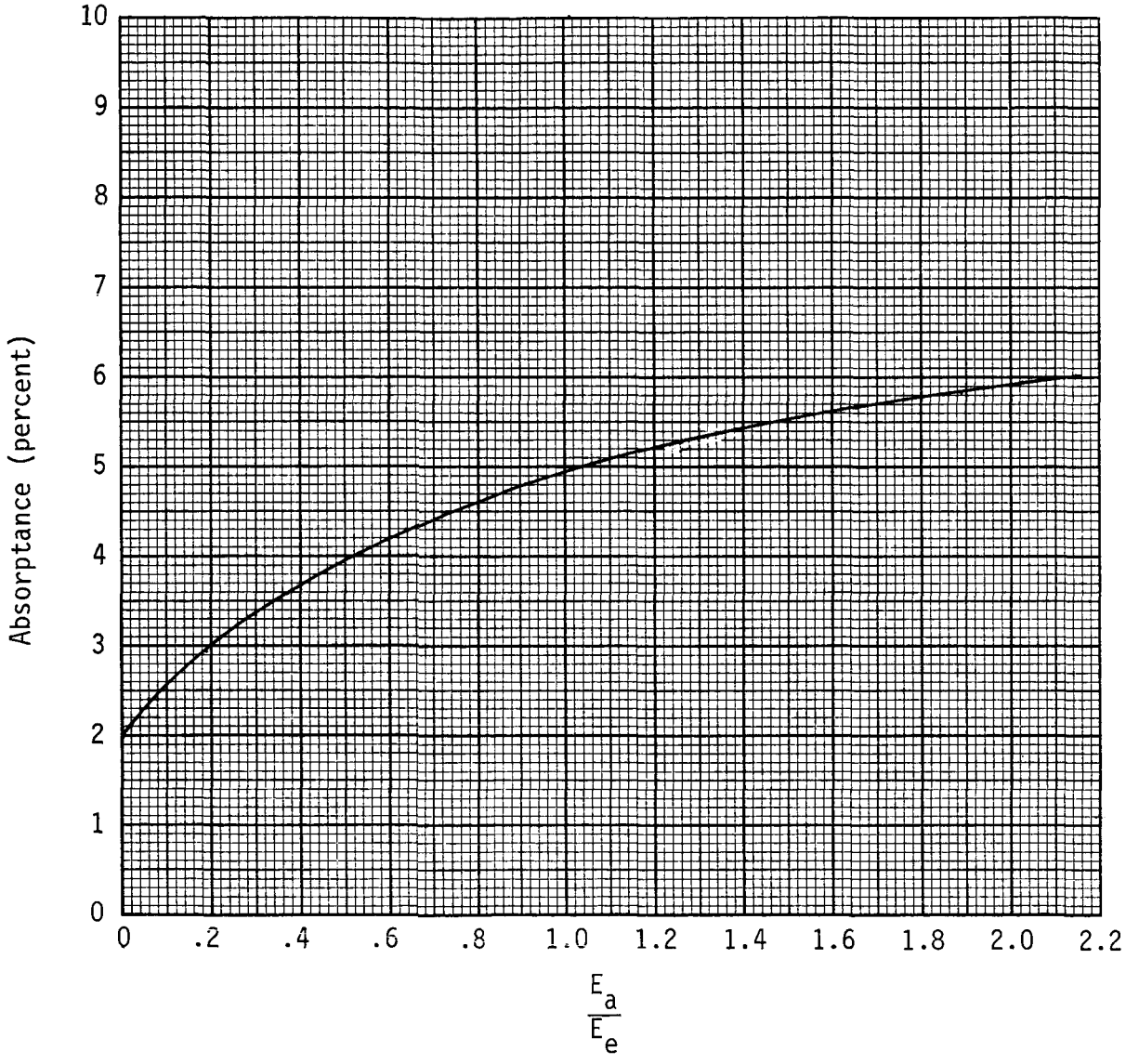

Figure V-15. Absorptance of freshly evaporated aluminum versus $\frac{E_a}{E_e}$

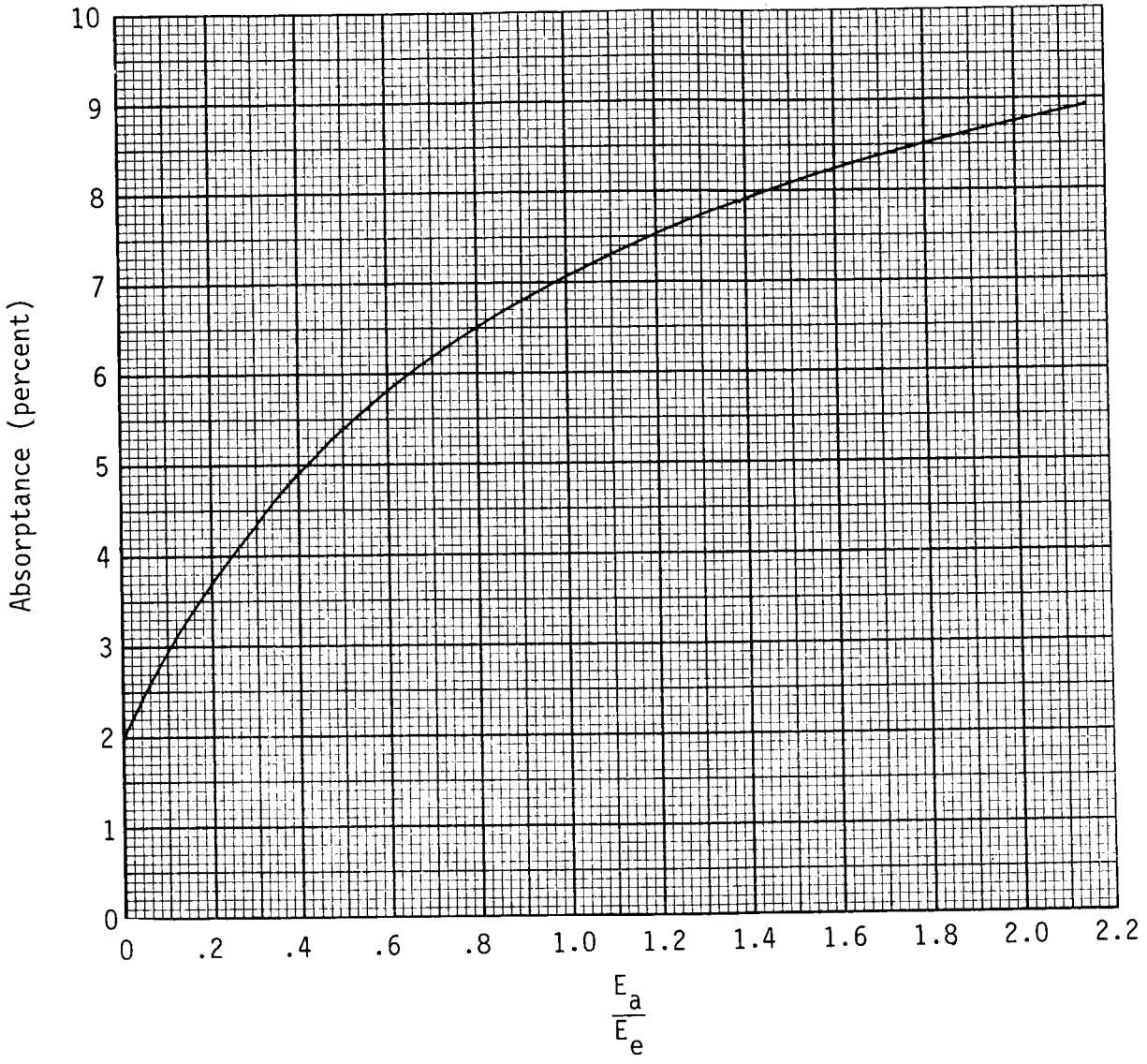

Figure V-16. Absorptance of evaporated aluminum which has been exposed to the atmosphere versus $\frac{E_a}{E_e}$

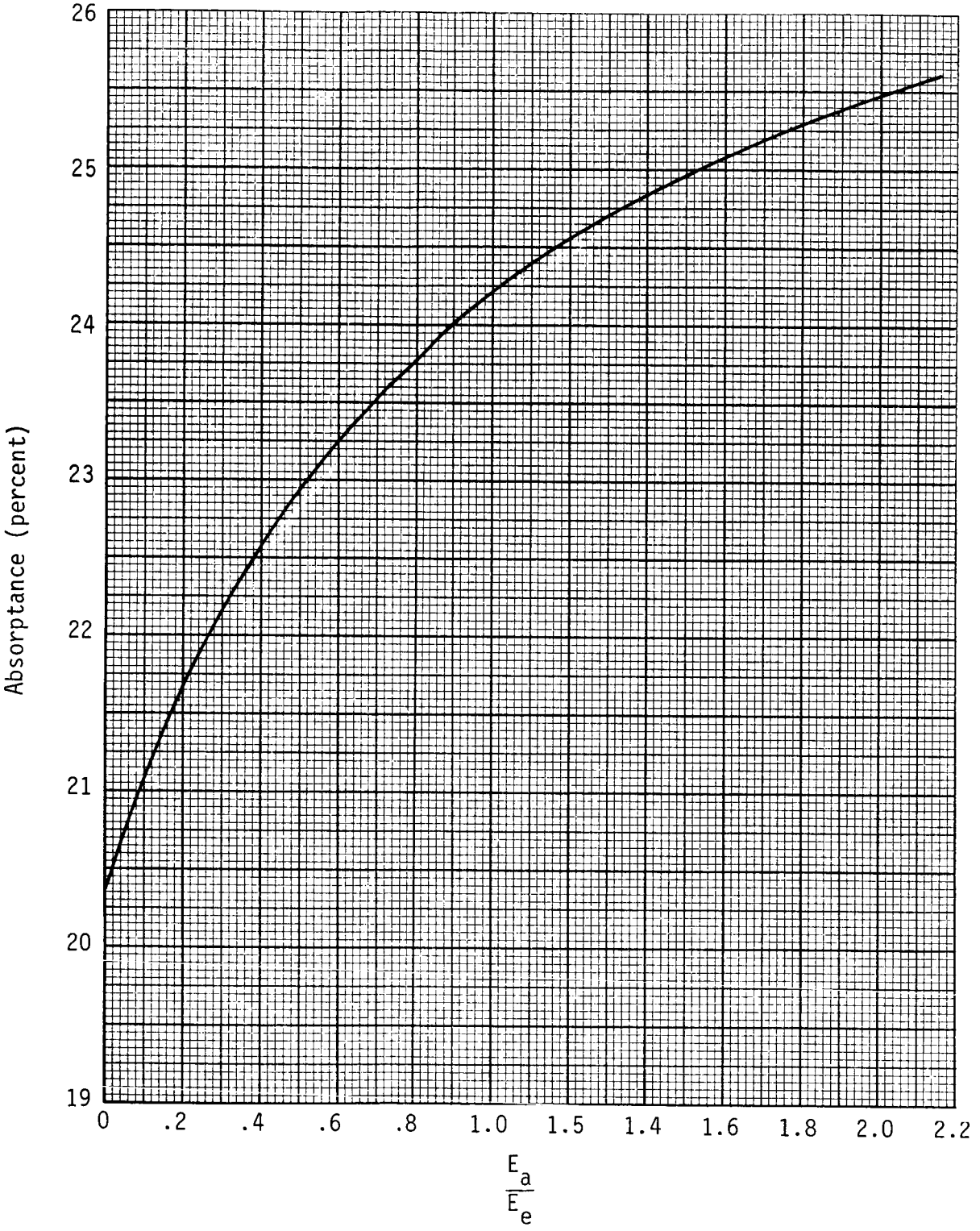

Figure V-17. Absorptance of leaf aluminum paint versus $\frac{E_a}{E_e}$

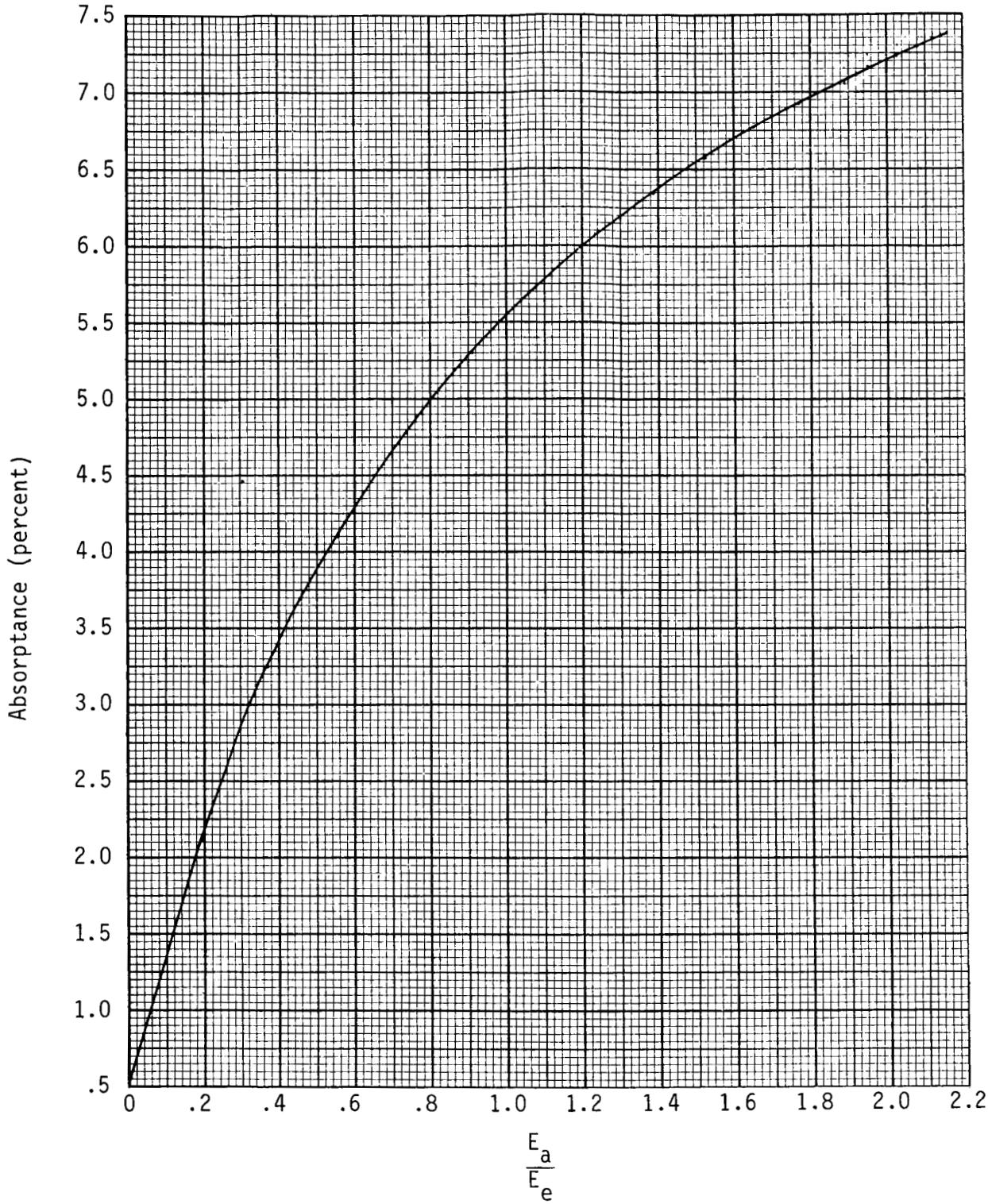

Figure V-18. Absorptance of aluminized mylar with no protective coating versus $\frac{E_a}{E_e}$

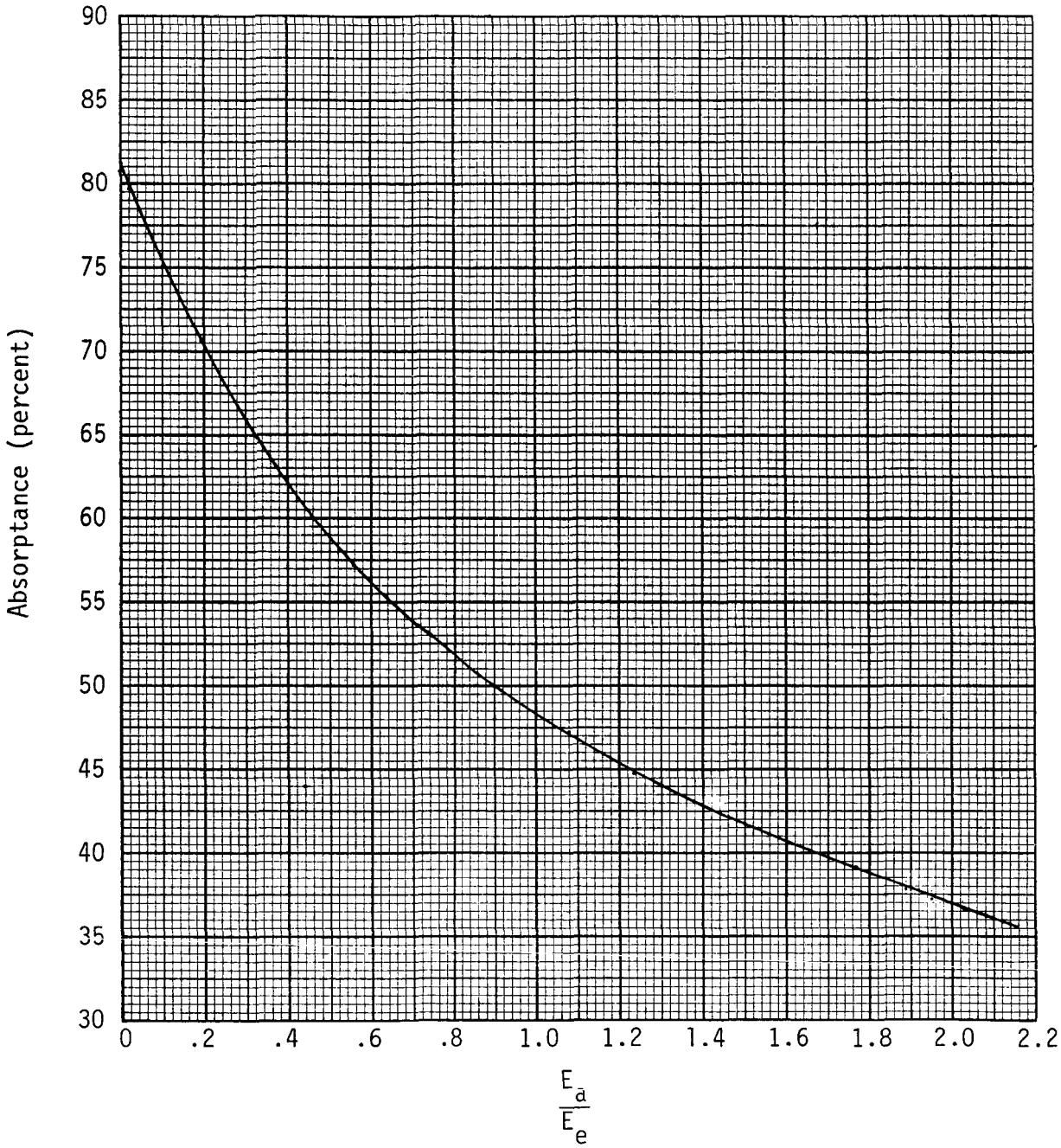

Figure V-19. Absorptance of ALZAC versus $\frac{E_a}{E_e}$

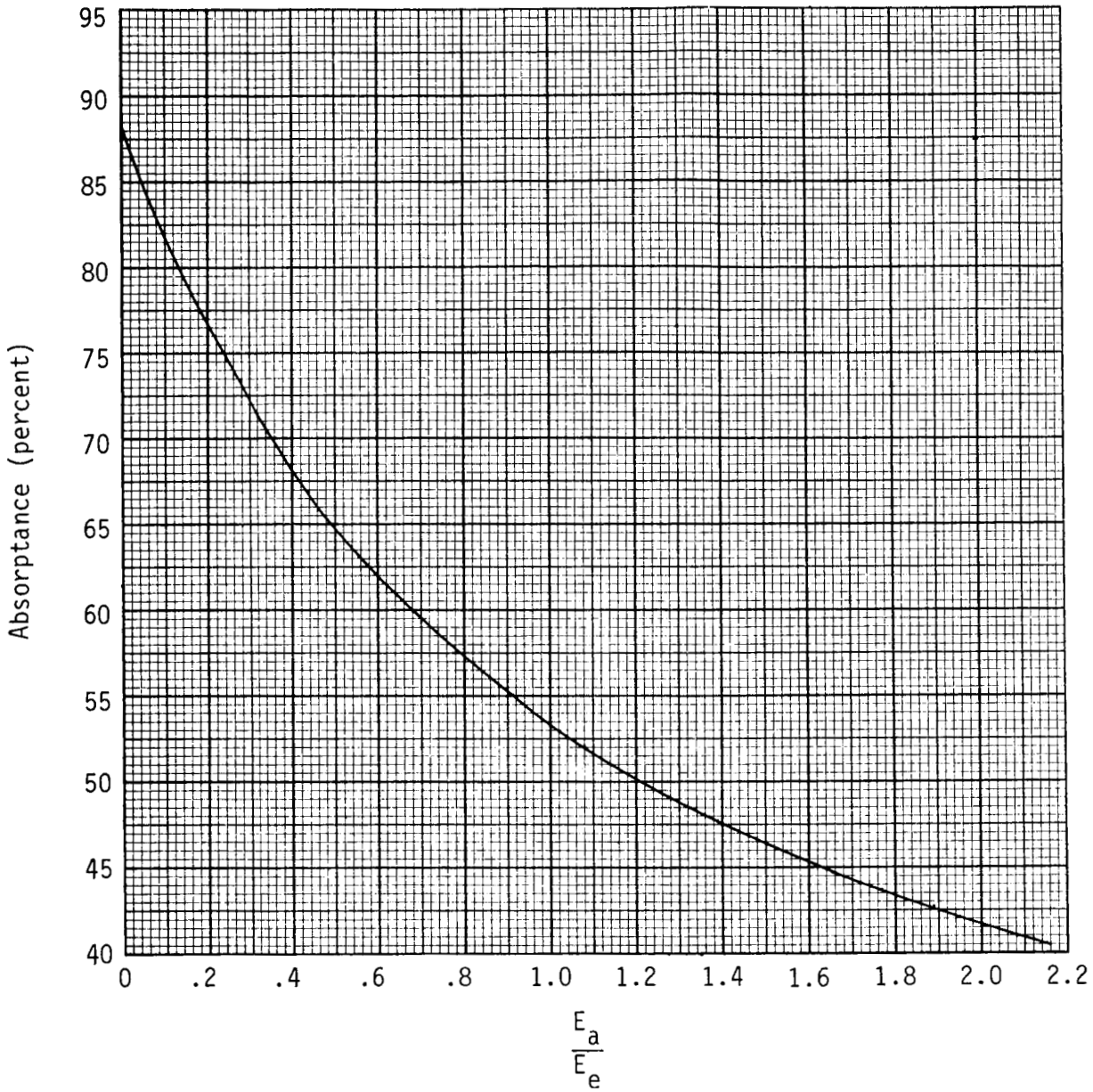

Figure V-20. Absorptance of white paint (titanium dioxide pigment in a silicone vehicle) versus $\frac{E_a}{E_e}$

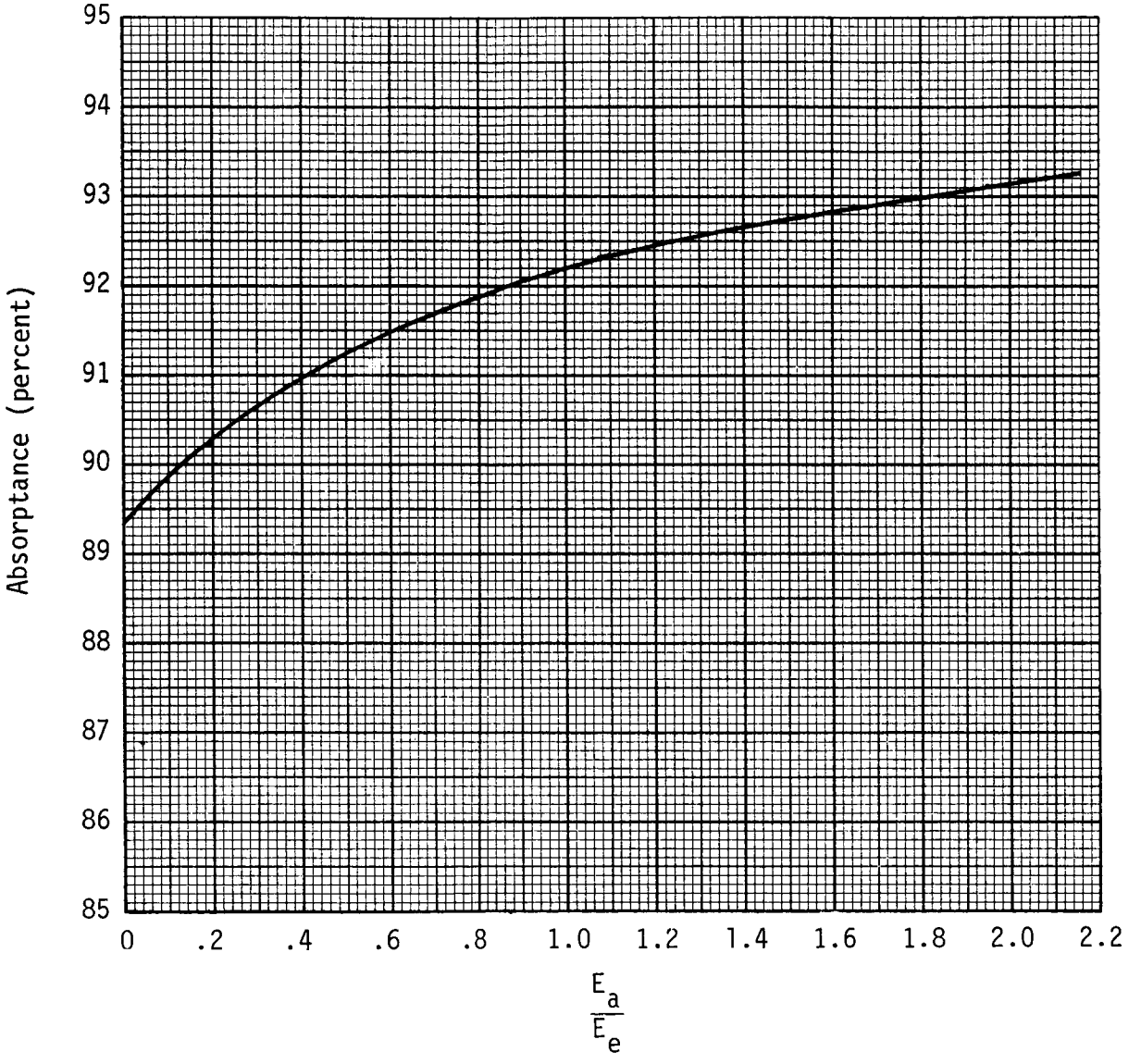

Figure V-21. Absorptance of black paint (CAT-A-LAC, sample 1) versus $\frac{E_a}{E_e}$

APPENDIX VI

RELATIONSHIP BETWEEN THE RADIANT INTENSITY DISTRIBUTION OF A SOURCE AND THE RADIANT INTENSITY DISTRIBUTION OF THE FLUX AFTER REFLECTION, AS A FUNCTION OF THE SHAPE OF THE REFLECTING SURFACE

Intuitively, it can be seen that the radiant intensity distribution of reflected radiant flux is a function of both the radiant intensity distribution of the radiant flux emitted by the source and the shape of the reflecting surface. The purpose of the following analysis is to define the various geometrical relationships which relate the radiant intensity distribution of the source to the radiant intensity distribution of the reflected radiant flux. Also, techniques are suggested whereby a reflecting surface can be defined to provide reflected radiant flux with a given (required) intensity distribution when the reflector is used with a source which has a given (known) radiant intensity distribution. To simplify the discussion, it has been assumed that the source is of negligible size.

To begin, consider figure VI-1 where a source is located on the axis of symmetry of a reflecting surface. The unit vector $\hat{s}$ defines the direction of a ray emitted by the source to a point (x,y) on the reflector; this ray is then reflected to the point Q. The unit vector $\hat{n}$ is normal to the reflector at the point (x,y) and the unit vector $\hat{r}$ defines the direction from the point Q to the point (x,y). Defining $\hat{i}$ and $\hat{j}$ as unit vectors parallel to the x-axis and the y-axis, respectively, then $\hat{s}$, $\hat{n}$, and $\hat{r}$ may be expressed as

$$\hat{s} = \hat{i} \cos \phi + \hat{j} \sin \phi \qquad \text{(VI-1)}$$

$$\hat{n} = \hat{i} \cos \left(\frac{\pi}{2} + \alpha\right) + \hat{j} \sin \left(\frac{\pi}{2} + \alpha\right) = - \hat{i} \sin \alpha + \hat{j} \cos \alpha \qquad \text{(VI-2)}$$

$$\hat{r} = \hat{i} \cos (\pi - \gamma) + \hat{j} \sin (\pi - \gamma) = - \hat{i} \sin \gamma + \hat{j} \sin \gamma \qquad \text{(VI-3)}$$

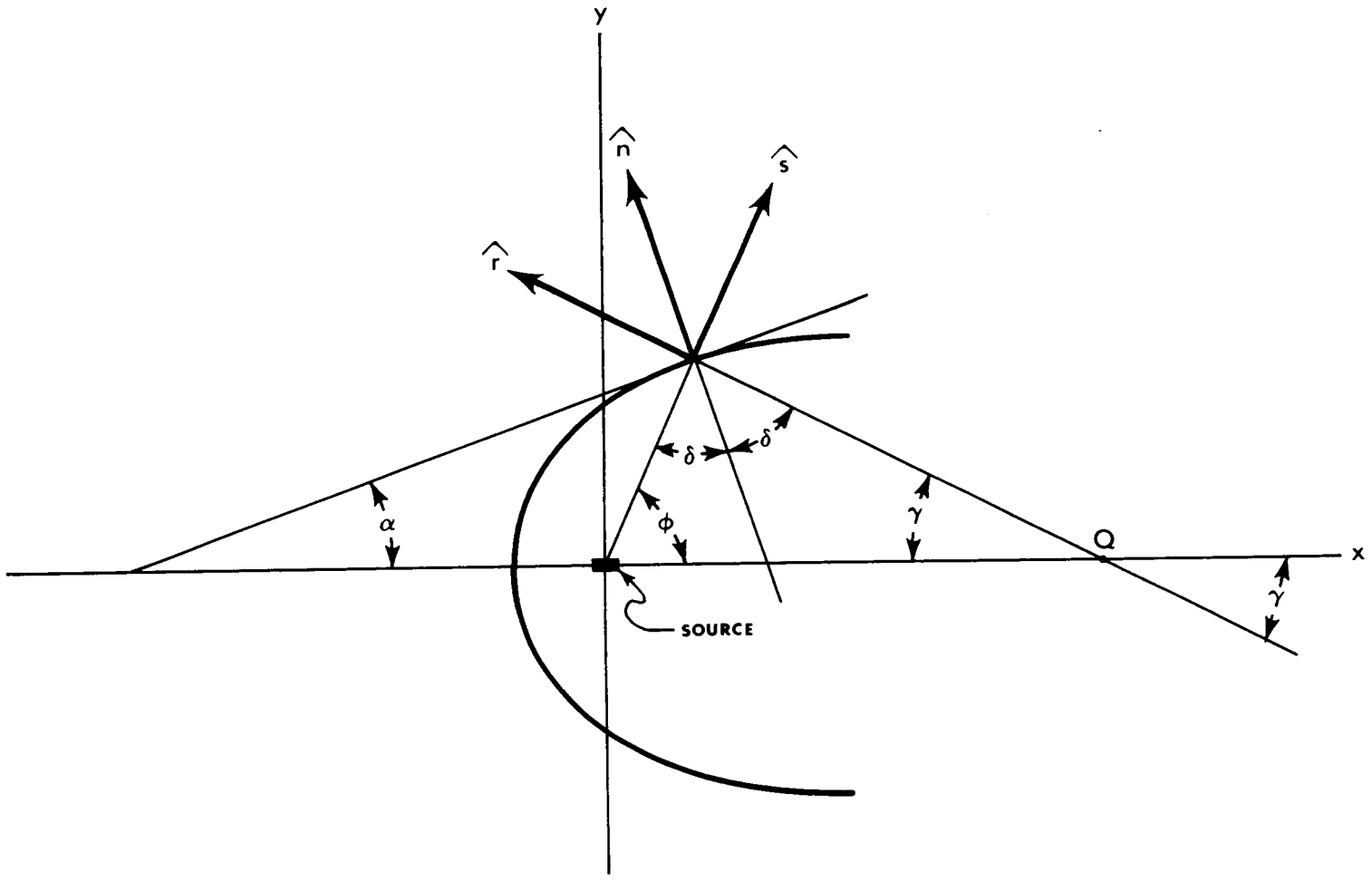

Figure VI-1. Schematic representation of the geometrical relationships which affect the intensity of reflected radiant flux when the source is located on the axis of an axially symmetric reflector.

Defining δ as the angle of incidence which is equal to the angle of reflection, then

$$\cos \delta = \hat{n} \cdot \hat{s} = \sin \phi \cos \alpha - \cos \phi \sin \alpha \qquad \text{(VI-4)}$$

$$\cos \delta = \hat{n} \cdot \hat{r} = \sin \gamma \cos \alpha + \cos \gamma \sin \alpha \qquad \text{(VI-5)}$$

Combining equations (VI-4) and (VI-5), the slope ($\tan \alpha$) of the reflector at the point (x,y) is

$$\frac{dy}{dx} \equiv \tan \alpha = \frac{\sin \phi - \sin \gamma}{\cos \phi + \cos \gamma} \qquad \text{(VI-6)}$$

From the geometry of figure VI-1

$$\cos \phi = \frac{x}{\sqrt{x^2 + y^2}} \qquad \text{(VI-7)}$$

$$\sin \phi = \frac{y}{\sqrt{x^2 + y^2}} \qquad \text{(VI-8)}$$

Taking the derivatives of equations (VI-7) and (VI-8)

$$d(\cos \phi) = \frac{y^2\, dx - xy\, dy}{(x^2 + y^2)^{\frac{3}{2}}} = - \sin \phi \, d\phi \qquad \text{(VI-9)}$$

$$d(\sin \phi) = \frac{x^2\, dy - xy\, dx}{(x^2 + y^2)^{\frac{3}{2}}} = \cos \phi \, d\phi \qquad \text{(VI-10)}$$

Substitution of equations (VI-6) and (VI-7) into equation (VI-9) yields

$$\frac{dx}{x} = \frac{d\phi}{\cos^2 \phi \, (\tan \alpha - \tan \phi)} \qquad \text{(VI-11)}$$

Substitution of equations (VI-6) and (VI-8) into equation (VI-10) yields

$$\frac{dy}{y} = \frac{d\phi}{\sin^2\phi\ (\text{ctn}\ \phi - \text{ctn}\ \alpha)} \qquad \text{(VI-12)}$$

If the angle γ can be defined in terms of the angle ϕ and various constants, then $\tan\alpha$ and $\text{ctn}\ \alpha$ can be expressed in terms of the variable ϕ and these same constants [see equation (VI-6)] and equations (VI-11) and (VI-12) can be utilized for a parametric determination of x and y. The angle γ can be defined in terms of the angle ϕ as follows.

Define dF' as the radiant flux emitted by the source at an angle ϕ with respect to the x-axis of figure VI-1. This flux is incident upon that element of area on the surface of the reflector whose normal $\hat{n}$ makes an angle $(\frac{\pi}{2} + \alpha)$ with the x-axis. Defining $d\omega'$ as the solid angle subtended by this surface element at the source and $d\omega$ as the solid angle ϕ subtended by this surface element at the point Q, then from the definition of solid angle

$$d\omega' = \sin\phi\ d\phi\ d\theta \qquad \text{(VI-13)}$$

$$d\omega = \sin\gamma\ d\gamma\ d\theta \qquad \text{(VI-14)}$$

Defining A_m as the albedo of the reflector for the source spectrum, I' as the intensity of the radiant flux emitted by the source in the direction ϕ, I as the intensity of the radiant flux reflected toward Q, and dF as the element of radiant flux contained within $d\omega$, then

$$A_m = \frac{dF}{dF'} = \frac{I\ d\omega}{I'd\omega'} = \frac{I\ \sin\gamma\ d\gamma}{I'\ \sin\phi\ d\phi} \qquad \text{(VI-15)}$$

If it is now required that the intensity of the reflected radiant flux be proportional to $\cos\gamma$, see equation (4-57), then from equation (VI-15)

$$\cos \gamma \sin \gamma \, d\gamma = \left(\frac{A_m}{I_o}\right) I' \sin \phi \, d\phi \qquad \text{(VI-16)}$$

For a uniformly radiating source (i.e., a spherical Lambertian source), I' is constant. Therefore, integrating equation (VI-16), the relationship between γ and ϕ for a uniformly radiating source is

$$\sin^2\gamma = \left(\frac{A_m I'}{I_o}\right) (1 - \cos \phi) \qquad \text{(VI-17)}$$

For a cylindrical Lambertian source, I' is given by equation (4-65). Substituting equation (4-65) into equation (VI-16) and integrating yields the relationship between γ and ϕ for a cylindrical Lambertian source which is coaxial with the reflector. That is

$$\sin^2\gamma = \left(\frac{A_m I'_{90}}{2I_o}\right) (\phi - \sin \phi \cos \phi) \qquad \text{(VI-18)}$$

where I'_{90} is the radiant intensity of the source in the directions normal to the axis of the cylinder.

The surface configuration required for a given source can be determined by dividing the range of ϕ into many small increments $\Delta\phi$ and utilizing equation (VI-16) and the trigonometric identities to determine the value of γ at the center of each interval. The value of α can be determined using equation (VI-6) and the trigonometric identities or, alternatively, using the relationship (from figure VI-1)

$$\alpha = \frac{\phi - \gamma}{2} \qquad \text{(VI-19)}$$

It is true that

$$\log_e x_i = \log_e x_{i-1} + \int_{x_{i-1}}^{x_i} \frac{dx}{x} \qquad \text{(VI-20)}$$

$$\log_e y_i = \log_e y_{i-1} + \int_{y_{i-1}}^{y_i} \frac{dy}{y} \qquad \text{(VI-21)}$$

Thus, from equations (VI-11) and (VI-12)

$$\log_e x_i = \log_e x_{i-1} + \left[\frac{\cos \alpha_i \, \Delta\phi}{\cos \phi_i \sin \left(\alpha_i - \phi_i \right)} \right] \qquad \text{(VI-22)}$$

$$\log_e y_i = \log_e y_{i-1} + \left[\frac{\sin \alpha_i \, \Delta\phi}{\sin \phi_i \sin \left(\alpha_i - \phi_i \right)} \right] \qquad \text{(VI-23)}$$

By evaluating equations (VI-22) and (VI-23) from an initial boundary condition defined by $\left(x_0 , y_0 \right)$, a set of coordinates $\left(x_i , y_i \right)$ can be calculated which describe the shape of the reflecting surface.

To test the above procedure, surfaces were determined, for a uniformly radiating source, for several values of C where

$$C = \frac{A_m I'}{I_0} \qquad \text{(VI-24)}$$

The values of C were determined using equation (4-82), by specifying as initial conditions that $\phi_0 = \pi - B$ and $\gamma_0 = 65^\circ$. It was also specified, as an initial condition, that $y_0 = 1.0$. Therefore, from the geometry of figure VI-1, $x_0 = y \operatorname{ctn} \phi_0$. The surfaces thus determined are plotted in figures VI-2 through VI-6,

In the derivation of the equations used to determine the surfaces represented in figures VI-2 through VI-6, the distance between the source and the position where the reflected ray intersects the axis (the point Q of figure VI-1) was allowed to vary. Because of this fact, the reflector introduces

C = 0.61206

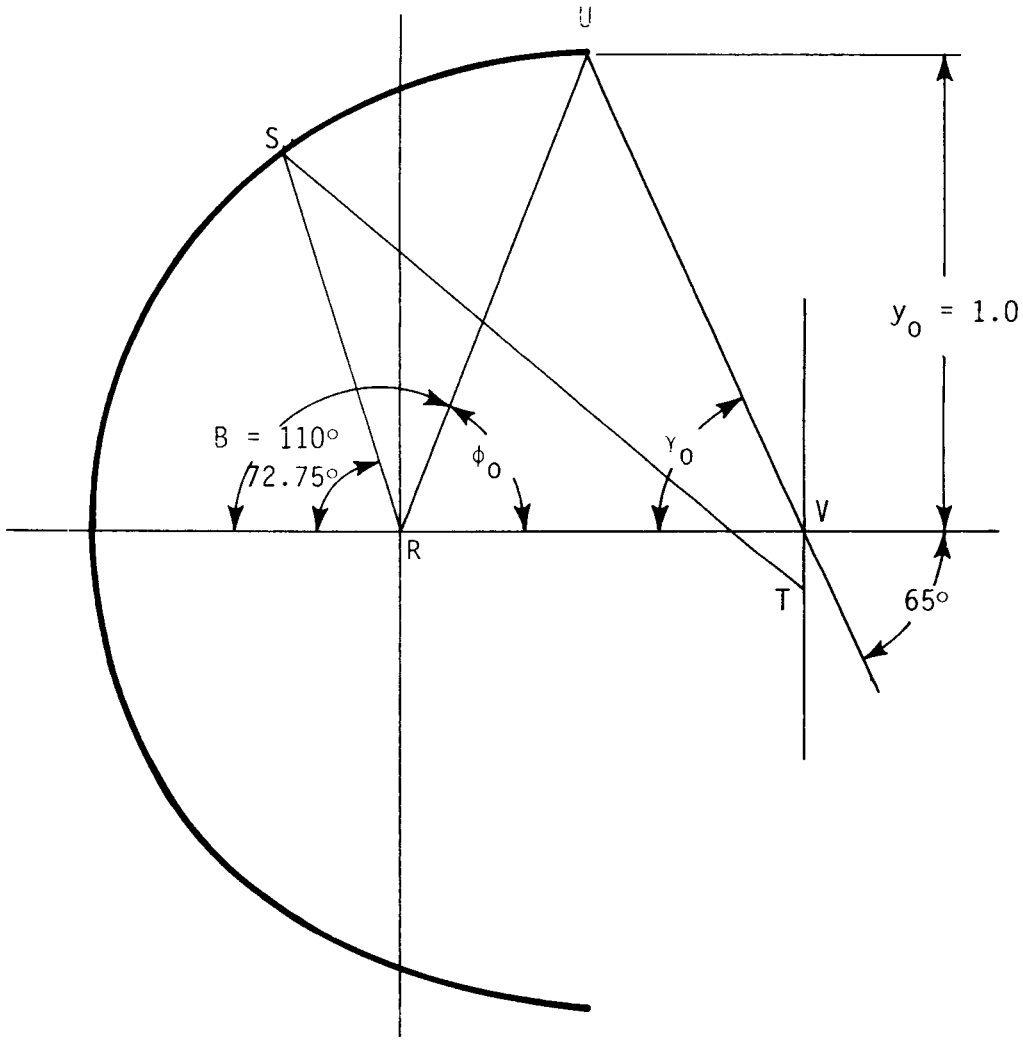

Figure VI-2. Geometry of a reflector which provides, for a point source, an output radiant intensity which is proportional to the cosine of the angle between the reflected ray and the axis.

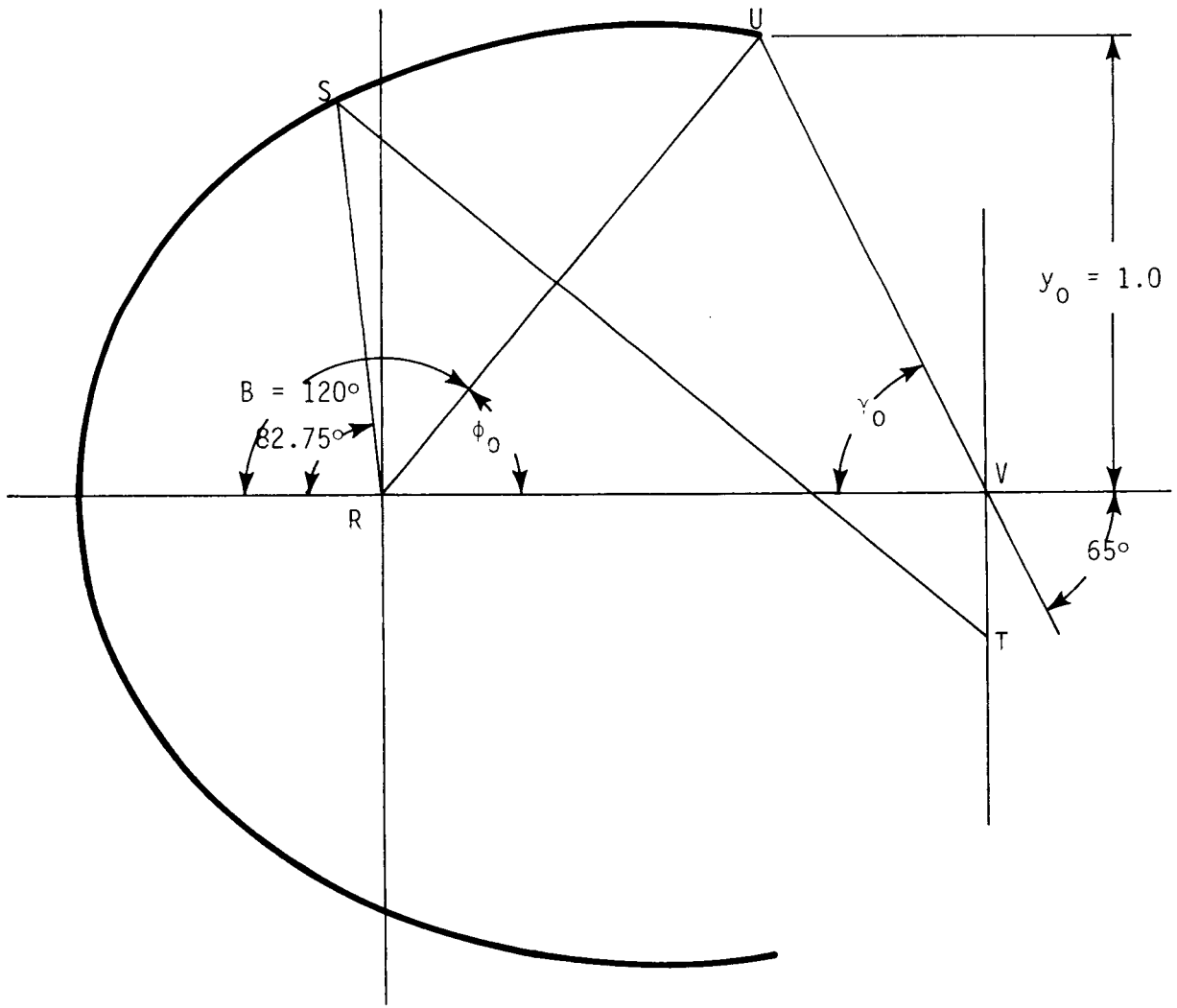

Figure VI-3. Geometry of a reflector which provides, for a point source, an output radiant intensity which is proportional to the cosine of the angle between the reflected ray and the axis.

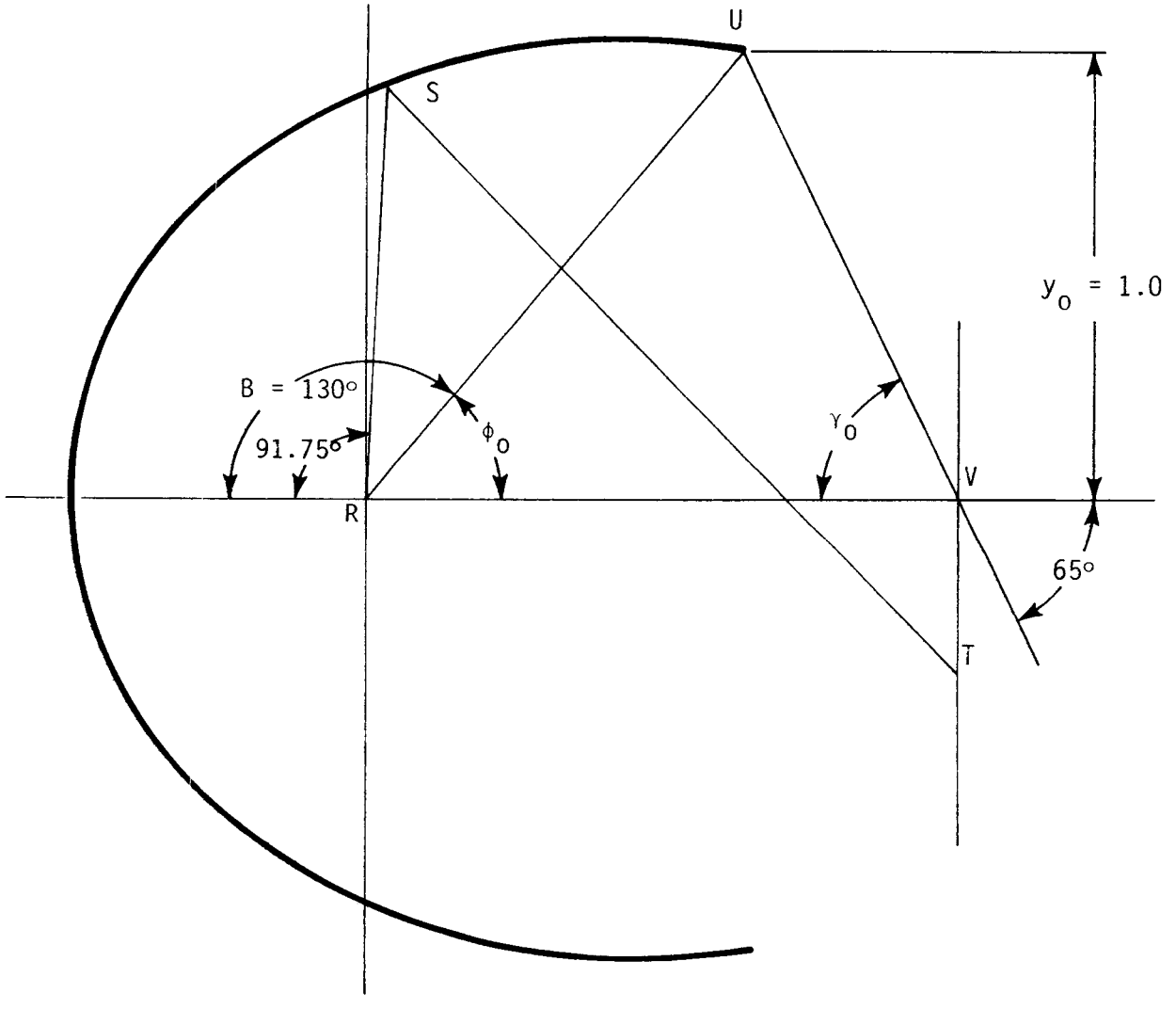

Figure VI-4. Geometry of a reflector which provides, for a point source, an output radiant intensity which is proportional to the cosine of the angle between the reflected ray and the axis.

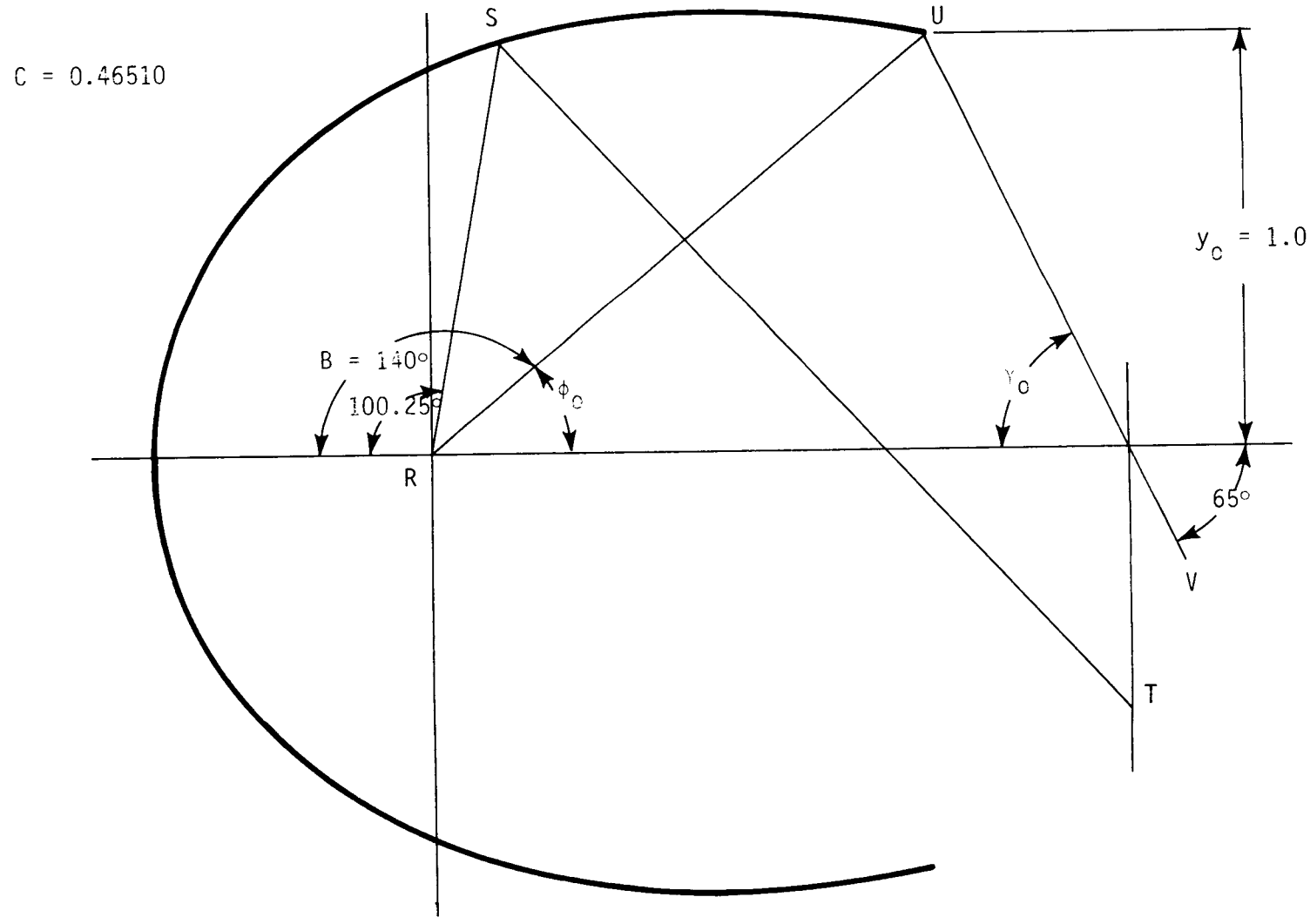

Figure VI-5. Geometry of a reflector which provides, for a point source, an output radiant intensity which is proportional to the cosine of the angle between the reflected ray and the axis.

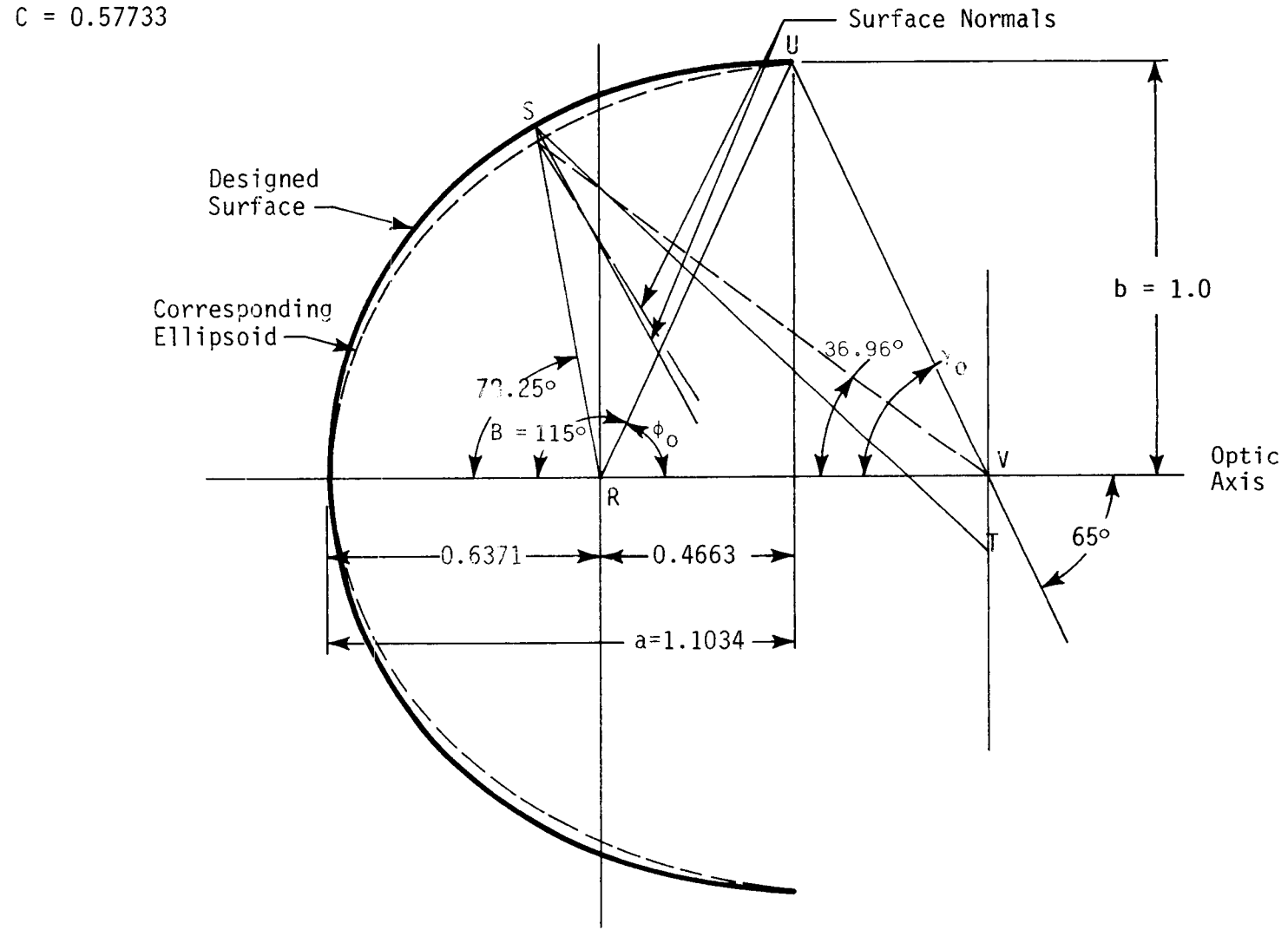

Figure VI-6. Geometry of a reflector (and the corresponding ellipsoidal approximation) which provides, for a point source, an output radiant intensity which is proportional to the cosine of the angle between the reflected ray and the axis

spherical aberration into the distribution of the reflected radiant flux. The amount of spherical aberration introduced by the surfaces plotted in figures VI-2 through VI-6 was determined by locating a reference plane normal to the axis at the intersection of the axis and the initial ray RUV. By tracing rays from the source to the reflector and then to the reference plane and determining the distance T between the axis and the ray intersection with the reference plane, it was possible to determine the ray path for which T is maximum. [The ray path RST plotted in figures VI-2 through VI-6 represents the ray for which T is maximum.] The range of T is a measure of the spherical aberration introduced by the reflector and, as can be seen from figures VI-2 through VI-6, increases as the value of C decreases.

In general, spherical aberration must be minimized. This can be seen from the fact that although the reflector has, in each case, been defined to provide radiant flux with the correct intensity along each ray path, the cosine intensity distribution defined by equation (4-57) has reference to radiant flux emanating from a well-defined position, a position which does not exist when spherical aberration is present. Further, if the reflecting surface is to be used in a module for the Planetary Radiation Environment Simulator, the presence of a large amount of spherical aberration makes it extremely difficult (if not impossible) to provide the required masking of the field into which the module emits radiant flux.

From figures VI-2 through VI-6, the surfaces defined for a uniformly radiating source (hereinafter denoted as the designed surfaces) resemble ellipsoids. This indicates that, if the source were located at the primary focus of the ellipsoid which each designed surface most closely resembles, the intensity of the radiant flux emanating from the secondary focus would be approximately proportional to the cosine of the angle γ between the axis and the reflected ray.

To illustrate, consider the designed surface, figure VI-6, which was determined by specifying the initial ray RUV so that $\phi_o = \gamma_o$. The corresponding ellipsoid, defined so that its primary focus is located at

R, so that its seconday focus is at V, and so that it passes through the point U, is plotted as the dashed curve in figure VI-6. The zone of the designed surface, at which the initial ray is reflected, defines the plane of the minor axis of the corresponding ellipsoid; since the corresponding ellipsoid contains this zone, the length of the semi-minor axis is $b = 1.0$ unit. The distance from the plane of the minor axis to either focus of the corresponding ellipsoid is $\sqrt{a^2 - b^2} = b \cot \phi_0 = 0.4663$ unit. Therefore, the corresponding ellipsoid has a semi-major axis of length $a = 1.1034$ unit and an eccentricity $e = 0.4226$. Further, since the designed surface intersects the optic axis at a distance of 0.6371 unit from the source, the designed surface and the corresponding ellipsoid are tangent at the optic axis.

If the designed surface were an ellipsoid, there would be no spherical aberration and the ray RST would pass through the point V. Spherical aberration of the same type as is introduced by the designed surface (indicated by the ray path RST) can be approximated by displacing the source toward the center between the foci of the corresponding ellipsoid. From the angular relationships indicated in figure VI-6, displacing the source in this manner will also tend to increase the intensity of the radiant flux in the vicinity of the optic axis. These angular realtionships also indicate that, if the interfocal distance is maintained, then as the length of the semi-minor axis b of the ellipsoid is reduced from 1.0 unit (thus increasing the eccentricity of the ellipsoid), the intensity of the radiant flux in the vicinity of the optic axis will increase.

To clarify the relationship between the source intensity distribution, the intensity distribution of the flux reflected from an ellipsoid, and the geometrical parameters of the ellipsoid, consider the case where a source of intensity I' in a direction ϕ is located at the primary focus of an ellipsoidal reflector. The geometry of an ellipsoid is such that

$$\cos \phi = \frac{\cos \gamma - G}{1 - G \cos \gamma} \qquad \text{(VI-25)}$$

where

$$G = \frac{2e}{1 + e^2} \tag{VI-26}$$

where e is the eccentricity of the ellipsoid, and where γ is the angle between the reflected ray and the optic axis. Differentiating equation (VI-25) yields

$$\frac{d(\cos \phi)}{d(\cos \gamma)} = \frac{\sin \phi \, d\phi}{\sin \gamma \, d\gamma} = \frac{1 - G^2}{(1 - G \cos \gamma)^2} \tag{VI-27}$$

Substitution of equation (VI-27) into equation (VI-15) yields an expression which relates the intensity I' of the radiant flux emitted by the source in the direction ϕ to the intensity I of the radiant flux reflected from the ellipsoid. This expression is

$$\frac{A_m I'}{I} = \frac{(1 - G \cos \gamma)^2}{1 - G^2} \tag{VI-28}$$

where A_m is the albedo of the reflecting surface for the spectrum of the source. If it is now required that the intensity I of the reflected radiant flux be proportional to the cosine of the angle γ between the reflected ray and the optic axis, see equation (4-57), then from equation (VI-28)

This equation is

$$I' = \left(\frac{I_o}{A_m}\right) \left[\frac{(1 - G \cos \gamma)^2 \cos \gamma}{1 - G^2}\right] \tag{VI-29}$$

From equation (VI-25)

$$\cos \gamma = \frac{\cos \phi + G}{1 + G \cos \phi} \tag{VI-30}$$

which, when substituted into equation (VI-29), yields an expression which defines the relationship required, between the source intensity I' in a direction ϕ and the ellipsoid geometrical parameter G, in order for the intensity I of the reflected radiant flux to be proportional to $\cos \gamma$. This equation is

$$I' = \left(\frac{I_o}{A_m}\right) \left[\frac{(1 - G^2)\ (G + \cos \phi)}{(1 + G \cos \phi)^3}\right] \tag{VI-31}$$

Thus, using equation (VI-31), it is possible to define an ellipsoidal reflector (or a reflector consisting of concentric zones of several ellipsoids, each ellipsoid having the same interfocal distance) which, when used with a given source, will provide radiant flux whose intensity I is approximately proportional to $\cos \gamma$.